University of Fort Hare
Together in Excellence

Preparation, Characterization and In vitro Analysis of Polyamidoamine Drug Conjugates Containing Ferrocene and Platinum Analogues.

By

Ansley Mugogodi

(Student Number: 201411572)

Dissertation Submitted in Fulfilment of the Requirements for the Degree of Master of Science in Chemistry

In the Department of Chemistry

Faculty of Science and Agriculture

University of Fort Hare

Supervisor: Prof. B.A. Aderibigbe

DECLARATION

I declare that this work is the result of my own research except where cited in references. The dissertation has not been submitted in part or in whole to any other university.

Signature :…….

Name :…….

Date :…….

ACKNOWLEDGEMENTS

Firstly I thank the Almighty God for the gift of life and His unconditional love in allowing me to pursue my studies in good health.

I extend my sincere gratitude to my supervisor, Dr B.A. Aderibigbe, for her support and guidance, without which this research would have been possible. I greatly appreciate the opportunity provided for me to contribute in this area of research.

I acknowledge all my colleagues in our research group for assistance in producing this work.

I'm thankful to the Department of Chemistry, GMRDC, MRC, NRF and Sasol Inzalo for securing the needs and financial resources for this research project.

Finally, I thank my parents, family members and friends for their love, prayers and support throughout the duration of my studies.

ABSTRACT

Polyamidoamine drug conjugates were prepared from analogues of ferrocene and platinum. Standard reaction procedures were followed in the synthesis of platinum and ferrocene analogues. Michael addition reaction of amines to the activated double bonds of methylenebisacrylamide was applied for preparation of the water soluble polyamidoamine carriers onto which drug analogues were attached. The drug release studies of the conjugates were evaluated at different pH environments. The results obtained from drug release studies showed that rate of drug release was variable depending on the conjugate and pH environment. Mathematical drug release models by Korsmeyer-Peppas were used to determine the drug release characteristics of the ferrocene and platinum based drugs from polyamidoamine drug conjugates.

Cytotoxicity potential of the analogues and polyamidoamine drug conjugates was tested on selected cell lines. Cisplatin was used as the standard for comparison of the IC_{50} values obtained for the compounds tested for cytotoxicity activity. The results from six polymer drug conjugates tested for cytotoxicity activity showed that conjugation of analogues to polyamidoamine carrier enhanced the activity of the analogues in some of the polyamidoamine drug conjugates. Various techniques such as Fourier Transform Infrared (FTIR) spectroscopy, Proton Nuclear Magnetic Resonance spectroscopy (^{1}H NMR), Scanning Electron Microscopy (SEM), transmission electron microscopy (TEM), Transmission Electron Microscopy (TEM) and Energy Dispersive X-ray (EDX) spectroscopy were employed for the characterization of the ferrocene and platinum analogues, polyamidoamine carriers and drug conjugates.

LIST OF ABBREVIATIONS

^{1}H NMR	Proton nuclear magnetic resonance spectroscopy
AAS	Atomic absorption spectroscopy
AEE	2-(2-Aminoethoxy) ethanol
APD	3-Amino-1,2-propanediol
ATCC	American Type Culture Collection
CMC	Critical micelle concentration
DACH	1, 2-Diaminocyclohexane
DACH $PtCl_2$	Cyclohexane-1,2-diamine dichloroplatinum(II)
DCC	N,N'-dicyclohexylcarbodiimide
DEP	3-Diethylaminopropylamine
DET	Diethylene triamine
DMEM	Dulbecco's Modified Essential Medium
DMP	3-Dimethylamino-1-propylamine
DNA	Deoxyribonucleic acid
EA	Ethanolamine
EA.hy926	Normal human cell line
EDA	Ethylenediamine
EDDA	2,2-(Ethlenedioxy) diethylamine
EDX	Energy dispersive x-ray spectroscopy

Fc	4-Ferrocenylketobutanoic acid
Fc-PDA	3-[4-Ferrocenylketobutamido]propylamine
FCS	Foetal Calf Serum
FDA	Food and Drug Administration
FTIR	Fourier transform infrared spectroscopy
IC_{50}	Concentration that inhibits the growth of 50% of the cell population
MBA	N, N'-methylenebisacrylamide
MCF-7	Michigan Cancer Foundation-7
MDA-MB-231	Human breast carcinoma cell line
MDR	Multidrug resistance
PAA	Polyamidoamine
PBS	Phosphate buffered saline
PDA	1,3-Propanediamine
PDI	Polydispersity index
PEG	Polyethylene glycol
pH	potential hydrogen
RNA	Ribonucleic acid
RT	Room temperature
SEM	Scanning electron microscope
SRB	Sulphorhodamine B

TEA	Triethylamine
TEM	Transmission electron microscopy
THF	Tetrahydrofuran
UV/Vis	Ultraviolet visible spectroscopy

LIST OF FIGURES

LIST OF TABLES

LIST OF SCHEMES

TABLE OF CONTENTS

CHAPTER 1

Introduction

1.1 Background

Polymers represent a sustainable mode of drug delivery and have been essential in the development and advancement of drug delivery technology by providing controlled release of therapeutic agents in required doses for sustained periods and tunable release of both hydrophobic and water soluble drugs (Liechty et al., 2010). As such polymer drug conjugates offer an exciting strategy for the delivery of drugs in the field of chemotherapy.

Researches carried out over the years have proved the possibility for the synthesis of polymer drug conjugates from linear polymers such as polyamidoamines (Ferruti, 1996; Ferruti et al., 2002). Cancer is among the leading causes of death worldwide, accounting for 8.8 million deaths in 2015. In that same period 571 000 deaths (6% of total cancer deaths) resulted from breast cancer (World Health Organisation, 2017). Historically, solid tumours such as breast cancer pose many challenges to systemic therapeutic treatment regimes. Common barriers to proper drug penetration in solid tumours include heterogeneous vascular supply and high interstitial pressures within tumour tissue. Encapsulation of drugs onto the synthetic carriers such as polyamidoamines can be useful in improving circulation lifetimes and hence enhance the drug efficacy (Park, 2002).

Breast cancer is one of the malignant diseases in which malignant tumours emanate from cells of the breast. Malignant tumours are a collection of abnormal cells that have the capability to invade surrounding tissues or replicate into distant body parts. Breast cancer poses a serious threat to humanity in both the developing and the developed world. Cisplatin, cis-diamminedichloroplatinum(II), is the most widely used antitumor agent, finding use in treatment of a wide variety of cancers such as testicular, ovarian, bladder, cervical, breast,

head and neck and non-small cell lung cancers (Miller et al., 2010). However, several second generation anticancer drugs have emerged as alternatives to cisplatin and its derivatives. Carboplatin, one of the second generation anticancer agents, has improved therapeutic index of cisplatin by ameliorating some of the undesirable side effects. Lobaplatin was approved in China and is currently used for treatment of cisplatin resistant ovarian cancer and also breast cancer (Wang & Guo, 2013).

Treatment of cancer by combination therapy is gaining in popularity because it causes synergistic anticancer effects, lowers individual drug related toxicity and suppresses multiple drug resistance (MDR) through different mechanisms of action (Parhi et al., 2012). It represents a mainstay treatment regime necessary for improvement of survival rates in cancers such as cancer of the breast (Ruiz-Esparza et al., 2014). The prevalence of MDR in the majority of cancers renders many clinically approved drugs ineffective, leading to poor prognosis (Wang & Guo, 2013). However, encapsulation of the anticancer drugs onto polymeric carriers can improve the water solubility of insoluble drugs, protection of the payload from prematurely degrading in the body, improved drug/payload residence time resulting in better pharmacodynamics profiles and improvement in efficacy and reduced non-specific drug toxicity (Singh et al., 2014).

1.2 Problem statement

Cancer is a leading cause of death on a global scale. Several treatment modalities such as chemotherapy, radiation therapy and surgery have been in use for treating cancer. Platinum anticancer agents have been the most widely used drugs for cancer chemotherapy. However, the platinum drugs inflict several forms of toxicity and they are also vulnerable to drug resistance. For example, the use of single drug agents for breast cancer therapy is usually prone to drug resistance especially after sustained period of use (Persidis, 1999). Many convectional anticancer drugs in clinical use today have problems with resistance against one

or multiple strains of cancers. Some major platinum based anticancer drugs such as oxaliplatin and carboplatin has been found to exhibit cross resistance with cisplatin in some cancer types (Gore et al., 1989; Talarico et al., 1999). In addition, traditionally used medicinal drugs cause toxicity to healthy tissues more than therapeutic drugs incorporated to carriers and hence the importance of polymer drug conjugates in the delivery of drugs (Allen & Cullis, 2004).

1.3 Aim and Objectives

1.3.1 Aim

The aim of this study was to synthesize polyamidoamine drug conjugates containing ferrocene and platinum analogues with enhanced therapeutic effects.

1.3.2 Specific objectives

- Preparation and characterization of ferrocene and platinum analogues.
- Encapsulation of ferrocene and platinum analogues onto polyamidoamine carriers to form polymer drug conjugates.
- Evaluation of drug release kinetics of encapsulated ferrocene and platinum drug conjugates.
- In vitro cytotoxicity evaluation of the drug conjugates on selected cancer cell lines.

1.4 Scope of study

This study focuses on the preparation of polyamidoamine drug conjugates from analogues of ferrocene and platinum. In vitro cytotoxicity evaluation was carried out on selected cell lines namely MCF-7, MDA-MB-231 and EA.hy926 to assess the anticancer activity of the prepared polymer drug conjugates. Drug release studies of the polymer drug conjugates was determined at pH 1.2 and 7.4 simulating conditions experienced in the stomach and normal blood environment respectively. The scope of this research design is to minimize the

resistance of tumour cells as well as improving the efficacy of platinum based drug and ferrocene based drug by combining the drugs by use of water soluble polyamidoamine carriers. The varied working mechanisms of the two drugs that result from combination should overcome for drug resistance of cancerous cells.

1.5 Significance of the study

The research is envisaged to contribute to the chemotherapeutic treatment of breast cancer by ameliorating some of the problems exhibited by traditionally used drugs. Encapsulation of ferrocene and platinum drugs onto polymeric carriers have potential to eradicate cross resistance of currently used chemotherapeutic anticancer agents. Moreover, polyamidoamine carriers are associated with high solubility in aqueous media which is favourable for drug assimilation in the human body. The low cost and relative ease of preparation and functionalization makes PAAs ideal for use in the current study.

CHAPTER 2

Literature Review

2.1 Introduction

This chapter focus on the literature based on carriers, drugs and polymer drug conjugates. Also included is a brief discussion on drug delivery systems such as nanoparticles, liposomes, hydrogels and polymeric micelles. Ferrocene and platinum analogues literature is also reviewed in this section. Substantial amounts of papers have been published on these topics, only a selected few publications have been made use of and referenced in this chapter.

2.2 Polymeric drug carriers

Drug carriers are materials that serve as devices to enhance the delivery and efficacy of drugs by increasing the hydrophilicity of drugs in water. They are employed in drug delivery systems such as controlled release technology to prolong in vivo actions, decrease drug metabolism and in the reduction of drug toxicity. Most anticancer drugs are not soluble in aqueous media, delaying their clinical effectiveness (Chadha et al., 2008). Hence, carriers are useful in improvement of drug delivery to the target sites of pharmacological actions.

Polymers exists as natural or synthetic forms which are used widely as components in various branches of science. Selected polymers used as drug carriers are either natural or synthetic macromolecules. In most cases synthetic polymers are more preferable for use as drug carriers because they can be tailor-made to match requirements of the biological conditions (Uchegbu & Schatzlein, 2006). In contrast, natural polymers which are present in living organisms suffer from low mechanical strength and high degradation rates. Polyethylene glycol (PEG) is one of the most used synthetic polymer for drug delivery applications (Greenwald et al., 2003). However, its application in therapeutics is limited by low drug

carrying capacity since only two terminal groups are available for drug conjugation (Banerjee et al., 2012; Li et al., 2013).

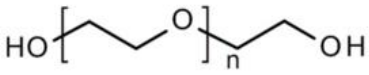

Figure 2.1: Structure of polyethylene glycol (PEG)

Polymeric drug carriers maximize their potential by ameliorating the toxicity and (or) increasing the therapeutic index of the anticancer drug (Larson & Ghandehari, 2012). Some of the major requirements of polymeric drug carriers include water solubility, biodegradability, biocompatibility and chemical composition as described in detail in the section below:

2.2.1 Water solubility

Solubility is a major requirement for a polymer intended to be employed as a drug carrier because of the predominantly aqueous central circulation system of humans. The polymer should be linear and highly flexible. Also, the presence of intra- or extra chain hydrophilic substituents such as hydroxyl and amino terminal enhances the dissolution of the whole structure. The hydrophilic entities are of excellent utility as they can easily undergo hydration. Additionally, the ability of a polymer to incorporate charged species also favours its hydrosolubility. The presence of the amide functional group which form the basis for linkage between carriers such as polyamidoamines (PAAs) and the drug also contribute to water solubility.

2.2.2 Biodegradability

Biodegradable polymers are an important collection of materials useful for the delivery of drugs (Liechty et al., 2010). The presence of labile bonds in polymeric backbone or linker of the carrier facilitates its chemical degradability. Many synthetic polymers which are

biodegradable depend on hydrolysis of ester linkages or derivatives of esters such as poly(lactic/glycolic acid) (Liechty et al., 2010). The carriers must be easily eliminated from the body after completion of their function or metabolized to smaller units below the renal threshold (Kopeèek & Ulbrich, 1983). However, the carrier should be sufficiently large to avoid premature excretion from the body through ultrafiltration of blood in the kidneys. Polymers such as poly(lactic acid) (PLA) break down to form lactic acid which is naturally present in muscles of the body. This acid is ejected by conversion to carbon dioxide and water during respiration (Gunatillake et al., 2003). Biodegradable polymers are normally designed to disintegrate as a result of hydrolysis of polymer chains into fragments that can be excreted out of the host. Failure for a drug carrier to be biodegradable may result in undesirable deposition and accumulation in body organs. Polyamidoamines are normally biodegradable especially if they contain an amide bond in the main chain and their rate of degradation depends on the structure (Ferruti et al., 1994; Ferruti et al., 1995).

2.2.3 Biocompatibility

Most importantly, a biodegradable polymer carrier is required to be biocompatible not only in terms of its physico-chemical properties but also with the qualities that define their characteristics when they come in contact with the body (Silva et al., 2004). Biocompatibility of a polymeric carrier is vital to ensure that rejection by the host does not happen through natural defence mechanisms. The polymer backbone of a carrier is required to be non-toxic, non-immunogenic, and non-thrombogenic in order to avoid carrier induced toxicity, immunogenic, and blood-clotting side effects. Methods of preparation and chemical structure of the polymer directly affects biocompatibility. Metabolic products resulting from the breakdown of the parent polymers must also be biocompatible.

2.2.4 Chemical composition

The drug carrier must contain reactive functional groups suited for incorporation and release of drugs. To avoid steric hindrances between the drug linkers, short side chains or spacers should be present to separate them. In addition, spacers must be stable in blood circulation but susceptible to degradation by enzymes or pH-dependent hydrolysis in the lysosomal compartment (Kopeček, 1984; Rejmanová et al., 1985). A polymeric carrier with a high drug loading capacity is advantageous as it enhances the targeting efficiency for the incorporated drug.

2.3 Polyamidoamine (PAA)

Polyamidoamine carriers are a class of synthetic biodegradable polymers that can be easily prepared by stepwise polyaddition of aliphatic amines to bisacrylamides (Scheme 2.1).

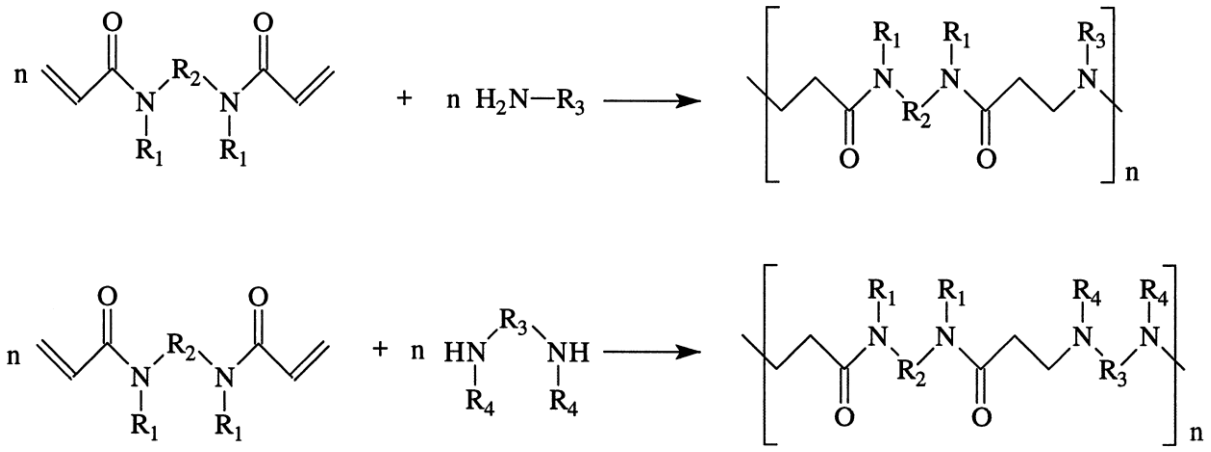

Scheme 2.1: Scheme showing synthesis of polyamidoamines (Hill et al., 1999; Mohammadifar et al., 2015)

These carriers contain tertiary amino and amido groups arranged along a backbone in regular sequences (Ferruti, 1996; Ferruti et al., 2002). Over the years linear PAAs have been principally synthesized in two forms, namely hydrogels and water-soluble entities which have shown potential for application as antimetastatic drugs, antivirals and antimalarials (Ferruti et

al., 1973; Cavalli et al., 2010; Urbán et al., 2014). The type of amide and amine present influence the properties of the PAAs including water solubility, degradability and biological toxicity. For example, the presence of primary amine and hydroxyl functional groups favours the solubility of polyamidoamines.

Ferruti pioneered the polyamidoamine carriers which are nontoxic, biocompatible, water soluble and biodegradable (Ferruti et al., 2002). As such polyamidoamine carriers are useful for biomedical applications (Ferruti et al., 2002; Aderibigbe et al., 2015). PAAs also do not exhibit the immunogenicity disadvantage as displayed by viral delivery systems (Malgesini et al., 2003). They have a special property of reacting with numerous functional groups in organic chemistry. Several chemical functions such as hydroxyl group, carboxyl group, allyl group and ether group can be easily introduced to the PAAs by using corresponding functional monomers (Ferruti et al., 2002; Malgesini et al., 2003). An endless variety of polyamidoamine structures can be synthesized based on corresponding choice of monomers i.e. functionalized amines and bisacrylamides (Cavalli et al., 2010). Polyamidoamine synthesis is carried out mainly in solvents such as alcohols and water. The mechanism for the reaction between the bisacrylamides and amines follows Michael addition as shown in the scheme below:

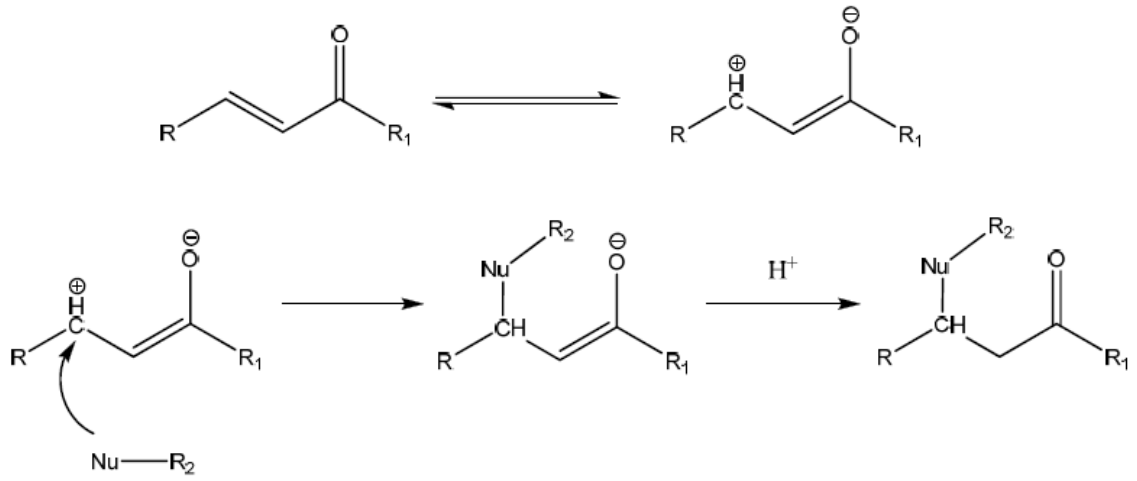

Scheme 2.2: Scheme showing Michael addition mechanism in polyamidoamine formation

The pioneering studies on PAA synthesis were reported around 1970 (Danusso & Ferruti, 1970) and thereafter their chemistry and properties have been reviewed in several publications (Ferruti et al., 1985; Ferruti et al., 2002). Water soluble polyamidoamines have been extensively researched as anticancer agents by Ferruti and co-workers (Ferruti et al., 1973; Ferruti et al., 2002; Emilitri et al., 2005). Polyamidoamine conjugates comprising ferrocene derivatives were synthesized in a research by Neuse et al (N'Da & Neuse, 2006). Aderibigbe et al. prepared PAA conjugates of neridronic acid and were characterized by several techniques including FTIR, NMR, TGA and SEM (Aderibigbe et al., 2015). In this current study, polyamidoamine conjugates of platinum drug and ferrocene derivatives will be prepared for drug release studies and evaluation of anticancer activity against breast cancer cell lines.

2.4 Drug delivery systems

One of the principal strategy of drug delivery is enhancement of pharmacological and pharmacokinetics of therapeutic drug molecules (Tong & Cheng, 2007). The drug molecules can be released to the target site by the dissociation of a covalent linker or by means of

diffusion. In designing drug delivery systems, it is important to regulate the quantity of drug released at a given time and the location in the body where the drug is released in order to optimise the efficiency of the therapeutic drug without causing harm to the host (Sing et al., 2014). Drug delivery systems can enhance the potential of antiproliferative agents by increasing the concentration and (or) by reducing the exposure in normal body tissues. Besides the potential shown by polyamidoamines, other delivery systems have been subject to numerous research. Nanoparticles, liposomes, micelles and hydrogels have been used for drug delivery for many years with good results.

2.4.1 Nanoparticles

Nanoparticles offer unique approaches as drug delivery systems for treatment of cancer with promising viability in the biopharmaceutical industry. Nanoparticles are useful for directly delivery of toxic drugs to the cancerous cells. Optimization of the physicochemical and biological properties of nanocarriers allows for ready uptake in the tumour tissue in comparison to larger molecules (Suri et al., 2007). Biodegradable nanoparticles are often used to enhance the therapeutic value of both hydrophilic and hydrophobic drugs by improving water solubility, bioavailability and retention time (Shenoy & Amiji, 2005; Wang et al., 2012). Nanoencapsulation of medicinal drugs offer many advantages including protection of premature drug degradation and interaction with biological environment, improved absorption into target tissue and increased intracellular penetration (Alexis et al., 2008). Studies on paclitaxel showed that nanoparticle formulation of the drug increased both its cytotoxicity profile in cell culture and its efficacy in in vivo analysis (Win & Feng, 2006). This is attributed to the increased retention time and bioavailability of nanoparticle formulation, which makes it possible for the concentration of the drug to remain higher than the minimum effective value for a longer period of time.

2.4.2 Liposomes

Another extensively researched delivery platform in clinical use is the liposome drug delivery system which consist of lipid bilayer that can be incorporated to drugs. Liposomes vary with composition, surface charge, size and the method used for preparation. Ever since their invention by Alec Bangham in 1961 (Bangham & Horne, 1964), liposomes have been long considered possible delivery vehicles for drug molecules into cells that would otherwise not be readily internalized. The biocompatibility, biodegradability, low toxicity and immunogenicity of liposomes make them suitable for drug delivery. Liposomes have been reported to improve drugs solubility and enhance their pharmacokinetic properties such as the therapeutic index of anticancer agents, rapid metabolism, reduction of side effects and increase of in vitro and in vivo antiproliferative activity (dos Santos Giuberti et al., 2011). Drug release from loaded liposomes can be initiated by pH, osmotic gradient, liposome composition, and the nature of the surrounding environment (dos Santos Giuberti et al., 2011).

Doxil (PEG liposomal doxorubicin) was the first liposome based drug delivery platform to be approved by FDA in 1995 for treatment of AIDS related Kaposi's Sarcoma. Other liposome based drug delivery systems in clinical application include DaunoXome (daunorubicin liposomes), DepotDur (morphine liposomes) and Ambisome (amphotericine B liposomes) (Farokhzad & Langer, 2006). The use of liposomes for drug delivery is firmly established with the clinical success of Doxil and more research is being done to find new liposome formulations of other anticancer drugs with better chemotherapy outcomes (Malam et al., 2009).

2.4.3 Polymeric micelles

Polymeric micelles are self-assembled nanocarriers that consists of a hydrophobic core and shell structure. Micelles form in aqueous media when the concentration of block copolymer

in solution exceeds the critical micelle concentration (CMC). Hydrophobic sections of block copolymers start to associate at CMC in order to reduce contact with molecules of water resulting in the formation of a core-shell micellar structure. Typically, polymeric micelles are composed of several hundred block copolymers and have diameters of about 20-50 nm (Kwon & Okano, 1996). Similar to polymer drug conjugates, polymeric micelles improve the hydrophilicity and bioavailability of hydrophobic drugs due to their unique core-shell structure which is useful for drug encapsulation. Polymeric micelles are usually made from biodegradable and biocompatible materials which makes them well suited as drug carrier systems.

Polymeric micelles are renowned for having high drug-loading capacity, high hydrophilicity, suitable size for long circulation in the blood and absorption to tumour tissues by the EPR effect (Rösler et al., 2001). Micelles have long half-life in the body and therefore advantageous for drug delivery since they are not susceptible to premature removal from blood stream via kidney ultrafiltration. The release of the drug from loaded polymeric micelle can be engineered to be triggered by physicochemical properties such as pH, temperature and the presence of certain types of enzymes (Rapoport, 2007).

2.4.4 Hydrogels

Hydrogels are three-dimensional, cross-linked networks of hydrophilic polymeric chains that do not dissolve but swell in water and hold a substantial amount of water while maintaining the structure (Qiu & Park, 2001; Hoffman, 2012). Hydrogels can be synthesized from both synthetic and natural polymers (Schwall & Banerjee, 2009). The pronounced biocompatibility of hydrogels emanate from their high water content and soft surface properties (Bae & Kim, 1993). The release of the drug and degradation of the polymer in the body is promoted by the ability of hydrogels to rapidly swell in aqueous medium (Liechty et al., 2010). Controlled release of the incorporated drug is also dependent on the diffusion

coefficient of the drug molecule across the hydrogel network (Ganta et al., 2008; Hoare & Kohane, 2008). Hydrogels exhibit several other properties useful for pharmaceutical and biomedical applications including stability in biological environment and patient compliance.

2.5 Polymer drug conjugates

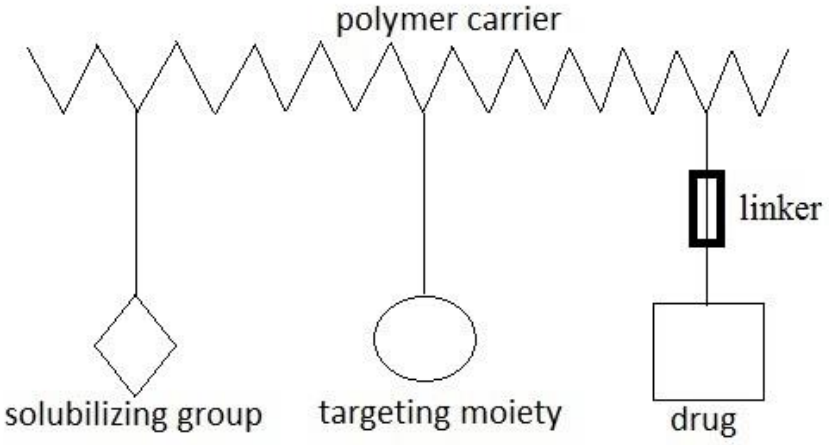

Figure 2.2: Generic structure of polymer drug conjugates

Polymer drug conjugates form a well-documented field of hydrophilic delivery systems termed polymer therapeutics (Duncan, 2006). This class of compounds also include polymeric drugs, polymer-protein conjugates and polymeric micelles. Polymer drug conjugates are mainly made up of the polymer backbone, solubilizing group, targeting moiety, linker and drug as shown on figure 2.2 above. Polymer drug conjugates offer several advantages compared to conventionally used anticancer drugs in chemotherapy. For example, specific targeting of drugs to the affected body organ can be used for polymer drug conjugates with minimal effect to healthy organs. Polymer drug conjugates, first proposed in 1970s, are technologies for drug delivery in which a drug and polymeric carrier such as polyamidoamines are covalently linked (Greco & Vicent, 2009).

Helmut Ringsdorf introduced the concept of polymer drug conjugates in 1975 and has been in application since then (Ringsdorf, 1975; Gros et al., 1981). Kopecek and Duncan employed the same strategy to develop the first synthetic polymer-drug conjugate containing N-(2-hydroxypropyl)methacrylamide (HPMA) (Duncan & Kopeček, 1984). Several other HPMA based copolymer drug conjugates such as HPMA copolymer-DACH palatinate and HPMA copolymer–carboplatin platinate have entered clinical trials to date [Table 2.1] (Duncan, 2003; Duncan, 2006; Duncan & Vicent, 2010).

Polymer drug conjugate	**Name**	**Indication**	**Clinical trials stage**
Polyglutamate–paclitaxel	CT-2103; Xyotax™; Opaxio®	Cancer-NSCLC, ovarian, various other cancers and combinations	Phase II/III
PEG-irinotecan	NKTR-102	Cancer-metastatic breast	Phase II
Polyglutamate–camptothecin	CT-2106	Various cancers	Phase I
HPMA copolymer-DACH platinate	Prolindac®	Cancer-melanoma, ovarian	Phase II
HPMA copolymer–doxorubicin	PK1; FCE28068	Various, particularly lung and breast cancer	Phase II
HPMA-doxorubicin galactosamine	PK2; FCE28069	Liver cell carcinoma	Phase 1, II
PEG-naloxone	NKTR-118	Opioid-induced constipation	Phase II
Polyacetal-camptothecin conjugate	XMT-1001 (Fleximer® technology)	Various cancers	Phase I
HPMA copolymer–carboplatin platinate	AP5280	Various cancers	Phase I/II

Table 2.1: Polymer drug conjugates at various stages of clinical trials (Vicent & Duncan, 2006; Li & Wallace, 2008; Duncan, 2011)

Polymer drug delivery system have been useful in delivery of hydrophobic drugs e.g. paclitaxel (Duncan, 2006; Satchi-Fainaro et al., 2006; Haag & Kratz, 2006). An effective drug delivery system is characterized by high stability in blood plasma (Galanski & Keppler, 2007), low toxicity and immunogenicity (Van Zutphen & Reedijk, 2005; Twaites et al., 2005). Polymer drug conjugates can protect the parent drug from premature degradation, prevent drug from interaction with the biological environment and enhance the absorption of the drug into the cancerous tissue by the EPR effect (Paramjot et al., 2015). For effective cytotoxicity, the drug conjugate should remain in the blood for at least six hours (Wang & Guo, 2013). In contrast, conjugates with the ester linkage between drug and polymer can release incorporated drug by chemical hydrolysis or esterase degradation extracellularly (Sugahara et al., 2007).

Polymer conjugation enhances the biodistribution of low-molecular-weight drugs and enables tumour-specific targeting with substantial reduction in toxicity. At present, over ten polymer-anticancer drug conjugates have progressed to phase I clinical trials including polyglutamate-camptothecin and polyacetal-camptothecin conjugate. Conjugates that have proceeded to phase II/III clinical trials include: polyglutamate-paclitaxel, PEG-irinotecan, HPMA copolymer-DACH palatinate, HPMA copolymer-doxorubicin (PK1), PEG-naloxone and HPMA copolymer-carboplatin palatinate (Li & Wallace, 2008). Doxorubicin is a widely used cytotoxic agent that has been transformed to PK1 (HPMA copolymer doxorubicin) by conjugation to a hydrophilic synthetic polymer, N-(2-hydroxypropyl) methacrylamide (HMPA) to reduce toxicity (Duncan et al., 1981; Duncan et al., 1982; Li & Wallace, 2008). PK1 has significantly improved plasma and tumour pharmacokinetics in comparison to the parent drug doxorubicin (Vasey et al., 1999).

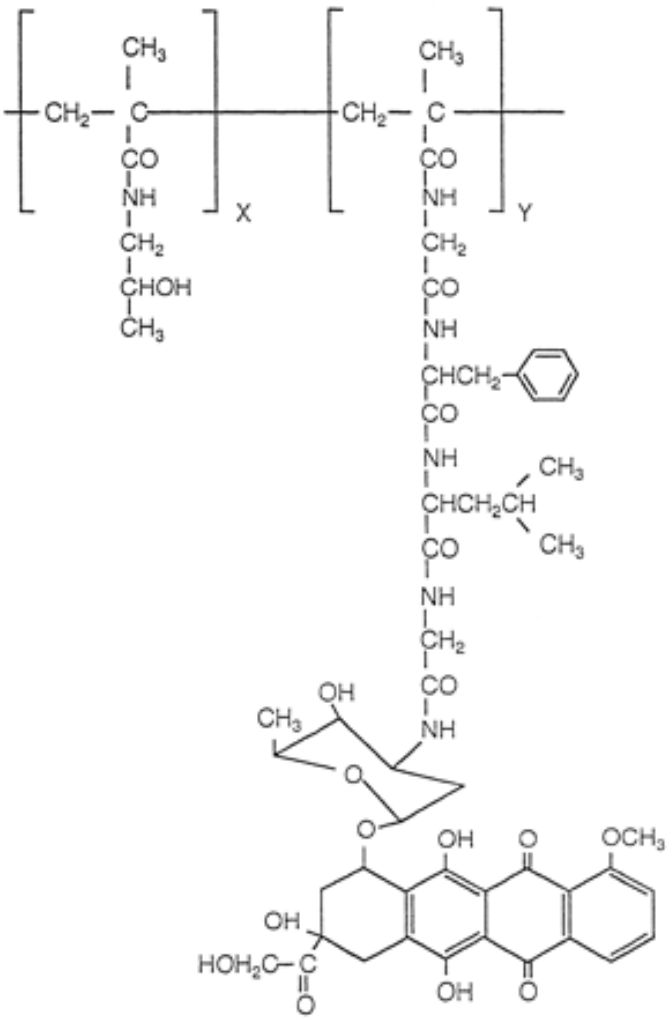

Figure 2.3: Structure of PK1 (HPMA copolymer doxorubicin)

Poly(l-glutamic acid)-paclitaxel (CT-2103) is a polymer drug conjugate of poly(1-glutamic acid) and paclitaxel. It was developed to improve the water solubility and hence the bioavailability of paclitaxel. The conjugate is highly hydrophilic and has showed enhanced antitumor activity compared to unconjugated paclitaxel in clinical studies (Li et al., 1998).

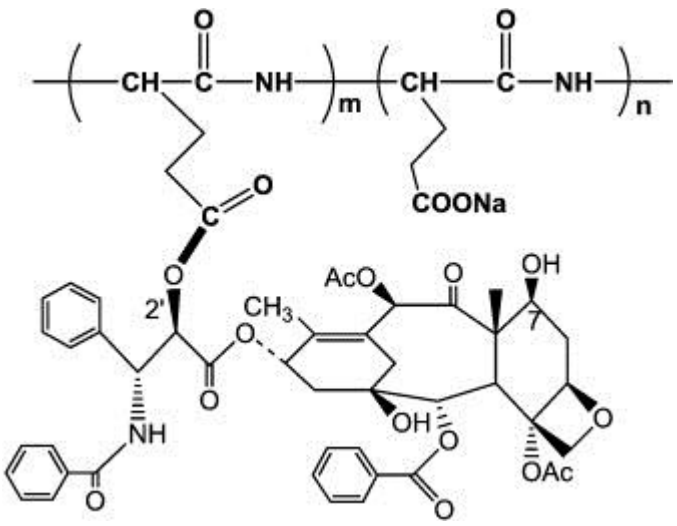

Figure 2.4: Structure of poly(l-glutamic acid)-paclitaxel conjugate (CT-2103)

2.6 The enhanced and permeability retention (EPR) effect

The enhanced and permeability retention effect plays a very important role in the targeting of polymer drug conjugates into the tumour tissue.

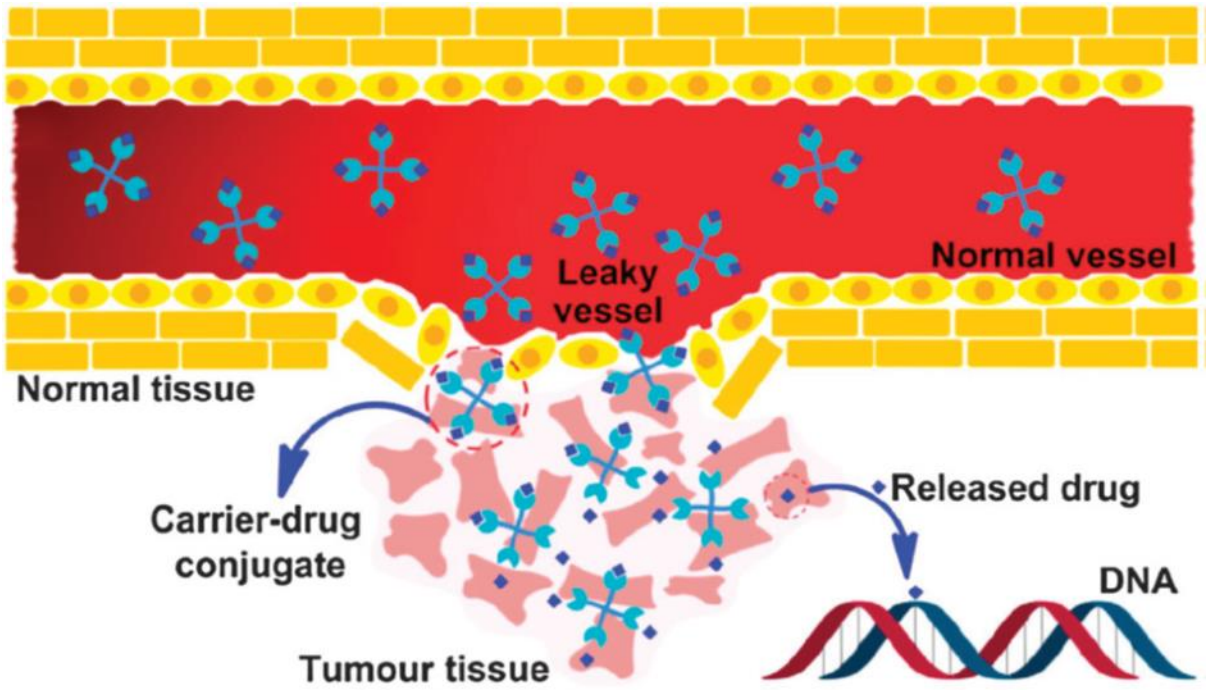

Figure 2.5: Schematic diagram showing absorption of drug conjugate into the tumour tissue by the EPR effect (Wang & Guo, 2013)

Hydrophilic polymers, proteins and other high molecular weight long circulating macromolecules have the capacity to accumulate into pathological sites such as solid tumours and inflammations via the EPR effect which was first identified by the works of Matsumura and Maeda (Matsumura & Maeda, 1986). Higher molecular weight conjugates accumulate in tumour tissue at higher therapeutic efficacy compared to lower molecular weight conjugates (Shiah et al., 2001). The blood vessels in tumours, unlike normal blood vessels, are much leakier due to accelerated growth and hence more permeable to macromolecules (Behlau & Bullinger, 2009). Furthermore, the accumulation of drugs in tumour tissue is facilitated by the lack of an efficient lymphatic system which is responsible for the effective drainage of macromolecules in normal tissue. The continued accumulation of the polymer drug into the tumour tissue by the EPR effect is also subject to its ability to stay in blood plasma for long period of time. Although the EPR effect contribute significantly to the delivery of chemotherapeutic agents to parts of the tumour which are well-vascularized, drugs may not reach regions lacking adequate blood supply, thereby limiting the drug efficacy (Thakor & Gambhir, 2013).

2.7 Cell cycle

The action of chemotherapy drugs operates by interfering with ability of a cancerous cell to grow and thus the importance of studying the cell cycle. Drugs affect cells at certain phases of the cell cycle than at others.

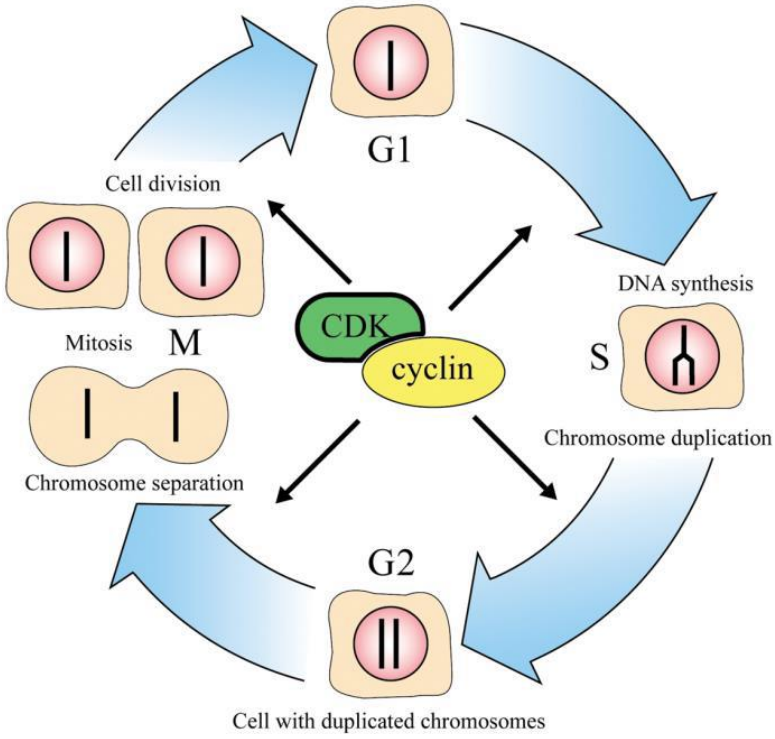

Figure 2.6: Stages of cell development (Nobelprize.org, 2001)

Cells undergo four sequential phases in order to replicate. In the first phase (G1), each cell prepares to replicate itself by synthesis of ribonucleic acid (RNA) and protein. Synthesis of deoxyribonucleic acid (DNA) occurs in the second phase (S) followed by duplication of chromosomes (Nobelprize.org, 2001). The third phase (G2) involves the duplication of RNA and protein. Finally, the cell undergoes mitosis (M) resulting in two identical functional cells (Burri & Lee, 2009). Cancerous cells become target of chemotherapeutic drugs because of their ability to replicate faster compared to normal cells.

2.7.1 pH of normal and cancerous cells

Normal body cells show healthy oxygen tension in aerobic state and respiration across the membrane of the cell. There is free exchange of oxygen and carbon dioxide across the cell membrane and its pH is normally around 7.34 (Altered-states.net, 2015). In contrast, a tumour cell is in anaerobic state. Oxygen cannot diffuse into the cell and glucose undergoes

fermentation to lactic acid resulting in the pH of the cell falling to 6.5 (Mellman, 1996). The lactic acid can attack DNA, destroying template action. RNA is changed and the control mechanism of the cell collapses. In acidic medium, enzymes within the cell become toxic, eventually leading to death of the cell as well as the host. In general, cancerous tissues are mildly acidic whereas healthy tissues are slightly alkaline.

2.8 Platinum Analogues

Platinum based anticancer drugs form a cornerstone of modern chemotherapy regimens for the treatment of a variety of solid tumours. The discovery of cisplatin anticancer properties marked the breakthrough for the successful use of platinum analogues for cancer treatment. Platinum-based chemotherapy agents act during any part of cell cycle and help in treating several types of cancers by impairing DNA synthesis, RNA transcription and function (Mesotheliomaweb.org, 2015). An important aspect of the chemistry of platinum drugs activity in vitro and in vivo is their ability to interact with the solvent environment. For instance, platinum drugs are activated by aquation whereby the leaving groups are replaced by water inside the cellular compartment (Knox et al., 1986; Martin, 1999). The toxicity profile of platinum based drugs is directly connected to the ease with which the leaving groups are aquated. As a result, platinum complexes with highly labile ligands like chloride or nitrate, are very toxic whereas ligands such as bis-carboxylates, which aquates at a slower rate, are significantly less toxic (Wheate et al., 2010).

However, platinum drugs use for chemotherapeutic treatment of cancer is associated with toxic side-effects, intrinsic and acquired resistance arising from various cancerous cells lines (Kartalou & Essigmann, 2001; Wheate et al., 2010). As a result, several thousands of platinum compounds have been developed, tested in vitro and only about 35 compounds in the last 40 years have reached clinical trials in order to evade the disadvantages posed by

cisplatin chemotherapy (Boulikas et al., 2007; Kaluderović & Paschke, 2011). Other platinum based drugs that have gained global approval or in use in at least one country include carboplatin, oxaliplatin, nedaplatin, lobaplatin and heptaplatin (Boulikas et al., 2007; Wang & Guo, 2013).

Platinum analogue	Cancer treatment	Year of approval	Status
Cisplatin	Various including testicular, ovarian, bladder, cervical, breast, head and neck and non-small cell lung cancers	1978	Worldwide approval
Carboplatin	Ovarian cancer, non-small cell lung cancers, small cell lung cancers, melanoma, head and neck cancer, thymic cancer, breast cancer	1989	Worldwide approval
Oxaliplatin	colorectal cancer	2002	Worldwide approval
Nedaplatin	non-small cell lung cancers, small cell lung cancers, esophageal cancer, head and neck tumors, bladder cancer	1996	Approved in Japan
Lobaplatin	Breast cancer, small cell lung cancers, chronic myeloid leukemia	2004	Approved in China
Heptaplatin	Gastric cancer	2005	Approved in Korea

Table 2.2: Summary of some platinum analogues approved for treatment of cancer (Kelland, 2007; Wheate et al., 2010; Kang et al., 2015)

2.8.1 Cisplatin

Cisplatin (figure 2.7) was first prepared by Peyrone in 1844 and the compound became known as Peyrone's chloride (Reedijk & Lohman, 1985). But it was until the 1960s when Rosenberg fortuitously discovered the therapeutic potential of cisplatin, cis-diamminodichloridoplatinum(II), while working on the effects of electric field on cell division of Escherichia coli bacteria (Rosenberg et al., 1965). Thereafter, Rosenberg and coworkers successfully carried out experiments with sarcoma 180 and leukemia L1210 bearing mice (Rosenberg & VanCamp, 1970; Kociba et al., 1970). This led to cisplatin progressing to phase I clinical trials in 1971 and its subsequent approval in 1978 for the treatment of testicular and ovarian cancer (Wong & Giandomenico, 1999; Farrell, 2005; Fricker, 2007). To date, cisplatin is used for the treatment of a wide spectrum of cancers including lung, head and neck, ovarian, bladder and testicular cancers (Reedijk & Lohman, 1985; Reedijk, 1996; Boulikas & Vougiouka, 2003).

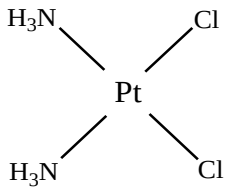

Figure 2.7: Chemical structure of cisplatin

Despite its success, clinical use of cisplatin is associated with several disadvantages that include severe toxicity such as nephrotoxicity, neurotoxicity, ototoxicity and emetogensis (Schaefer et al., 1985; Goren et al., 1986; Alberts & Noel, 1995). In addition, cisplatin administration is associated with poor oral bioavailability and hence it is administered intravenously with extensive hydration to lower the risk of renal toxicity (Wang & Lippard, 2005). While some side effects can be contained by combining with other drugs, neurotoxicity remains a major dose-limiting toxic effect. Other ways to reduce cisplatin

toxicities have included liposomal encapsulation and use of other approved platinum drugs to achieve anticancer activity close to that of cisplatin but with reduced nephrotoxicity (Muggia et al., 2015).

Cisplatin resistance is either inherent within or acquired by cancerous cells (Siddik, 2003). The major mechanisms of resistance to cisplatin chemotherapy have been identified to result from several factors including reduction in cisplatin uptake into cells, modulation of apoptotic pathways and increased DNA repair (Boulikas & Vougiouka, 2003; Siddik, 2003; Rabik & Dolan, 2007; Kelland, 2007). Consequently, derivatives of cisplatin have been developed over the years in order to reduce the toxicity of the parent compound and also to reduce other problems of the parent compound such as drug resistance.

2.8.2 Carboplatin

Carboplatin, cis-diammine-1,10-cyclobutanedicarboxylatoplatinum(II), $[Pt(C_6H_6O_4)(NH_3)_2]$, (figure 2.8) is a second generation anticancer agent that was introduced in the early 1980s as a result of intensive work towards the improvement of cisplatin which was discovered earlier. Major endeavours have been devoted to determine the anticancer activity of carboplatin in order to come up with novel platinum based drugs with better pharmacological profiles.

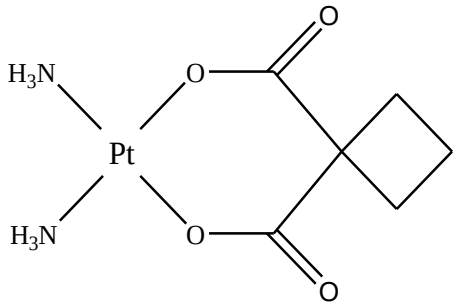

Figure 2.8: Chemical structure of carboplatin

Carboplatin and cisplatin have similar clinical activity and both drugs are prone to resistance. However, carboplatin is relatively better tolerated clinically, causing less side effects such as

nausea, neurotoxicity, ototoxicity, and nephrotoxicity than cisplatin (dos Santos Guimarães et al., 2013). The reduced toxicity of carboplatin compared to cisplatin can be attributed to the presence of less labile leaving groups on carboplatin. Carboplatin resistance can be caused by the reduction in platinum uptake, increased efflux, increased DNA repair, decreased mismatch repair, modulation of signalling pathways or presence of quiescent non-cycling cells (Stewart, 2007). In clinical practice, carboplatin has replaced cisplatin in a number of indications treatment modalities though carboplatin chemotherapy remains more expensive than cisplatin (Desoize & Madoulet, 2002).

2.8.3 Oxaliplatin

Although carboplatin has become the dominant second-generation platinum drug, oxaliplatin is the most commonly used third generation platinum drug. Oxaliplatin, (trans-R,R-1,2-diaminocyclohexane) oxalate platinum(II), (Figure 2.9) is a platinum based anticancer drug with a 1,2-diaminocylohexane ligand (DACH) entity. It is one of the few platinum based drugs to achieve global approval for various cancer treatment. Oxaliplatin and other related 1,2 diaminocyclohexane drugs were originally prepared by Kidani and co-workers (Kidani et al., 1978). Oxaliplatin is the more hydrophilic derivative of tetraplatin which failed clinical trials (Kelland, 2007).

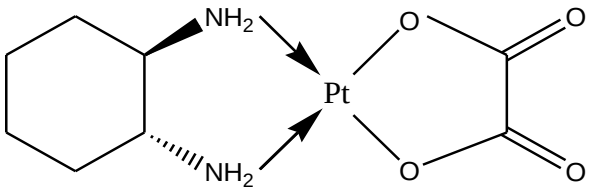

Figure 2.9: Chemical structure of oxaliplatin

Oxaliplatin was selected for further development because it displayed higher efficacy and lower toxicity compared to cisplatin in in vivo preclinical studies and most importantly, it

exhibit anticancer activity against some tumours resistant to cisplatin (Desoize & Madoulet, 2002; Muggia et al., 2015). Oxaliplatin exhibits a variety of antineoplastic activity such as against colorectal and gastric cancers which differs from other platinum based chemotherapy agents (Brunton et al., 2011). A number of phase II and III trials in solid tumours administering oxaliplatin in combination with other anticancer drugs against several tumours have suggested increased activity as compared to unconjugated oxaliplatin. Furthermore, in comparison to cisplatin, oxaliplatin lack nephrotoxic effects, which is attributed to the absence of platinum accumulation in blood plasma (Pasetto et al., 2006).

Oxaliplatin undergo different mechanism of action to that of classical cisplatin or carboplatin (Boulikas et al., 2007). In spite of the fact that the actual cellular and molecular aspects of mechanism of oxaliplatin have not been fully understood, it appears that the intrinsic chemical and steric features of the non-hydrolysable diaminocyclohexane platinum adducts on DNA contribute to the lack of cross-resistance with both cisplatin and carboplatin drugs (Francesco et al., 2002). The anticancer effects of oxaliplatin are enhanced when it is taken in combination with established anticancer drugs such as gemcitabine, cisplatin, carboplatin and taxanes (Ranson & Thatcher, 1999; Raymond et al., 2002).

2.9 Ferrocenyl Drug System

Despite the dominance of platinum-based anticancer drugs such as cisplatin and carboplatin, ferrocene based compounds have exhibited significant anticancer properties to be utilised for the chemotherapeutic treatment of cancer. Several metal compounds have been studied as anticancer agents preclinically in vivo and in vitro. Ferrocene was the first metallocene to be discovered, and its structure was deduced by Geoffrey Wilkinson in the early 1950s (Wilkinson et al., 1952). Ever since, the study of ferrocene and its derivatives have increased rapidly due to several factors including their highly promising antiproliferative activity

against various murine and human cancer lines, favourable electrochemical properties and their unusual stability in aqueous and aerobic media (van Staveren & Metzler-Nolte, 2004).

Several scientific researchers have indicated that some ferrocene derivatives are highly active in vitro and in vivo, against infections from bacteria and fungus and cancer. Ferrocene-based compounds that have exhibited anticancer activity include ferricenium salts, ferrocene conjugated to biologically active molecules and ferrocenyl compounds coordinated to other metals (Ornelas, 2011). The salts of ferrocenium picrate and ferrocenium trichloroacetate were the first iron based complexes for which antitumour activity was observed in pioneering research by Köpf-Maier and co-workers (Köpf-Maier et al., 1984). Unsubstituted ferrocene on the other hand is not active as it is not soluble in water. In this current study, an attempt has been made to introduce substituents to ferrocene and assess anticancer activity.

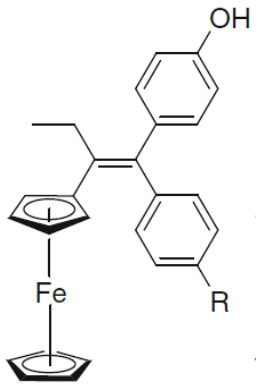

Figure 2.10: Structure of a ferrocene based organometallic compound, ferrocifen (Pizarro et al., 2010)

Jaouen et.al explored the potential of ferrocene based organometallic, ferrocifen on treatment of breast cancer and other cancers. They reported that it is the presence of an organometallic component (ferrocene) and a pharmacophore fragment (hydroxytamoxifen), that contributes to the cytotoxicity and anti-oestrogenicity properties of the compounds generated (Nguyen et al., 2007).

CHAPTER 3

Methodology

3.1 Introduction

This chapter describes the materials, reagents and procedures carried out in the preparation of analogues, carriers and drug conjugates. Characterization techniques employed in this study are also discussed.

3.2 Materials and reagents

All preparative work for experiments in this study were carried out using distilled water. Ferrocene (98% Merck) and potassium tetrachloride (98% Aldrich) were used for the reactions to form of platinum and ferrocene analogues. Solvents such as tetrahydrofuran (99.5% Merck) and dichloromethane (99% Merck) were dried over molecular sieves 4 Å (Sigma-Aldrich) for 24 hours before use for preparation of analogues. Methylenebisacrylamide (Sigma-Aldrich) was used for synthetic reactions for carriers and conjugates. Amines such as 3-dimethylamino-1-propylamine (98% Sigma-Aldrich), 1,3-propanediamine (Sigma-Aldrich), 4-(3-aminopropyl)morphine (Aldrich), 3-diethylaminopropylamine (Sigma-Aldrich), dopamine (98.5% Sigma-Aldrich), 2-(2-aminoethoxy) ethanol (Acros Organics), ethylenediamine (Sigma-Aldrich) and 2,2-(ethlenedioxy) diethylamine (Sigma-Aldrich) were used in various stages of the preparation of carriers and conjugates. Triethylamine (Sigma-Aldrich) was used in the reactions forming carriers and drug conjugates. 1,3-propanediamine (Sigma-Aldrich), 3-dimethylamino-1-propylamine (98% Sigma-Aldrich) and 3-diethylaminopropylamine (Sigma-Aldrich) were employed as linkers for the drug conjugates. Dialysis of polymer carriers and drug conjugates was done using cellulose dialysing membranes with molecular cut-off limits of 6000 and 12000 respectively which were purchased from Sigma-Aldrich.

3.3 Preparation of platinum and ferrocene analogues

3.3.1 Synthesis of cyclohexane-1,2-diamine dichloroplatinum(II) (DACH $PtCl_2$)

Potassium tetrachloroplatinate (1000 mg, 2.41 mmol) was dissolved in 13 mL distilled water followed by dropwise addition of DACH (275 mg, 2.41 mmol) with stirring. The resultant mixture was stirred at RT overnight and placed at -30°C for 24 hours. The precipitate formed was filtered off and washed with cold water and cold methanol. The precipitated was dried in an oven at 40°C for 6 hours.

3.3.2 Synthesis of 4-Ferrocenylketobutanoic acid (Fc)

$AlCl_3$ (1440 mg, 10.8 mmol) was added to a stirred solution of ferrocene (2000 mg, 10.75 mmol) dissolved in dichloromethane (10 mL). Succinic anhydride (540 mg, 5.4 mmol) was added in small portions followed by refluxing for 2 hours. The resulting mixture was poured on ice water and extraction was performed using dichloromethane. The ketoacid was extracted from the organic layer using sodium carbonate solution (10%) and precipitated with concentrated hydrochloric acid. The yellow-tan precipitate formed was filtered off, washed with ice-water and dried in an oven at 50-60ºC (Mukaya et al., 2015).

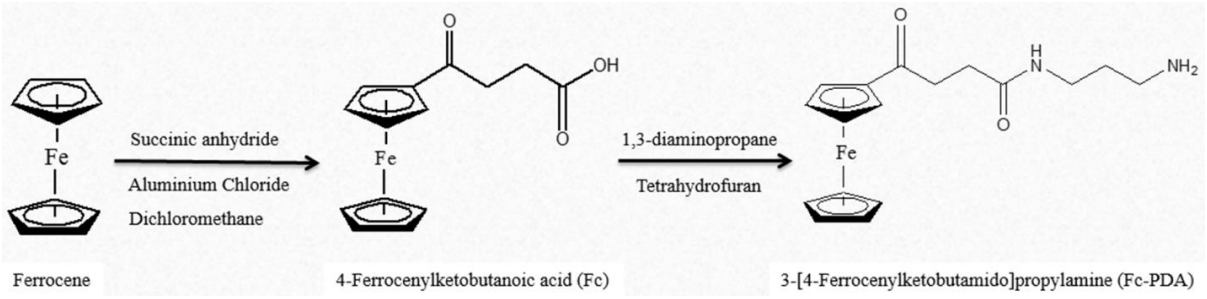

Scheme 3.1: Reaction scheme for the synthesis of 4-Ferrocenylketobutanoic acid (Fc) and 3-[4-Ferrocenylketobutamido]propylamine (Fc-PDA)

3.3.3 Synthesis of 3-[4-ferrocenylketobutamido]propylamine (Fc-PDA)

To a stirred solution of Fc (1500 mg, 5.2 mmol) dissolved in tetrahydrofuran (11 mL) was added N-hydroxysuccinimide (600 mg, 5.2 mmol) in small portions at RT followed by stirring in an ice-bath for 15 min. Thereafter DCC (1080 mg, 5.2 mmol) in THF (3 mL) was added dropwise and stirred for a further 4 hours in the ice-water bath, then at room temperature for 48 hours. The solid was filtered off and washed with THF. Thereafter, the filtrate and washings were combined and added dropwise to stirred solution of PDA (580 mg, 7.9 mmol) in THF (14 mL). Stirring was carried for another 24 hours in an ice-water bath and then 6 hours at room temperature. The solid formed was filtered off and washed with THF. The filtrate and washes were combined and spun to an oily viscous liquid on a rotary evaporator (65°C bath temperature) (Mukaya et al., 2015).

3.4 Reaction procedures for the preparation of carriers

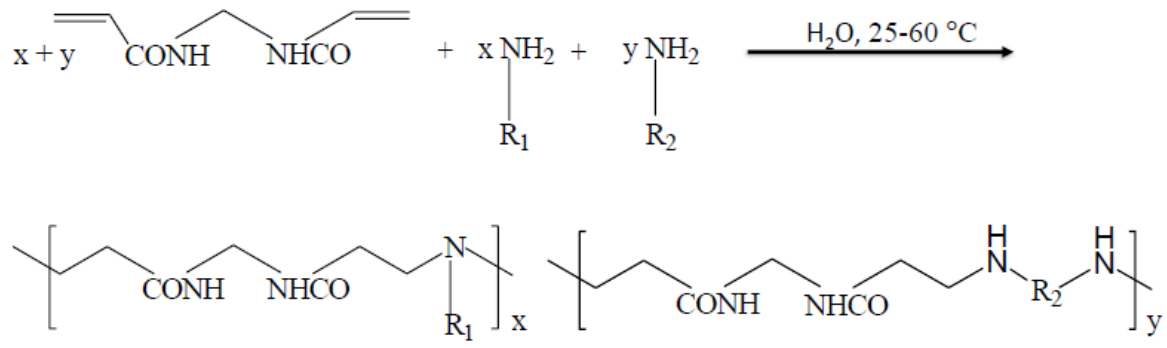

Scheme 3.2: General reaction equation for the formation of polyamidoamine drug carriers (Mufula & Neuse, 2011)

Carrier 1 (PC1): MBA (500 mg, 3.24 mmol) was dissolved in 20 mL of hot distilled water. Upon cooling, DEP (337 mg, 2.59 mmol) and TEA (1 mL) were added and stirred for 2 hours, followed by cooling the reaction in an ice bath and dropwise addition of PDA (71.9 mg, 0.97 mmol). The resultant solution was flushed with argon gas and stirred at RT for an

additional 2 days. The solution was adjusted to pH 7 by using concentrated HCl. Exhaustive dialysis was performed against water, using cellulose membrane with molecular weight cut-off 6000 for 1 day. Freeze-drying of the resulting solution produced a water soluble solid.

Carrier 2 (PC2): By the same procedure as for carrier 1 above, MBA (500 mg, 3.24 mmol) in 20 mL water was reacted with APM (374 mg, 2.59 mmol) and TEA (1 mL). The mixture was stirred for 2 hours, followed by cooling the reaction in an ice bath and dropwise addition of DET (100 mg, 0.97 mmol). The resultant solution was worked up as before, dialysed and freeze dried to produce a water soluble solid.

Carrier 3 (PC3): Following the same procedure for synthesis of carrier 1 above, MBA (500 mg, 3.24 mmol) in 20 mL water was reacted with AEE (272 mg, 2.59 mmol) and TEA (1 mL). The mixture was stirred for 2 hours, followed by cooling the reaction in an ice bath and dropwise addition of EDDA (144 mg, 0.97 mmol). The resultant solution was worked up as before, dialysed and freeze dried to produce a water soluble solid.

Carrier 4 (PC4): By the same procedure for carrier 1 above, MBA (500 mg, 3.24 mmol) in 20 mL water was reacted with AEE (272 mg, 2.59 mmol) and TEA (1 mL). The mixture was stirred for 2 hours, followed by cooling the reaction in an ice bath and dropwise addition of EDA (58.3 mg, 0.97 mmol). The resultant solution was worked up as before, dialysed and freeze dried to produce a water soluble solid.

	Amount of reactant (mg)												
	MBA	DEP	PDA	APM	APD	DET	DMP	EDA	AEE	EA	DPM	EDDA	Yield (mg)
PC1	500	337	72	-	-	-	-	-	-	-	-	-	683
PC2	500	-	-	374	-	100	-	-	-	-	-	-	559
PC3	500	-	-	-	-	-	-	-	272	-	-	144	370
PC4	500	-	-	-	-	-	-	58	272	-	-	-	308
PC5	500	-	-	-	88	100	198	-	-	-	-	-	496
PC6	500	-	-	-	-	100	198	-	-	-	184	-	703
PC7	500	253	-	-	88	100	-	-	-	-	-	-	480
PC8	500	253	-	-	88	100	-	-	-	-	-	-	837
PC9	500	-	-	-	-	100	198	-	-	59	-	-	451
PC10	500	-	48	-	-	-	264	-	-	-	-	-	653

Table 3.1: Summary of the yield and quantity of reactants used in the formation of polyamidoamine carriers

Carrier 5 (PC5): By the same procedure for carrier 1 above, MBA (500 mg, 3.24 mmol) in 20 mL water was reacted with DMP (198 mg, 1.94 mmol) and TEA (1 mL). The mixture was stirred for 2 hours, followed by cooling the reaction in an ice bath and dropwise addition of APD (88.4 mg, 0.97 mmol). The solution obtained was stirred at RT for an additional 24 hours and then cooled on an ice bath before DET (100 mg, 0.97 mmol) was added dropwise. The resultant solution was worked up as before, dialysed and freeze dried to produce a water soluble solid.

Carrier 6 (PC6): By the same procedure as for carrier 1 above, MBA (500 mg, 3.24 mmol) in 20 mL water was reacted with DMP (198 mg, 1.94 mmol) and TEA (1 mL). The mixture was stirred for 2 hours, followed by cooling the reaction in an ice bath and addition of dopamine (184 mg, 0.97 mmol). The solution obtained was stirred at RT for an additional 24 hours and then cooled on an ice bath before DET (100 mg, 0.97 mmol) was added dropwise. The resulting solution was worked up as before, dialysed and freeze dried to produce a water soluble solid.

Carrier 7 (PC7): By the same procedure as for carrier 1 above, MBA (500 mg, 3.24 mmol) in 20 mL water was reacted with DEP (253 mg, 1.94 mmol) and TEA (1 mL). The mixture was stirred for 2 hours, followed by cooling the reaction in an ice bath and addition of APD (88.4 mg, 0.97 mmol). The solution obtained was stirred at RT for an additional 24 hours and then cooled on an ice bath before DET (100 mg, 0.97 mmol) was added dropwise. The resultant solution was worked up as before, dialysed and freeze dried to produce a water soluble solid.

Carrier 8 (PC8): By the same procedure as for carrier 1 above, MBA (500 mg, 3.24 mmol) in 20 mL water was reacted with DEP (253 mg, 1.94 mmol) and TEA (1 mL). The mixture was stirred for 2 hours, followed by cooling the reaction in an ice bath and addition of

dopamine (184 mg, 0.97 mmol). The solution obtained was stirred at RT for an additional 24 hours and then cooled on an ice bath before DET (100 mg, 0.97 mmol) was added dropwise. The resultant solution was worked up as before, dialysed and freeze dried to produce a water soluble solid.

Carrier 9 (PC9): By the same procedure as for carrier 1 above, MBA (500 mg, 3.24 mmol) in 20 mL water was reacted with DMP (198 mg, 1.94 mmol) and TEA (1 mL). The mixture was stirred for 2 hours, followed by cooling the reaction in an ice bath and addition of EA (59 mg, 0.97 mmol). The solution obtained was stirred at RT for an additional 24 hours and then cooled on an ice bath before dropwise addition of DET (100 mg, 0.97 mmol). The resultant solution was worked up as before, dialysed and freeze dried to produce a water soluble solid.

Carrier 10 (PC10): Following the same procedure for carrier 1 above, MBA (500 mg, 3.24 mmol) in 20 mL water was reacted with DMP (264 mg, 2.59 mmol) and TEA (1 mL). The mixture was stirred for 6 hours, followed by cooling the reaction in an ice bath and dropwise addition of PDA (48 mg, 0.65 mmol). The resultant solution was worked up as before, dialysed and freeze dried to produce a water soluble solid.

The structures of polyamidoamines carriers prepared in this study are shown below:

Carrier 1:

X:Y = 8:2

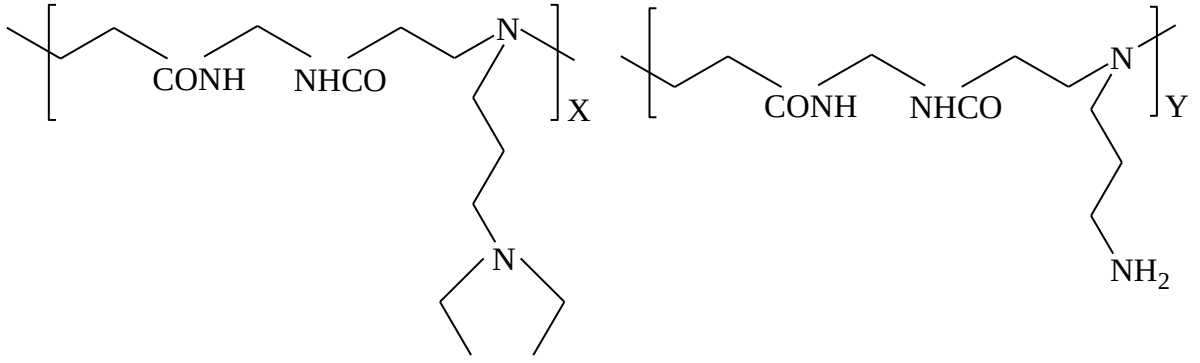

Carrier 2:

X:Y = 8:2

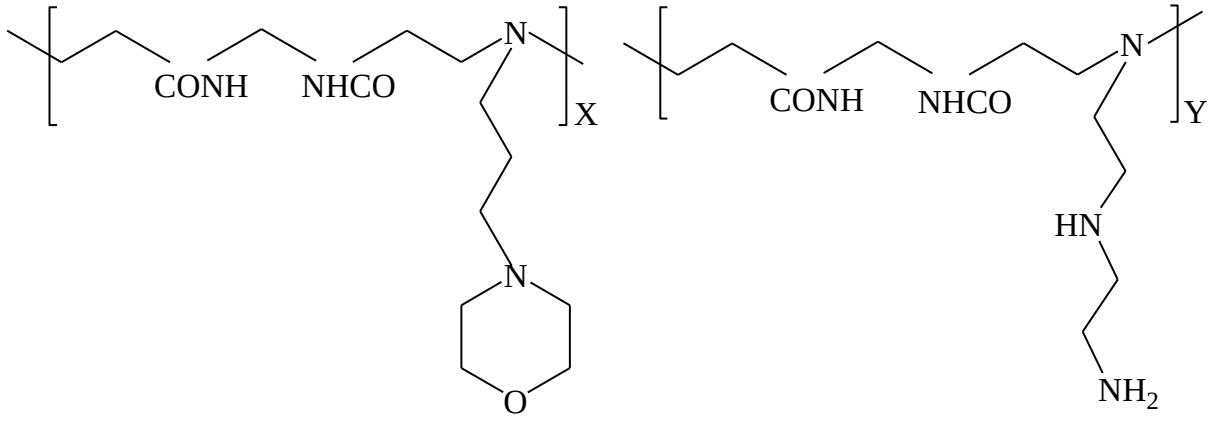

Carrier 3:

X:Y = 8:2

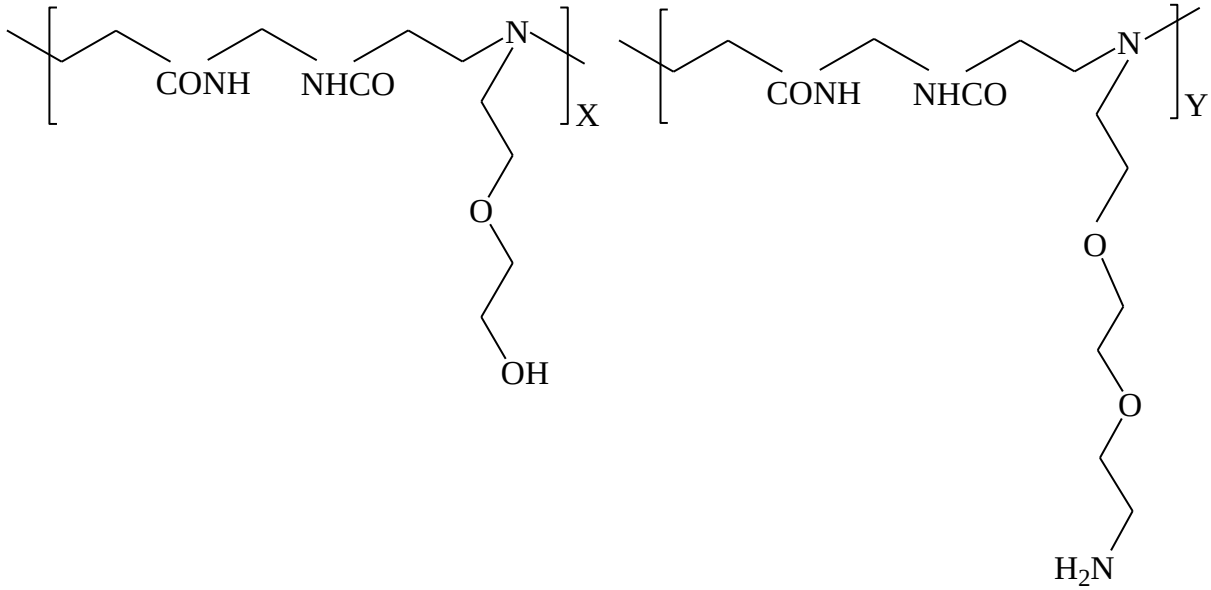

Carrier 4:

X:Y = 8:2

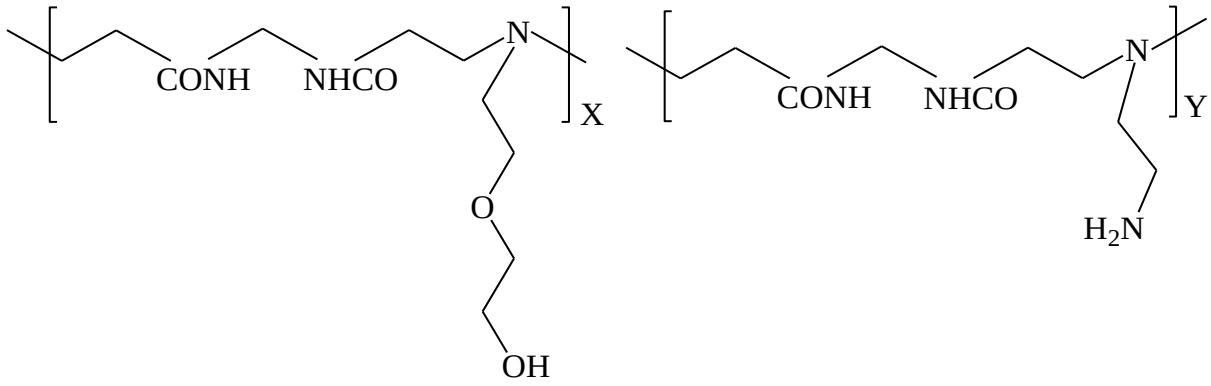

Carrier 5:

X:Y:Z = 6:3:1

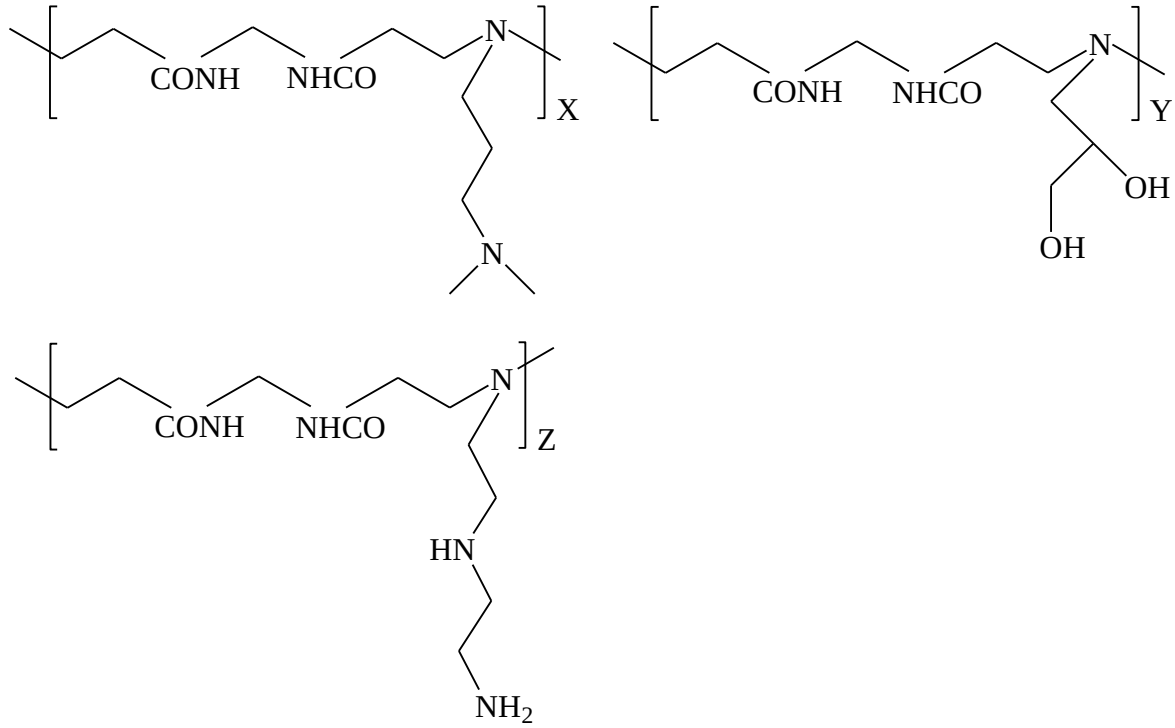

Carrier 6:

X:Y:Z = 6:3:1

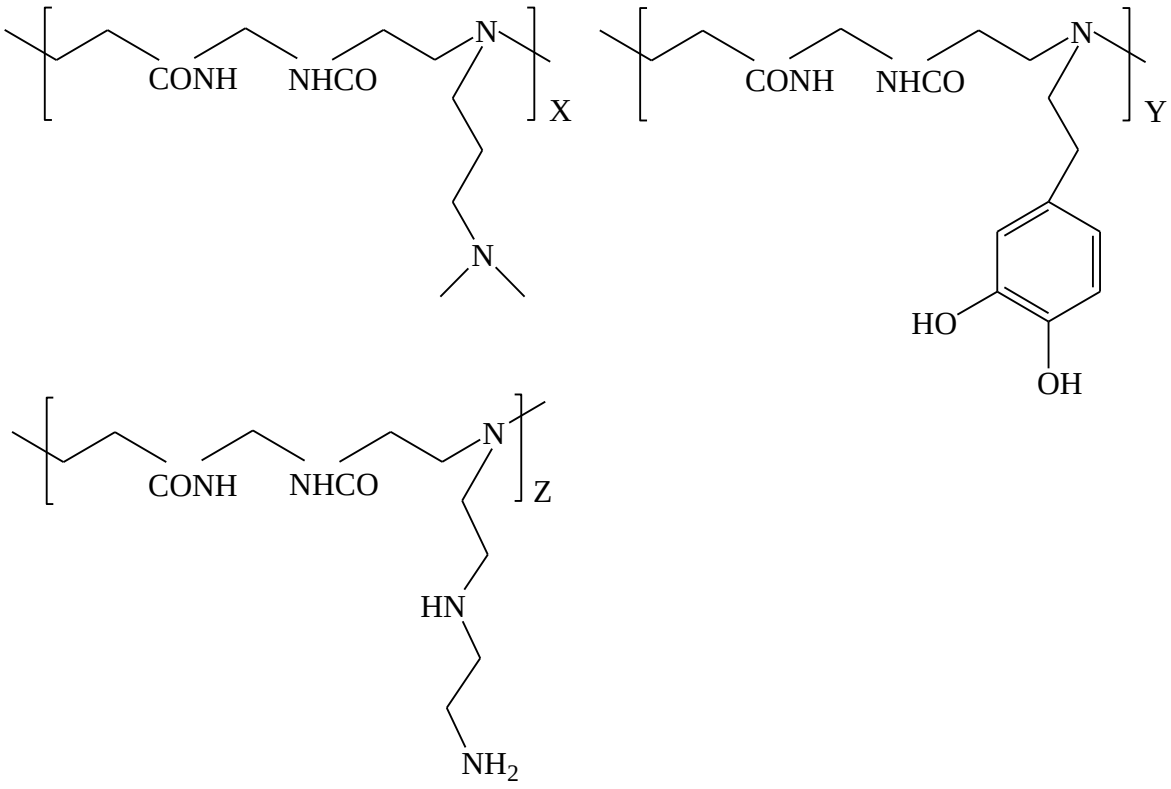

Carrier 7:

X:Y:Z = 6:3:1

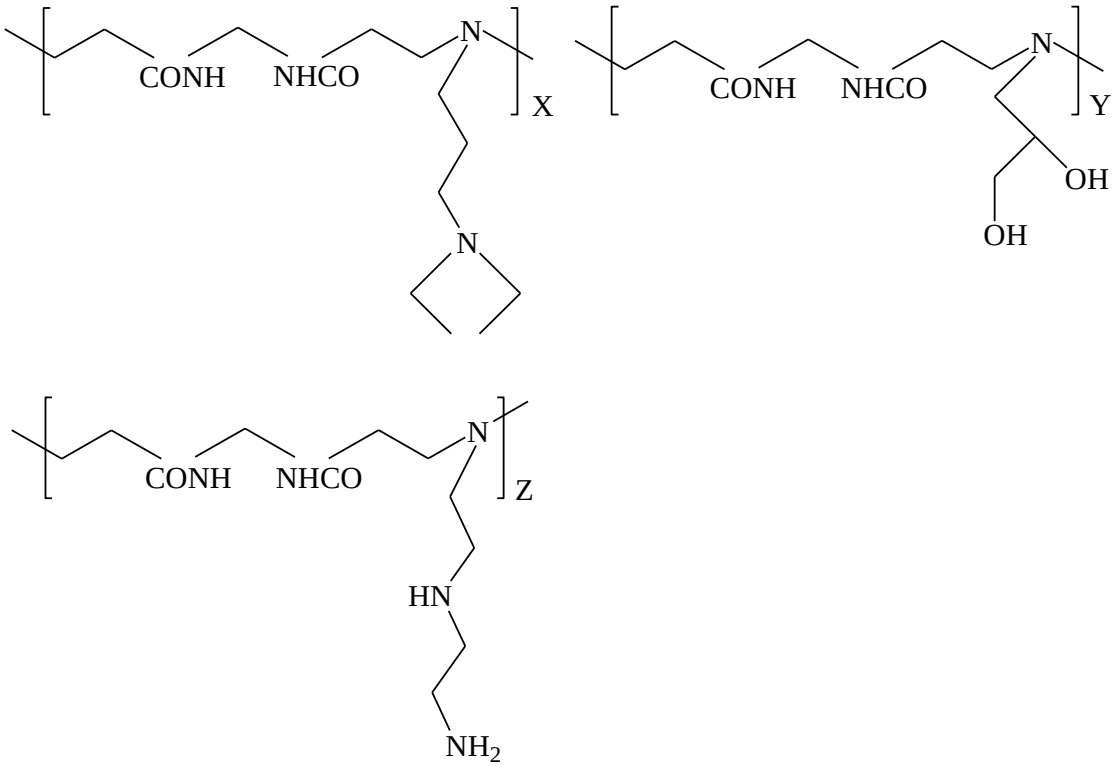

Carrier 8:

X:Y:Z = 6:3:1

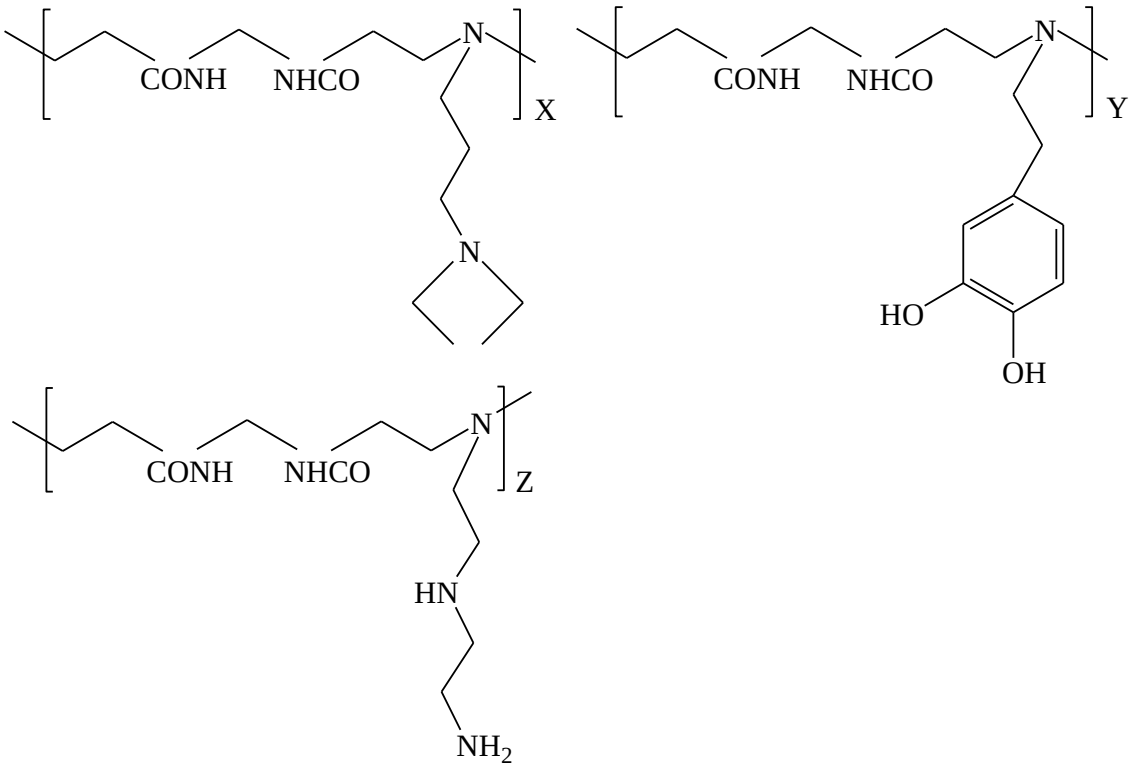

Carrier 9:

X:Y:Z = 6:3:1

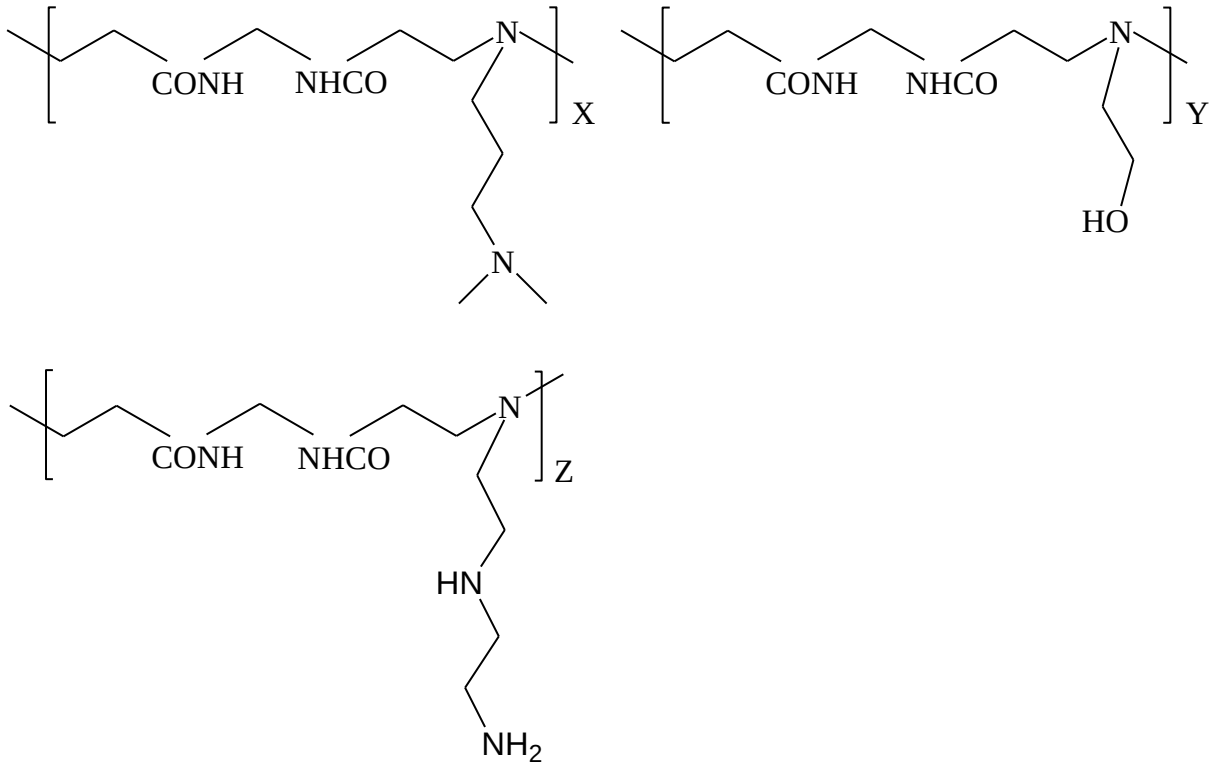

Carrier 10:

X:Y = 8:2

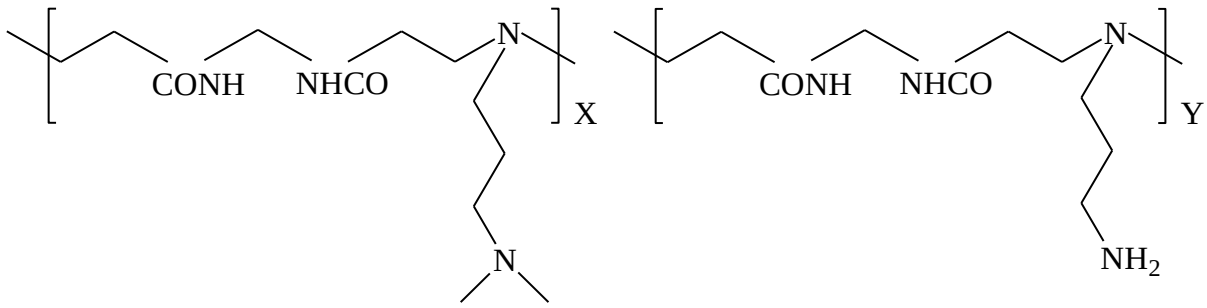

3.5 Synthesis of polyamidoamine drug conjugates

Conjugate 1 (PD1): MBA (500 mg, 3.24 mmol) was dissolved in 10 mL of hot distilled water. Upon cooling, DEP (358 mg, 2.75 mmol) was added and stirred for 6 hours at RT, followed by dropwise addition of DET (51 mg, 0.49 mmol) in an ice bath. The resultant solution was flushed with argon gas and stirred at RT for an additional 3 days. DACH $PtCl_2$ (186 mg, 0.49 mmol) was added to the solution of the carrier protected from light and pH was

adjusted to 5.5. The solution was stirred for a further 3 days with light protection after saturation with inert gas. The resulting solution was stirred at 65°C for 24 hours. The mixture was filtered and exhaustive dialysis was performed for 1 day followed by freeze-drying.

Conjugate 2 (PD2): Following the same procedure for conjugate 1 above, MBA (500 mg, 3.24 mmol) in 10 mL water was reacted with DMP (281 mg, 2.75 mmol). The mixture was stirred for 6 hours, followed by cooling the reaction in an ice bath and addition of PDA (36 mg, 0.49 mmol). The resultant solution was flushed with argon gas and stirred at RT for an additional 3 days. DACH $PtCl_2$ (186 mg, 0.49 mmol) was added to the solution of the carrier protected from light and pH was adjusted to 5.5. The resultant solution was worked up as before, dialysed and freeze dried to produce a water soluble solid.

Amount of reactant (mg)									
	MBA	DEP	PDA	DET	DMP	DACH $PtCl_2$	K_2PtCl_4	Fc-PDA	Yield (mg)
PD1	500	358	-	51	-	186	-	-	390
PD2	500	-	36	-	281	186	-	-	285
PD3	500	358	-	51	-	-	203	-	491
PD4	500	-	36	-	281	-	203	-	464
PD5	500	337	-	-	-	-	-	222	145
PD6	1000	676	48	-	-	-	135	222	133
PD7	-	-	-	-	-	123	-	-	112

Table 3.2: Summary of yield and quantity of reactants used in the formation of polyamidoamine drug conjugates

Conjugate 3 (PD3): MBA (500 mg, 3.24 mmol) was dissolved in 10 mL of hot distilled water. Upon cooling, DEP (358 mg, 2.75 mmol) was added and stirred for 6 hours, followed by dropwise addition of DET (51 mg, 0.49 mmol) in an ice bath. The resultant solution was flushed with argon gas and stirred at RT for an additional 3 days. K_2PtCl_4 (203 mg, 0.49 mmol) was added to the solution of the carrier and stirring was continued for a further 24 hours with light protection after saturation with inert gas. The resulting solution was stirred at 45°C for 40 hours and pH was strictly maintained at 5-6 for the last 0.5 hours. The mixture was filtered and dialysis was performed for 1 day followed by freeze-drying.

Conjugate 4 (PD4): Following the same procedure for conjugate 3 above, MBA (500 mg, 3.24 mmol) in 10 mL water was reacted with DMP (281 mg, 2.75 mmol). The mixture was stirred for 6 hours, followed by cooling the reaction in an ice bath and addition of PDA (36 mg, 0.49 mmol). The resultant solution was flushed with argon gas and stirred at RT for an additional 3 days. K_2PtCl_4 (203 mg, 0.49 mmol) was added to the solution of the carrier and stirring was continued for a further 24 hours with light protection after saturation with inert gas. The resultant solution was worked up as before, dialysed and freeze dried to produce a water soluble solid.

Conjugate 5 (PD5): MBA (500 mg, 3.24 mmol) was dissolved in 10 mL of hot distilled water. Upon cooling, DEP (337 mg, 2.59 mmol) and TEA (1 mL) were added and stirred for 6 hours. The resultant solution was protected from light followed by addition of Fc-PDA (222 mg, 0.65 mmol) dissolved in 2 mL methanol. The solution was flushed with argon gas and stirred at RT for an additional 3 days. The resulting mixture was concentrated on roti evaporator (water bath temperature 60°C) to remove the volatiles and then filtered. Dialysis was performed against water for 1 day followed by freeze drying.

Conjugate 6 (PD6): MBA (1000 mg, 6.49 mmol) was dissolved in 20 mL of hot distilled water. Upon cooling, DEP (676 mg, 5.19 mmol) and TEA (1 mL) were added and stirred for 6 hours at RT. The resultant solution was protected from light followed by addition of Fc-PDA (222 mg, 0.649 mmol) dissolved in 2 mL methanol. The solution was flushed with argon gas and stirred at room temperature for an additional 3 days. PDA (48 mg, 0.649 mmol) was then added to the resulting solution followed by stirring for further 24 hours. The solution was concentrated on roti evaporator (water bath temperature 60°C) to remove the volatiles and then filtered. Dialysis was performed against water for 1 day followed by freeze drying.

The resultant solid was divided into two portions for preparation of co-conjugates with platinum based drugs. 234 mg of the first portion was dissolved in 7 mL distilled water and protected from light with aluminium foil. K_2PtCl_4 (135 mg, 0.649 mmol) was added to the solution and stirring was continued for a further 24 hours with light protection after saturation with inert gas. The resulting solution was stirred at 45°C for 40 hours and pH was strictly maintained at 5-6 for the last 0.5 hours. The mixture was filtered and dialysis was performed for 1 day followed by freeze-drying.

Conjugate 7 (PD7): 231 mg of the second portion of the conjugate prepared in the procedure above was dissolved in 7 mL distilled water and protected from light using aluminium foil. DACH $PtCl_2$ (123 mg, 0.649 mmol) was added to the solution protected from light and pH was adjusted to 5.5. The solution was stirred for a further 3 days with light protection after saturation with inert gas. The resulting solution was stirred at 65°C for 24 hours. The mixture was filtered and dialysis was performed for 1 day followed by freeze-drying.

The structures of polyamidoamine drug conjugates prepared in this study are shown below:

Conjugate 1:

X:Y = 8.5:1.5

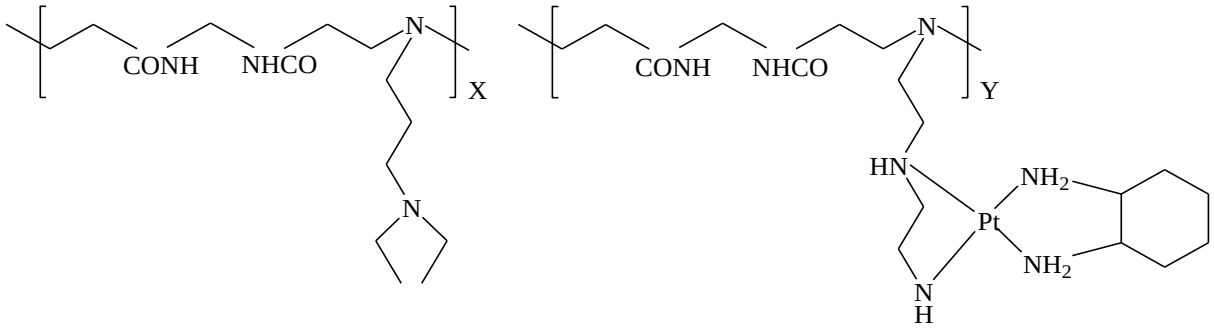

Conjugate 2:

X:Y = 8.5:1.5

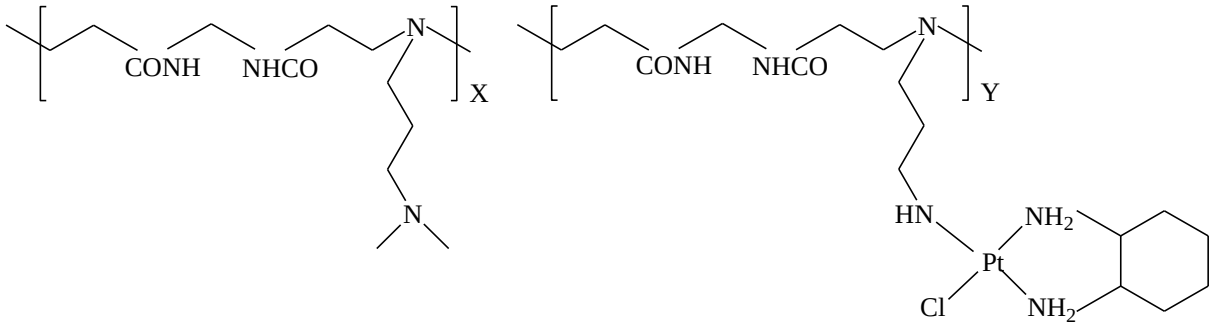

Conjugate 3:

X:Y = 8.5:1.5

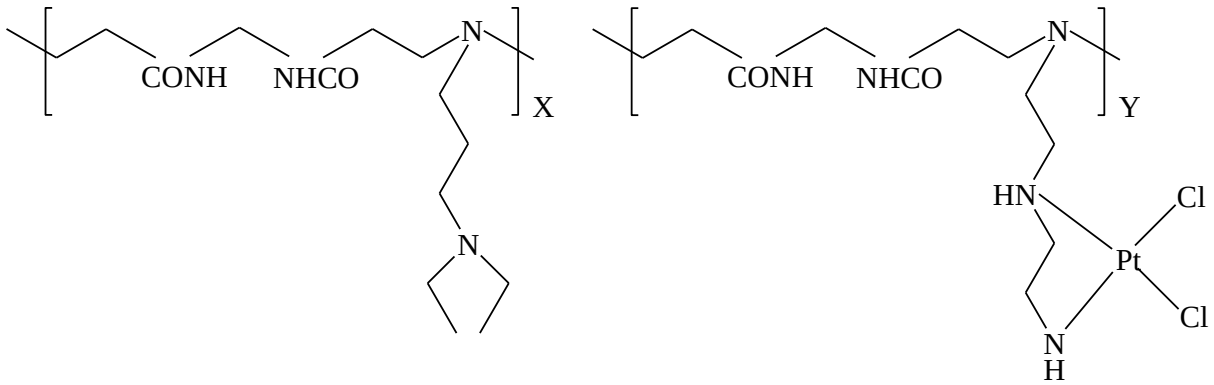

Conjugate 4:

X:Y = 8.5:1.5

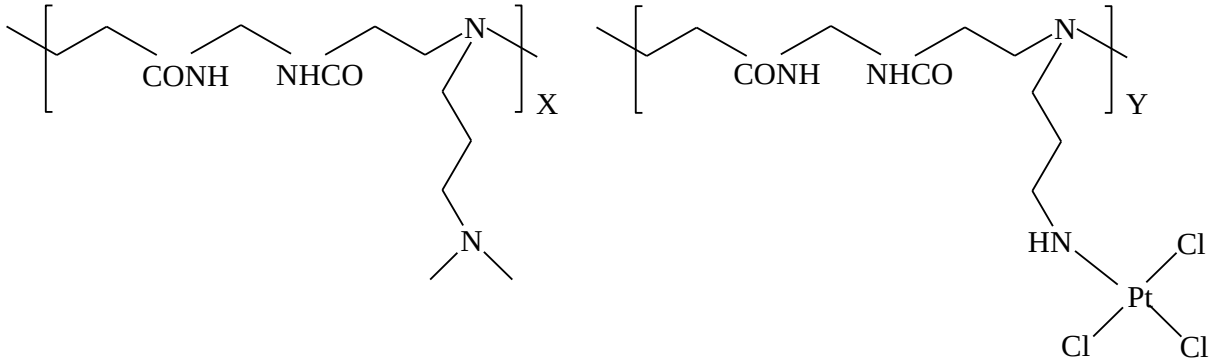

Conjugate 5:

X:Y = 8:2

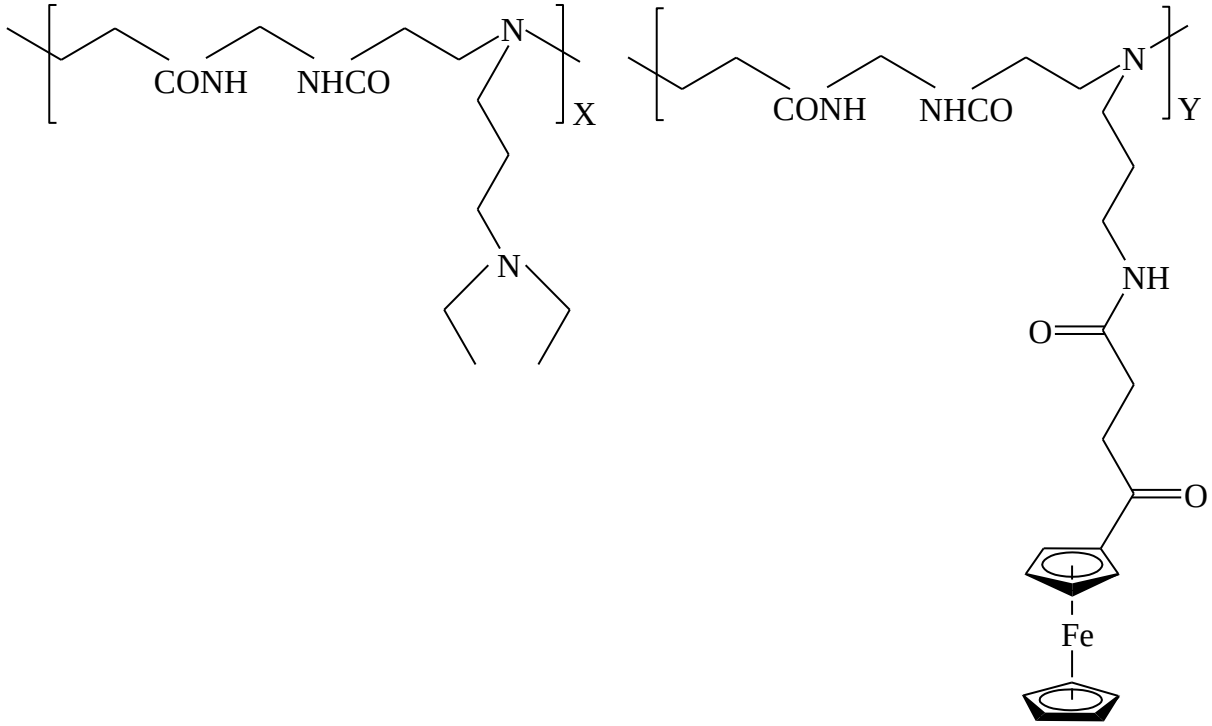

Conjugate 6:

X:Y:Z = 8:1:1

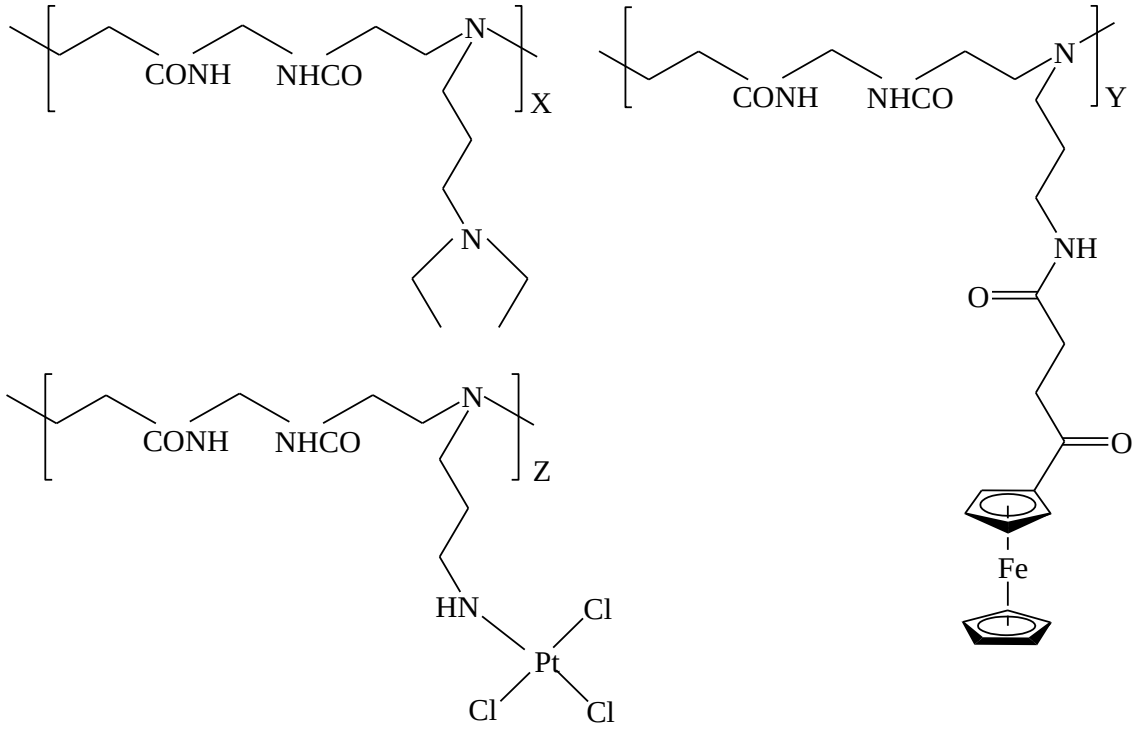

Conjugate 7:

X:Y:Z = 8:1:1

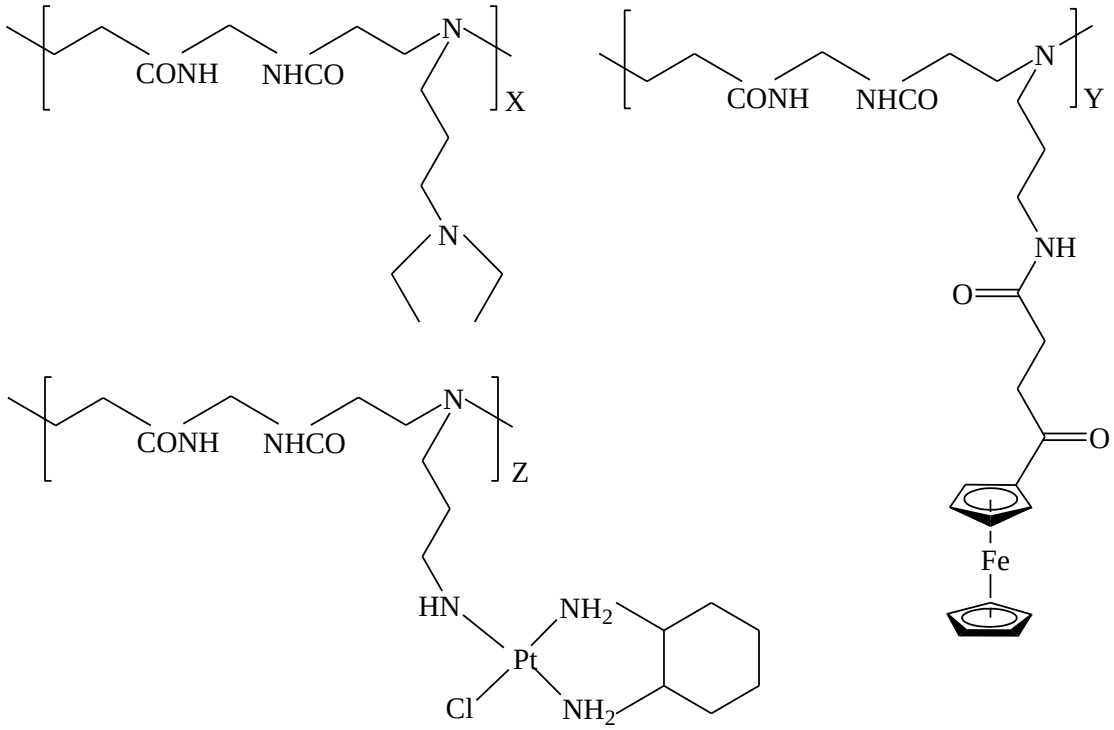

3.6 Characterization techniques

This subsection describes the analytical techniques that were used for characterization of the ferrocene and platinum analogues, carriers and drug conjugates that were prepared. Samples were characterized using various techniques including the following: Fourier transform infrared spectroscopy (FTIR), Transmission electron microscopy (TEM), Nuclear magnetic resonance (NMR), Energy dispersive X-ray spectroscopy (EDX) and Particle Size Analysis.

3.6.1 Fourier Transform Infrared Spectroscopy (FTIR)

In this study, FTIR analysis on analogues, carriers and drug conjugates was used to determine the presence of functional groups. FTIR scan for each sample was carried out in wavenumber range 400-4000 cm^{-1}. PerkinElmer Two FTIR spectrometer was employed to obtain FTIR data.

3.6.2 Proton Nuclear Magnetic Resonance Spectroscopy (^{1}H NMR)

^{1}H NMR was carried out using D_2O in a Varian Unity INOVA 300 MHz Nuclear Magnetic Resonance Spectrometer to elucidate the chemical structure of the analogues, carriers and drug conjugates. The samples for drug conjugates were set to pH 10-11 using sodium hydroxide to get rid of protonation.

3.6.3 Scanning Electron Microscopy (SEM)

Scanning electron microscopy is an analytical technique useful for obtaining surface morphology and crystallographic information of a sample. In this study, SEM analysis was carried out on JEOL JSM-6390LV scanning electron microscope instrument at an accelerating voltage of 15 kV. All samples were coated with a thin layer of gold before SEM images were obtained in order to improve the quality of results.

3.6.4 Transmission Electron Microscopy (TEM) and Energy Dispersive X-Ray Spectroscopy (EDX)

TEM was used to determine the morphology and to provide an estimate of particle thickness of polyamidoamine drug conjugates. The TEM images were recorded on JEM-1200EX JEOL instrument. Samples of conjugates were dispersed in ethanol before a drop of the solution was deposited onto copper grids and allowed to dry on a filter paper at RT for 15 minutes prior to TEM analysis. EDX was used to determine elemental composition of polyamidoamine drug conjugates.

3.6.5 Particle Size Analysis

The particle size analysis was carried out on Malvern Zetasizer Nano ZS instrument. Each sample of the conjugate was dissolved in 1 mL of deionized water to form a stock solution. 0.1 mL of the stock solution was diluted to 1 mL with deionized water, vortexed and filtered through 0.45 µm disc syringe filter. Refractive index of 1.348 and absorption value of 0.001 were used in the determination of the particle sizes of samples.

3.7 Drug release studies

Drug release was performed on conjugates PD3, PD5 and PD6. 20 mg of conjugate dissolved in 2 mL distilled water was placed in a dialyses membrane. The membrane was placed in buffer solution of pH 1.2 and 7.4 (simulating gastric pH and blood serum pH respectively) and dialysis was performed using a shaker (Memmert, Germany) maintained at 37°C. 4 mL aliquots were withdrawn and replaced by equal amount of fresh buffer solution at 40 minutes time intervals for the first 8 hours and then at 24 hour spacing for the next 5 days. Concentration of drug released were quantified by ultraviolet visible spectroscopy and atomic absorption spectroscopy. Pt drug released was obtained by atomic absorption spectroscopy

while Fe drug released was quantified using ultraviolet visible spectroscopy at wavelength 228 nm as discussed in sections 3.7.1 and 3.7.2 below.

3.7.1 Ultraviolet Visible Spectroscopy (UV/Vis)

Ultraviolet visible spectroscopy was performed on Perkin Elmer Lambda 365 UV/Vis spectrometer. The UV/Vis spectrum of Fc-PDA was evaluated for the wavelength range of 200 nm to 700 nm as shown in figure 3.1 below. The maximum absorption wavelength was obtained at 228 nm and was used for the calibration of the instrument before determining the quantity of ferrocene drug released.

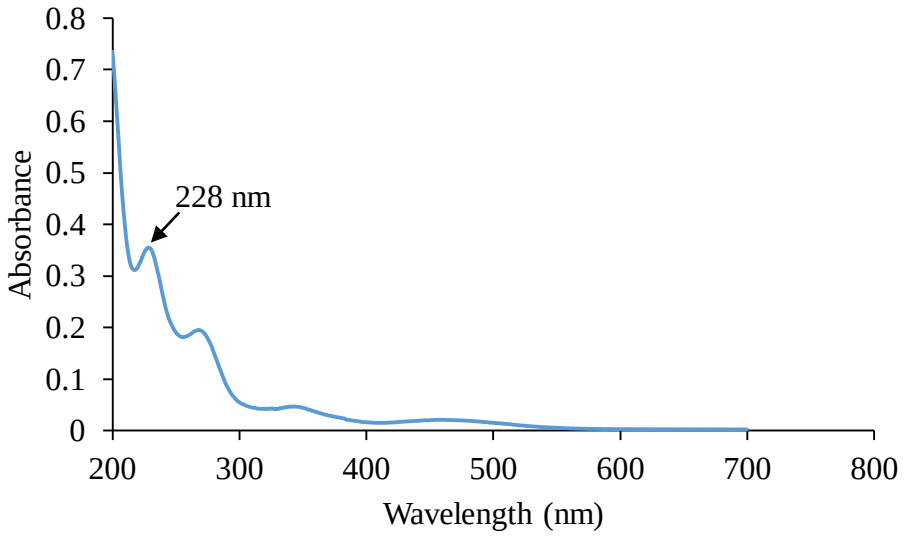

Figure 3.1: UV/Vis spectrum for Fc-PDA

A stock solution of 1000 mg/L was prepared and diluted accordingly to form standard solutions of Fc-PDA of concentrations 100, 10, 1 and 0.1 mg/L. Figure 3.2 shows the calibration curve for the ferrocene based drug, Fc-PDA. After calibration, concentrations of samples from drug release studies were obtained at wavelength 228 nm. Each sample concentration was obtained in triplicates and average values were taken.

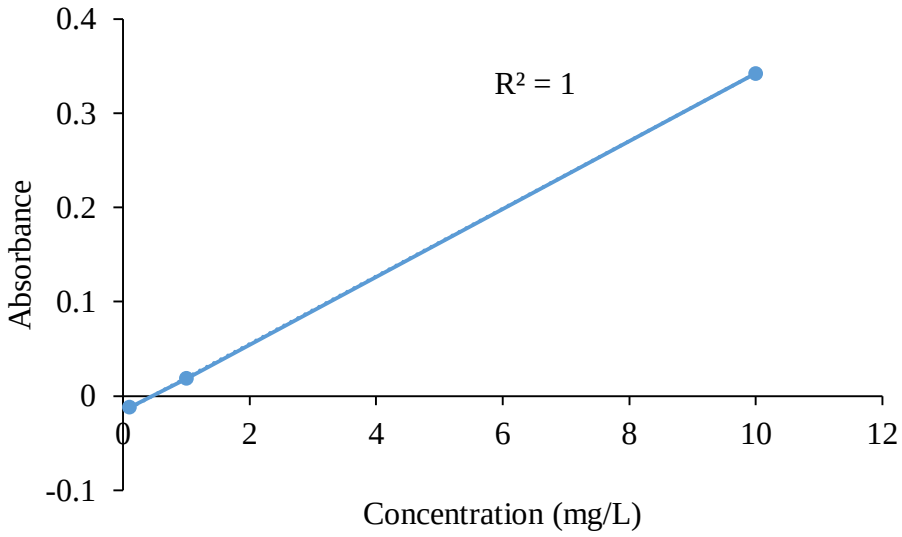

Figure 3.2: Calibration curve for Fc-PDA

3.7.2 Atomic absorption spectroscopy (AAS)

Thermo Scientific iCE 3500 Series AA Spectrometer was used to determine the concentration of platinum drug. A stock solution of 150 mg/L was prepared and diluted accordingly to form standard solutions of K_2PtCl_4 of concentrations 100, 50, 20 and 5 mg/L. Figure 3.3 shows the calibration curve for the platinum based drug, K_2PtCl_4. After calibration of the instrument, aliquots were withdrawn from each sample solutions obtained in drug release studies and the concentration was recorded. Each sample concentration was obtained in triplicates and average values were taken.

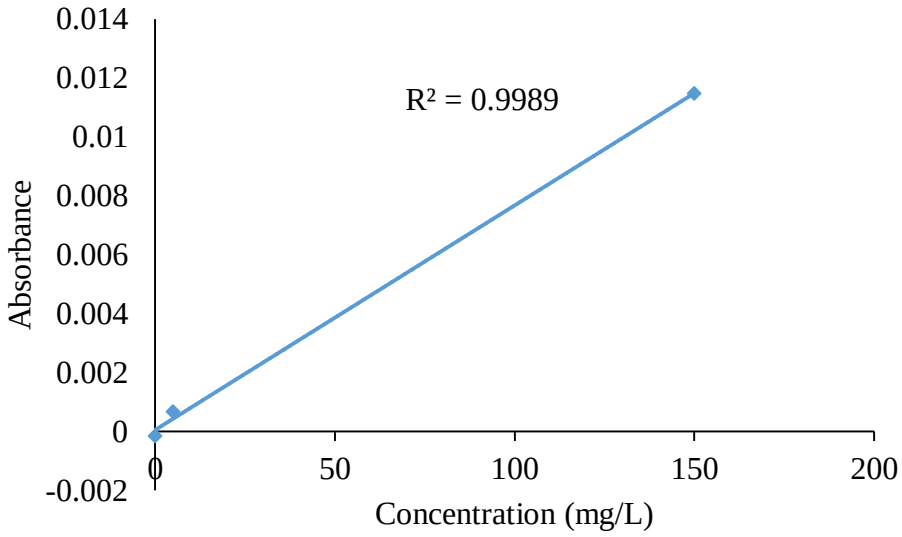

Figure 3.3: Calibration curve for K_2PtCl_4

3.8 In vitro analysis

3.8.1 Cell lines

Cytotoxicity was evaluated against breast cancer cell lines (MCF-7 and MDA-MB-231) and normal cell line (EA.hy926). MCF-7 (HBT-22) and MDA-MB-231 (HBT-26) cell lines were obtained from the American Type Culture Collection (ATCC) and the EA.hy926 cell line was provided as a gift from the University of North Carolina's Lineberger Comprehensive Cancer Centre.

All cells were maintained in Dulbecco's Modified Essential Medium (DMEM) supplemented with 10% Foetal Calf Serum (FCS) and 2 mM glutamine in 75 mL flasks. The cells were maintained at 37°C in an incubator humidified with an atmosphere of 5% CO_2. When confluent, cells were washed with phosphate buffered saline (PBS) and harvested by detachment using 0.25% trypsin/EDTA. Centrifugation was performed on the detached cells in complete medium at 200 g for 5 minutes. The trypan blue (0.1%) exclusion method was

employed to count cell which were diluted to 5 x 104 (MCF-7 and EA.hy926) and 2.5 x 104 (MDA-MB-231) cells/mL 10% FCS medium.

3.8.2 Cytotoxicity assay

Cytotoxicity was evaluated by determination of cell density with sulforhodamine B assay as reported by Vichai and Kirtikara with minor changes (Vichai & Kirtikara, 2006). A 100 μL of cell suspension was seeded into a sterile, clear 96-well plates and incubated overnight in an atmosphere of 5% CO_2 at a temperature of 37°C. During incubation, cells were allowed to attach and then exposed to 100 μL of the experimental compounds (0.01 – 100 μM for conjugates, 0.03 – 32 μM for platinum drug). Medium was used as the negative control. Blank and colour controls without cells were included to check for background noise and sterility. The plates were incubated for a period of 72 hours in 5% CO_2 at a temperature of 37°C and then cells were fixed with 50 μL of 50% trichloroacetic acid overnight at 4°C. Fixed cells were washed three times with tap water before staining with 100 μL of 0.057% SRB in 1% acetic acid for 30 minutes. The stained cells were washed four times with 100 μL of 1% acetic acid and then air dried. The bound dye was dissolved using 200 μL Tris-buffer (10mM, pH 10.5). Absorbance was measured on Synergy 2 plate (Bio-tek Instruments, Inc) at 510 nm with reference 630 nm. Assays were carried out using both three intra- and three inter-replicates. Graphpad Prism 5 was used to calculate the IC_{50} values.

CHAPTER 4

Results and Discussion

4.1 Introduction

This chapter describes the results of the characterization of analogues, carriers and drug conjugates that were prepared in this project. Drug release studies and in vitro cytotoxicity evaluation results are also discussed in this chapter.

4.2 FTIR analysis

Fig 4.1 shows the FTIR spectrum of platinum analogue cyclohexane-1,2-diamine dichloroplatinum(II) (DACH $PtCl_2$) which was employed in the preparation of polyamidoamine drug conjugates.

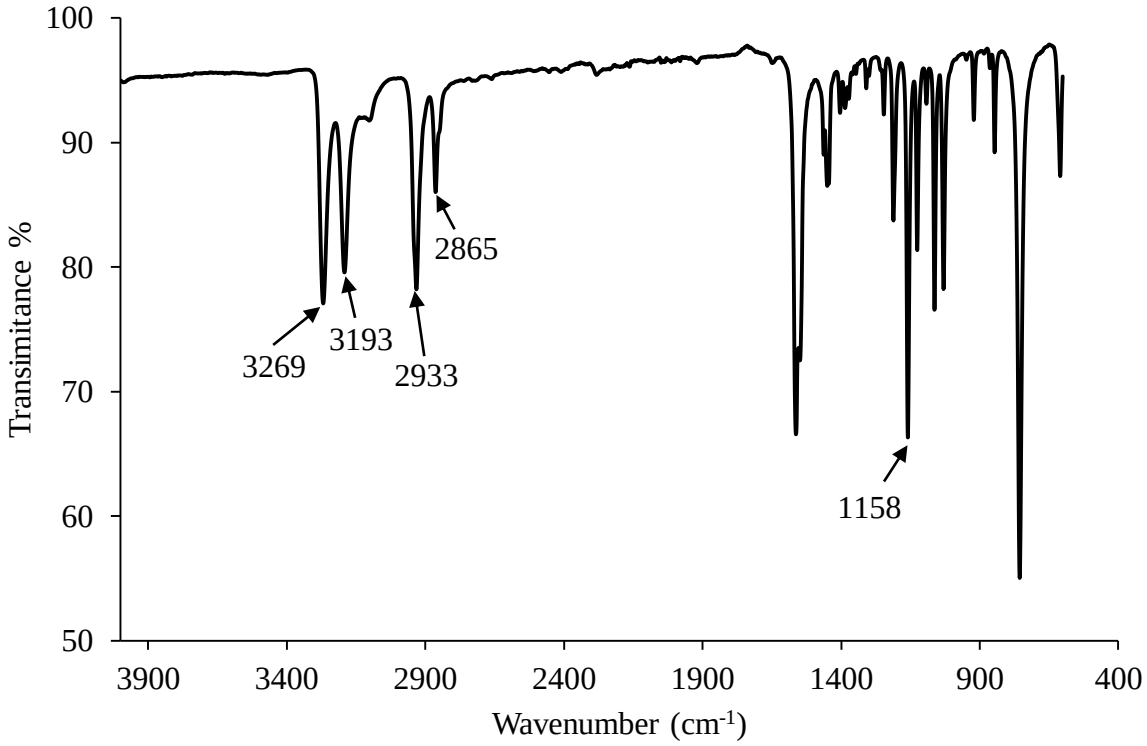

Figure 4.1: FTIR spectrum of DACH $PtCl_2$

In the spectrum for DACH $PtCl_2$, two sharp peaks at 3269 cm^{-1} and 3193 cm^{-1} are attributed to the primary amine N-H stretch. Also observed are peaks corresponding to the C-N stretch on 1158 cm^{-1}, C-H stretch on 2933 cm^{-1} and 2865 cm^{-1}. An extremely weak band for Pt-N stretch appear at about 545 cm^{-1}. Wysokiński and co-workers reported similar findings on carboplatin (Wysokiński et al., 2006). The FTIR analysis confirms the successful synthesis of the platinum analogue since all major peaks are clearly observable on the spectrum.

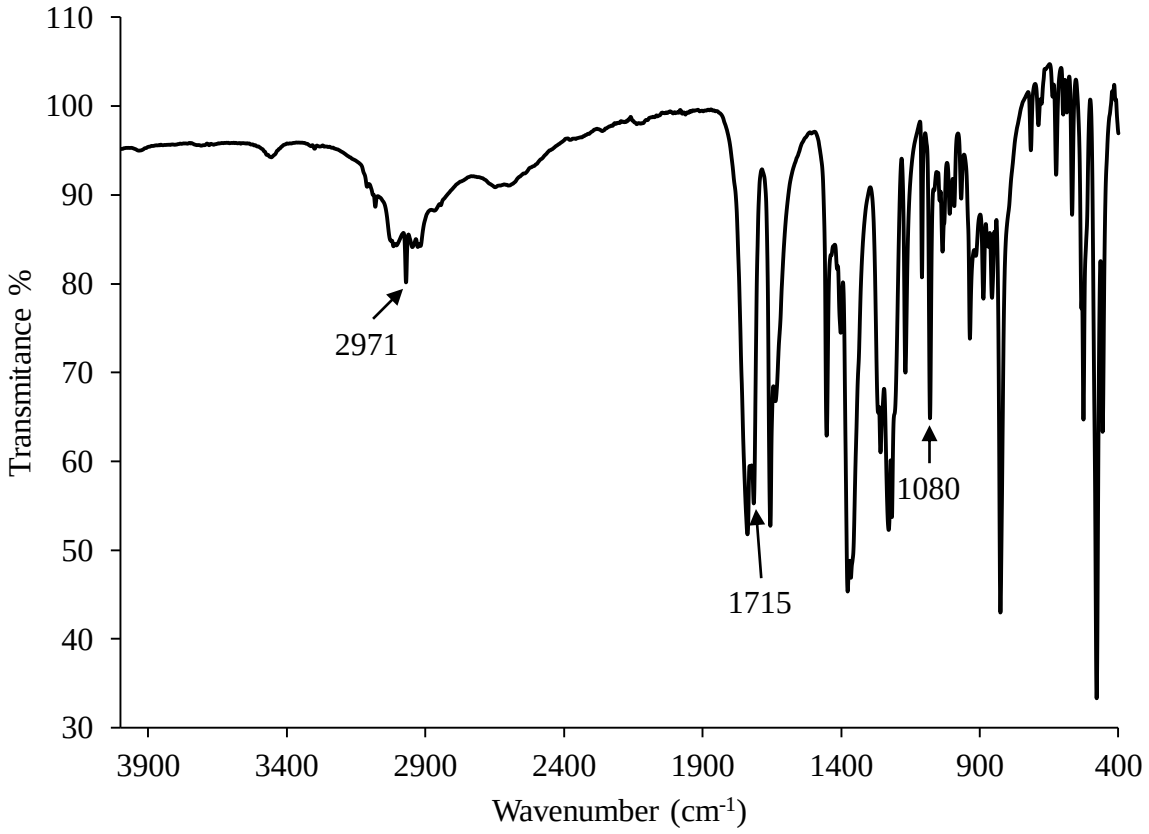

Figure 4.2: FTIR spectrum of 4-ferrocenylketobutanoic acid

The spectrum for 4-ferrocenylketobutanoic acid shows labelled sharp peak at 1715 cm^{-1} ascribed to C=O stretch of a carboxylic acid. The broad peak centred on 2971 cm^{-1} also confirms the presence of O-H stretch carboxylic acid functional group. On the other hand, peaks on 1080 cm^{-1}, 1656 cm^{-1} and 1229 cm^{-1} correspond to C-O stretch, C=C stretch and C-N stretch respectively.

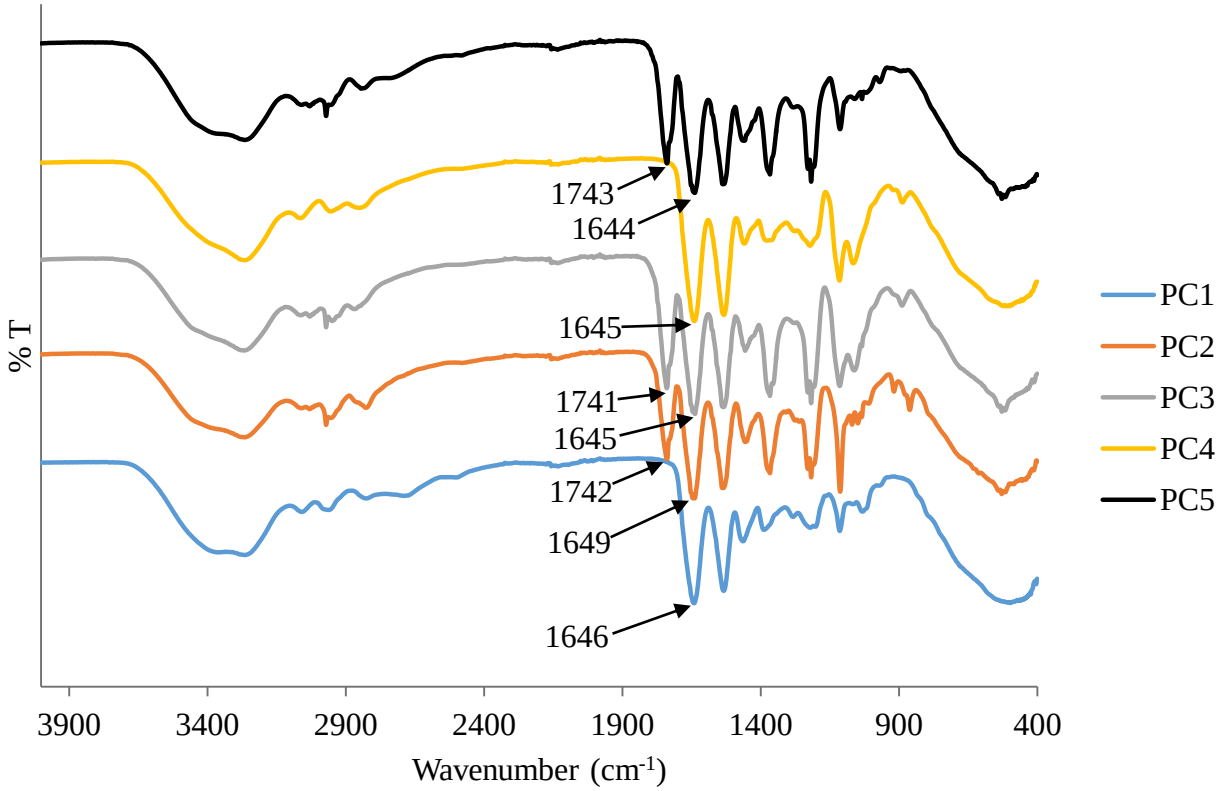

Figure 4.3: FTIR spectra of polyamidoamine carriers PC1-5

FTIR spectra of polyamidoamine carriers (PC1-10) are shown in figs 4.3 and 4.4. Spectra for the carriers showed a similar trend for the major absorption peaks across all compounds. The presence of the broad peak centred around 3300 cm^{-1} (amide N-H stretch) and sharp peak in the range 1655-1635 cm^{-1} (C=O stretch) in all spectrums for polyamidoamine carriers PC1 to PC10 represent the amide bond and confirm the successful preparation of the carriers. Peaks on the range 3100-3000 cm^{-1} and 3000-2850 cm^{-1} are attributed to C-H stretching for alkene and alkane functional groups respectively. Sharp peaks corresponding to N-H bending were also observed for carriers at about 1530 cm^{-1} of each spectrum. For carriers PC6 and PC8, peaks corresponding to aromatic C-H stretch were observed at about 3053 cm^{-1} confirming the presence of dopamine in the polyamidoamine carriers. The peak at about 1217 cm^{-1} in each spectrum is attributed to C-N stretch.

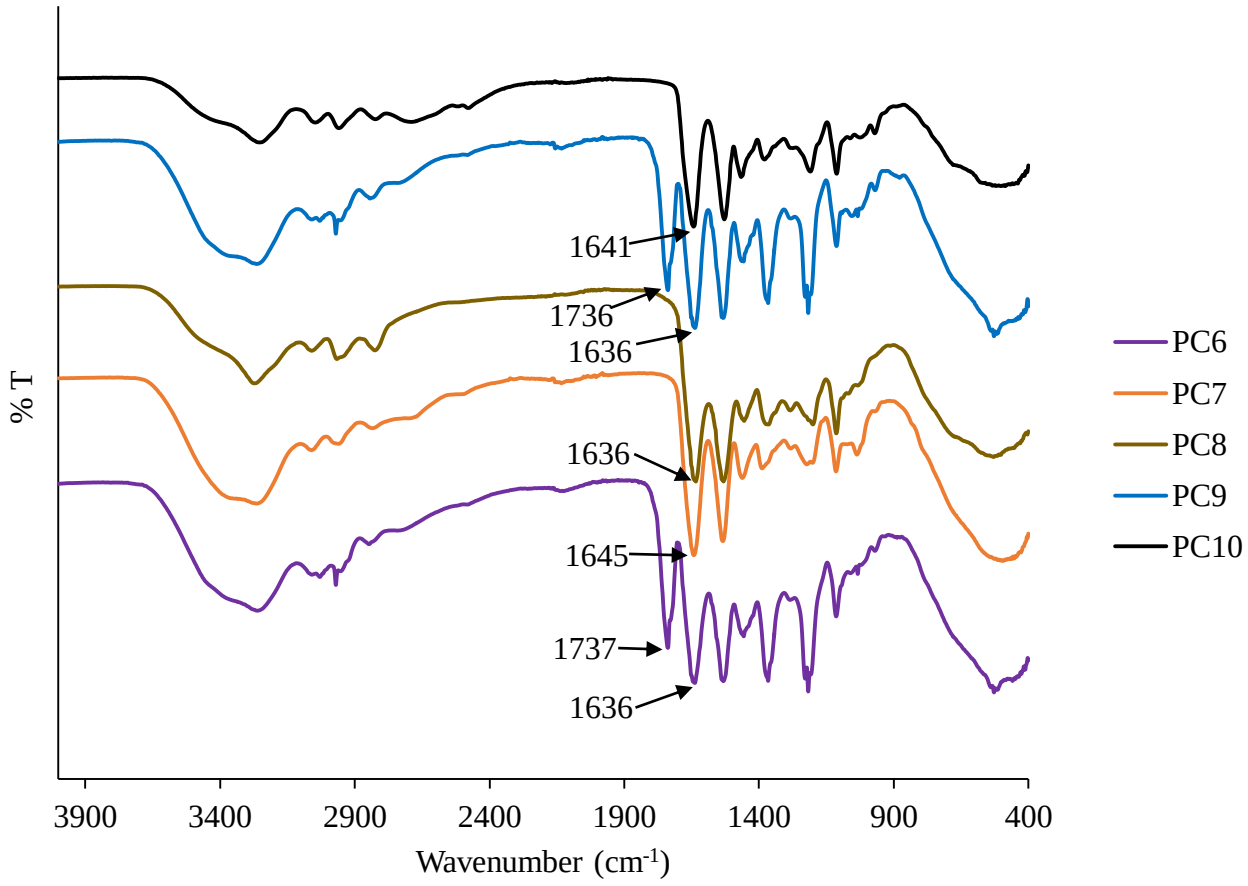

Figure 4.4: FTIR spectra of polyamidoamine carriers PC6-10

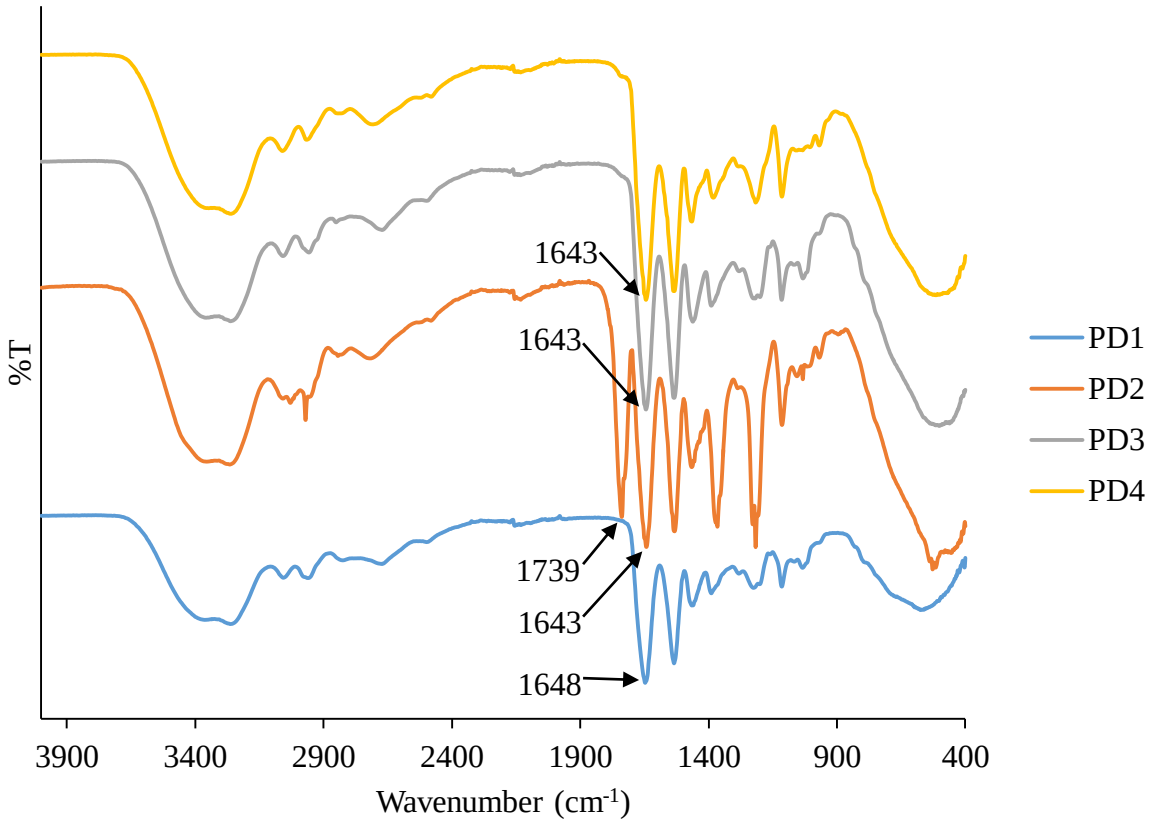

Figure 4.5: FTIR spectra of polyamidoamine drug conjugates PD1-4

The FTIR spectra of polyamidoamine drug conjugates (PD1-7) are shown in figs 4.5 and 4.6. The spectra of the conjugates did not differ from that of carriers to a larger extent. The broad peak centred around 3300 cm^{-1} (amide N-H stretch) and sharp peak in the range 1655-1635 cm^{-1} (C=O stretch) in all spectrums for polyamidoamine conjugates PD1 to PD7 represent the amide bond and confirm the successful preparation of the conjugates. The presence of the amide bond also confirm the successful incorporation of the ferrocenyl analogue, 4-ferrocenylketobutanoic acid (Fc) on conjugates PD5, PD6 and PD7. The peak on 545 cm^{-1} corresponds to Pt-N and confirm the conjugation of the platinum analogues on the conjugates (Wysokiński et al., 2006). Peaks on the range 3100-3000 cm^{-1} and 3000-2850 cm^{-1} are attributed to C-H stretching for alkene and alkane functional groups respectively. Sharp peaks corresponding to N-H bending were also observed for the conjugates at about 1530 cm^{-1} of

each spectrum. The peak at about 1217 cm^{-1} in each spectrum of the conjugates correspond to C-N stretch.

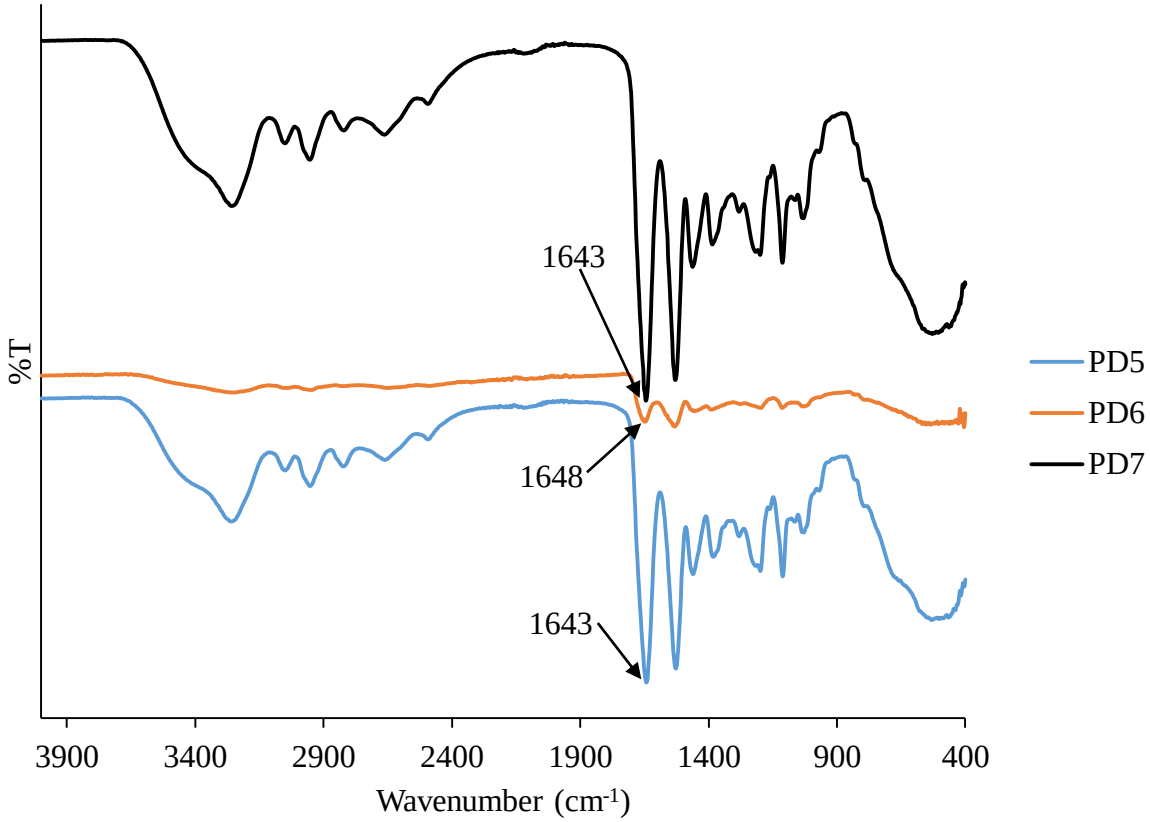

Figure 4.6: FTIR spectra of polyamidoamine drug conjugates PD5-7

4.3 ^{1}H NMR analysis

Results obtained for ^{1}H NMR analysis confirmed the observations obtained from FTIR analysis. The proton count expected and the proton count obtained were close to each other indicating the successful isolation of the compounds. ^{1}H NMR spectra of the analogues and polymers prepared in this study were analysed and tabulated as shown in table 4.1 and 4.2 below.

Compound	Assignment	Chemical shift (ppm)	Proton count	
			Expected	Found
Fc-PDA	$CH_2C\mathbf{H_2}CH_2NH_2$	2.75-2.73	2	2
	$CH_2CH_2C\mathbf{H_2}NH_2$	3.08-3.05	2	2
	$COC\mathbf{H_2}C\mathbf{H_2}CO$	4.22	4	5
	$CONHC\mathbf{H_2}CH_2CH_2$	4.50	2	2
	C**H** (ferrocenyl)	4.80	9	2
PC1	$CH_2N(CH_2\mathbf{CH_3})_2$	1.01-0.97	48	48
	$CH_2C\mathbf{H_2}CH_2N(CH_2CH_3)_2$, $CH_2C\mathbf{H_2}CH_2NH_2$	1.57	20	16
	$CH_2C\mathbf{H_2}CONH$, $NHCOC\mathbf{H_2}CH_2$	2.30-2.25	40	49
	$C\mathbf{H_2}CH_2C\mathbf{H_2}N(C\mathbf{H_2}CH_3)_2$, $C\mathbf{H_2}CH_2CONH$, $COCH_2C\mathbf{H_2}N$, $C\mathbf{H_2}CH_2C\mathbf{H_2}NH_2$	2.73-2.34	112	117
	$CONHC\mathbf{H_2}NHCO$	4.41-4.40	20	22
PC2	$CH_2C\mathbf{H_2}CH_2N(CH_2)_2$	1.50	16	16
	$C\mathbf{H_2}CH_2CONH$, $COCH_2C\mathbf{H_2}N$, $C\mathbf{H_2}CH_2C\mathbf{H_2}N(C\mathbf{H_2})_2$, $C\mathbf{H_2}C\mathbf{H_2}NHC\mathbf{H_2}C\mathbf{H_2}NH_2$	2.41-2.18	120	128
	$CH_2C\mathbf{H_2}CONH$, $COC\mathbf{H_2}CH_2N$	2.66-2.61	40	46
	$C\mathbf{H_2}OC\mathbf{H_2}$	3.59	32	31
	$CONHC\mathbf{H_2}NHCO$	4.39	20	22.5
PC3	$C\mathbf{H_2}CH_2CONH$, $COCH_2C\mathbf{H_2}N$, $NC\mathbf{H_2}CH_2O$, $OCH_2C\mathbf{H_2}NH_2$	2.31-2.26	64	64
	$CH_2C\mathbf{H_2}CONH$, $COC\mathbf{H_2}CH_2N$	2.57-2.53	28	28
	$C\mathbf{H_2}OC\mathbf{H_2}C\mathbf{H_2}OH$, $C\mathbf{H_2}OC\mathbf{H_2}C\mathbf{H_2}OC\mathbf{H_2}$	3.51-3.45	64	60
	$CONHC\mathbf{H_2}NHCO$	4.41-4.40	20	31
PC4	$CH_2C\mathbf{H_2}CONH$, $COC\mathbf{H_2}CH_2N$	2.28-2.25	40	40
	$C\mathbf{H_2}CH_2CONH$, $COCH_2C\mathbf{H_2}N$, $NC\mathbf{H_2}CH_2O$, $C\mathbf{H_2}C\mathbf{H_2}NH_2$	2.70-2.51	64	59
	$C\mathbf{H_2}OC\mathbf{H_2}C\mathbf{H_2}OH$	3.57-3.44	48	39
	$CONHC\mathbf{H_2}NHCO$	4.40-4.39	20	19
PC5	$CH_2C\mathbf{H_2}CH_2N(CH_3)_2$	1.65	12	12
	$C\mathbf{H_2}CH_2CONH$, $COCH_2C\mathbf{H_2}N$, $C\mathbf{H_2}CH_2C\mathbf{H_2}N(C\mathbf{H_3})_2$, $C\mathbf{H_2}CH(OH)$, $C\mathbf{H_2}C\mathbf{H_2}NHC\mathbf{H_2}C\mathbf{H_2}NH_2$	2.37-2.25	114	59.5
	$CH_2C\mathbf{H_2}CONH$, $COC\mathbf{H_2}CH_2N$	2.54-2.46	40	49
	C**H**(OH)$C\mathbf{H_2}OH$	2.75-2.54	9	76.5
	$CONHC\mathbf{H_2}NHCO$	4.44-4.41	20	23

PC6	$CH_2C\mathbf{H_2}CH_2N(CH_3)_2$	1.47	12	12
	$CH_2C\mathbf{H_2}CONH$, $COC\mathbf{H_2}CH_2N$	2.03	40	50
	$C\mathbf{H_2}CH_2CONH$, $COCH_2C\mathbf{H_2}N$, $C\mathbf{H_2}CH_2C\mathbf{H_2}N(C\mathbf{H_3})_2$, $C\mathbf{H_2}CH_2C(CH)_2$, $C\mathbf{H_2}C\mathbf{H_2}NHC\mathbf{H_2}C\mathbf{H_2}NH_2$	2.41-2.13	114	96
	$CH_2C\mathbf{H_2}C(CH)_2$	2.53	6	12
	$CONHC\mathbf{H_2}NHCO$	4.40	20	17
	C**H** (aromatic)	5.66-5.63	1	1
		6.09-6.08	2	2
PC7	$CH_2N(CH_2C\mathbf{H_3})_2$	0.86-0.84	36	36
	$CH_2C\mathbf{H_2}CH_2N(CH_2CH_3)_2$	1.47-1.43	12	11
	$C\mathbf{H_2}CH_2CONH$, $COCH_2C\mathbf{H_2}N$, $C\mathbf{H_2}CH_2C\mathbf{H_2}N(C\mathbf{H_2}CH_3)_2$, $C\mathbf{H_2}CH(OH)$, $C\mathbf{H_2}C\mathbf{H_2}NHC\mathbf{H_2}C\mathbf{H_2}NH_2$	2.44-2.24	102	100
	$CH_2C\mathbf{H_2}CONH$, $COC\mathbf{H_2}CH_2N$	2.70-2.52	40	41
	C**H**(OH)$C\mathbf{H_2}OH$	3.45-3.31	9	5
	$CONHC\mathbf{H_2}NHCO$	4.40	20	20
PC8	$CH_2N(CH_2C\mathbf{H_3})_2$	0.85-0.82	36	36
	$CH_2C\mathbf{H_2}CH_2N(CH_2CH_3)_2$	1.44	12	10
	$C\mathbf{H_2}CH_2CONH$, $COCH_2C\mathbf{H_2}N$, $C\mathbf{H_2}CH_2C\mathbf{H_2}N(C\mathbf{H_2}CH_3)_2$, $C\mathbf{H_2}CH_2C(CH)_2$, $C\mathbf{H_2}C\mathbf{H_2}NHC\mathbf{H_2}C\mathbf{H_2}NH_2$	2.41-2.01	102	103
	$CH_2C\mathbf{H_2}CONH$, $COC\mathbf{H_2}CH_2N$	2.61-2.60	40	46
	$CH_2C\mathbf{H_2}C(CH)_2$	3.13-3.09	6	4
	$CONHC\mathbf{H_2}NHCO$	4.39	20	18
	C**H** (aromatic)	6.08-6.06	1	0.2
		7.92-7.74	2	0.5
PC9	$CH_2C\mathbf{H_2}CH_2N(CH_3)_2$	1.50-1.44	12	12
	$C\mathbf{H_2}CH_2CONH$, $COCH_2C\mathbf{H_2}N$, $C\mathbf{H_2}CH_2C\mathbf{H_2}N(C\mathbf{H_3})_2$, $NC\mathbf{H_2}CH_2OH$, $C\mathbf{H_2}C\mathbf{H_2}NHC\mathbf{H_2}C\mathbf{H_2}NH_2$	2.55-2.02	114	115
	$CH_2C\mathbf{H_2}CONH$, $COC\mathbf{H_2}CH_2N$	2.69-2.61	40	43
	$NCH_2C\mathbf{H_2}OH$	3.52-3.48	6	5
	$CONHC\mathbf{H_2}NHCO$	4.40	20	20
PC10	$CH_2C\mathbf{H_2}CH_2N(CH_3)_2$, $CH_2C\mathbf{H_2}CH_2NH_2$	1.60	20	20
	$C\mathbf{H_2}CH_2CONH$, $COCH_2C\mathbf{H_2}N$, $C\mathbf{H_2}CH_2\mathbf{CH_2}N(C\mathbf{H_3})_2$, $C\mathbf{H_2}CH_2C\mathbf{H_2}NH_2$	2.52-2.15	128	140
	$CH_2C\mathbf{H_2}CONH$, $NHCOC\mathbf{H_2}CH_2$	2.72	40	47
	$CONHC\mathbf{H_2}NHCO$	4.54-4.52	20	23

Table 4.1: ^{1}H NMR data for polyamidoamine drug carriers

Compound	Assignment	Chemical shift (ppm)	Proton count	
			Expected	Found
PD1	$CH_2N(CH_2C\mathbf{H_3})_2$	0.99-0.98	51	51
	$CH_2C\mathbf{H_2}CH_2N(CH_2CH_3)_2$, $CHC\mathbf{H_2}C\mathbf{H_2}C\mathbf{H_2}C\mathbf{H_2}CH$	1.57	29	16
	$CH_2C\mathbf{H_2}CONH$, $NHCOC\mathbf{H_2}CH_2$	2.30-2.26	40	42
	$C\mathbf{H_2}CH_2CONH$, $COCH_2C\mathbf{H_2}N$, $C\mathbf{H_2}CH_2C\mathbf{H_2}N(\mathbf{CH_2}CH_3)_2$, $C\mathbf{H_2}C\mathbf{H_2}NHC\mathbf{H_2}C\mathbf{H_2}$, $C\mathbf{H}CH_2CH_2CH_2CH_2C\mathbf{H}$	2.69-2.33	123	128
	$CONHC\mathbf{H_2}NHCO$	4.41	20	21
PD2	$CH_2C\mathbf{H_2}CH_2N(CH_3)_2$, $CH_2C\mathbf{H_2}CH_2NH$, $CHC\mathbf{H_2}C\mathbf{H_2}C\mathbf{H_2}C\mathbf{H_2}CH$	1.61	32	32
	$C\mathbf{H_2}CH_2CONH$, $COCH_2C\mathbf{H_2}N$, $C\mathbf{H_2}CH_2C\mathbf{H_2}N(C\mathbf{H_3})_2$, $C\mathbf{H_2}CH_2C\mathbf{H_2}NH$, $C\mathbf{H}CH_2CH_2CH_2CH_2C\mathbf{H}$	2.38-2.32	134	133
	$CH_2C\mathbf{H_2}CONH$, $NHCOC\mathbf{H_2}CH_2$	2.58-2.54	40	40
	$CONHC\mathbf{H_2}NHCO$	4.41	20	40
PD3	$CH_2N(CH_2C\mathbf{H_3})_2$	0.86-0.83	51	51
	$CH_2C\mathbf{H_2}CH_2N(CH_2CH_3)_2$	1.45	17	16
	$C\mathbf{H_2}CH_2CONH$, $COCH_2C\mathbf{H_2}N$, $C\mathbf{H_2}CH_2C\mathbf{H_2}N(\mathbf{CH_2}CH_3)_2$, $C\mathbf{H_2}C\mathbf{H_2}NHC\mathbf{H_2}C\mathbf{H_2}$	2.38-2.24	120	105
	$CH_2C\mathbf{H_2}CONH$, $NHCOC\mathbf{H_2}CH_2$	2.64-2.61	40	34
	$CONHC\mathbf{H_2}NHCO$	4.40	20	16
PD4	$CH_2C\mathbf{H_2}CH_2N(CH_3)_2$, $CH_2C\mathbf{H_2}CH_2NH$	1.47	20	20
	$C\mathbf{H_2}CH_2CONH$, $COCH_2C\mathbf{H_2}N$, $C\mathbf{H_2}CH_2C\mathbf{H_2}N(C\mathbf{H_3})_2$, $C\mathbf{H_2}CH_2C\mathbf{H_2}NH$	2.31-2.03	131	146
	$CH_2C\mathbf{H_2}CONH$, $NHCOC\mathbf{H_2}CH_2$	2.67-2.62	40	46
	$CONHC\mathbf{H_2}NHCO$	4.40	20	20
PD5	$CH_2N(CH_2C\mathbf{H_3})_2$	0.99	48	48
	$CH_2C\mathbf{H_2}CH_2N(CH_2CH_3)_2$, $CH_2C\mathbf{H_2}CH_2NH$	1.59	20	19
	$C\mathbf{H_2}CH_2CONH$, $COCH_2C\mathbf{H_2}N$, $C\mathbf{H_2}CH_2C\mathbf{H_2}N(C\mathbf{H_2}CH_3)_2$, $C\mathbf{H_2}CH_2C\mathbf{H_2}NH$	2.50-2.40	112	99
	$CH_2C\mathbf{H_2}CONH$, $NHCOC\mathbf{H_2}CH_2$, $COC\mathbf{H_2}C\mathbf{H_2}CO$	2.76	48	45
	$CONHC\mathbf{H_2}NHCO$, $C\mathbf{H}$ (ferrocenyl)	4.54	38	28
PD6	$CH_2N(CH_2C\mathbf{H_3})_2$	0.98-0.96	48	48
	$CH_2C\mathbf{H_2}CH_2N(CH_2CH_3)_2$, $CH_2C\mathbf{H_2}CH_2NH$	1.57	20	13

	$C\mathbf{H_2}CH_2CONH$, $COCH_2C\mathbf{H_2}N$, $C\mathbf{H_2}CH_2C\mathbf{H_2}N(C\mathbf{H_2}CH_3)_2$, $C\mathbf{H_2}CH_2C\mathbf{H_2}NH$	2.49-2.38	112	101
	$CH_2C\mathbf{H_2}CONH$, $NHCOC\mathbf{H_2}CH_2$, $COC\mathbf{H_2}C\mathbf{H_2}CO$	2.74	44	41
	$CONHC\mathbf{H_2}NHCO$, C**H** (ferrocenyl)	4.51	29	8
PD7	$CH_2N(CH_2C\mathbf{H_3})_2$	1.18	48	48
	$CH_2C\mathbf{H_2}CH_2N(CH_2CH_3)_2$, $CH_2C\mathbf{H_2}CH_2NH$, $CHC\mathbf{H_2}C\mathbf{H_2}C\mathbf{H_2}C\mathbf{H_2}CH$	1.77	28	16
	$CH_2C\mathbf{H_2}CONH$, $NHCOC\mathbf{H_2}CH_2$, $COC\mathbf{H_2}C\mathbf{H_2}CO$	2.44-2.39	44	42
	$C\mathbf{H_2}CH_2CONH$, $COCH_2C\mathbf{H_2}N$, $C\mathbf{H_2}CH_2C\mathbf{H_2}N(C\mathbf{H_2}CH_3)_2$, $C\mathbf{H_2}CH_2C\mathbf{H_2}NH$, C**H**$CH_2CH_2CH_2CH_2C$**H**	2.98-2.51	114	113.5
	$CONHC\mathbf{H_2}NHCO$, C**H** (ferrocenyl)	4.54	29	20

Table 4.2: ^{1}H NMR data for polyamidoamine drug conjugates

All spectrum of carriers and conjugates showed the signal of CONHC**H$_2$**NHCO at about 4.40 ppm indicating the successful formation of the polyamidoamine backbone which form the basis of both polyamidoamine carriers and conjugates. The expected proton count and found proton count for the polymers were similar which indicate that the polyamidoamines carriers and conjugates were successfully isolated. ^{1}H NMR spectrum for PC1 displayed signals of the methyl and methylene protons of 3-diethylaminopropylamine at 1.01-0.97 ppm, 1.57 ppm and 2.73-2.34 ppm. Peaks at 1.57 ppm and 2.73-2.43 ppm confirmed the incorporation of 1,3-propanediamine to the carrier PC1. The spectra for PC2 showed signals at 1.50 ppm, 2.41-2.31 ppm and 3.59 ppm with indicate the presence of 4-(3-aminopropyl) morphine and diethylene triamine in the carrier. The spectrum for PC3 showed signal 2.31-2.26 ppm and 3.51-3.45 ppm suggesting the presence of the amines; 2-(2-aminoethoxy)ethanol and 2,2-(ethlenedioxy) diethylamine. Spectrum for PC4 displayed peaks for methylene protons of 2-(2-aminoethoxy) ethanol at 2.70-2.51 ppm and 3.57-3.44 ppm. Signals at 2.70-2.51 ppm indicate methylene protons of ethylenediamine in carrier PC4. The spectrum for PC5 showed peaks at 1.65 ppm, 2.37-2.25 ppm and 2.75-2.54 ppm which indicate the incorporation of amines; 3-dimethylamino-1-propylamine, 3-amino-1,2-propanediol and diethylene triamine. Spectrum for PC6 showed peaks at 2.41-2.13 ppm and 2.53 ppm which indicate the presence of 3-dimethylamino-1-propylamine and diethylene triamine. Peaks at 1.47 ppm, 2.41-2.13 ppm, 5.66-5.63 ppm and 6.09-6.08 ppm confirm the incorporation of dopamine to the carrier. The spectrum for PC7 showed the peaks of the methyl and methylene protons of 3-diethylaminopropylamine at 0.86-0.84 ppm, 1.47-1.43 ppm and 2.44-2.24 ppm. Signals at 2.44-2.24 ppm and 3.45-3.31 ppm indicate the methylene protons of the amines; 3-amino-1,2-propanediol and diethylene triamine. On the other hand, peaks at 0.86-0.84 ppm, 1.47-1.43 ppm and 2.44-2.24 ppm indicate the presence of 3-diethylaminopropylamine in the carrier. The spectrum for PC8 displayed signals for the methyl and methylene protons of 3-

diethylaminopropylamine at 0.85-0.82 ppm, 1.44 ppm and 2.41-2.01 ppm. Signals at 2.41-2.01 ppm, 3.13-3.09 ppm, 6.08-6.06 ppm and 7.92-7.74 ppm indicate the presence of diethylene triamine and dopamine in the carrier. Spectrum for PC9 showed signals at 1.50-1.44 ppm and 2.55-2.02 ppm which confirmed the incorporation of 3-dimethylamino-1-propylamine. On the other hand, signals at 2.55-1.44 ppm and 3.52-3.48 ppm indicate the presence of diethylene triamine and ethanolamine. The spectrum for PC10 showed signals at 1.60 ppm and 2.52-2.15 ppm which confirm the successful incorporation of 3-dimethylamino-1-propylamine and 1,3-propanediamine to the carrier.

The spectrum for polyamidoamine drug conjugate PD1 showed signals at 0.99-0.98 ppm, 1.57 ppm and 2.69-2.33 ppm indicated the presence of 3-diethylaminopropylamine. Peaks at 1.57 ppm and 2.69-2.33 ppm confirm the presence of diethylene triamine and cyclohexane-1,2-diamine dichloroplatinum(II) in the conjugate. Spectrum for PD2 showed signals at 1.61 ppm and 2.58-2.32 ppm indicated the presence of 3-dimethylamino-1-propylamine, 1,3-propanediamine and cyclohexane-1,2-diamine dichloroplatinum(II). The spectrum for PD3 displayed signals at 0.86-0.83 ppm, 1.45 ppm and 2.38-2.24 ppm which confirm the presence of 3-diethylaminopropylamine. Signals at 2.38-2.24 ppm indicate presence of diethylene triamine and potassium tetrachloroplatinate in the conjugate. Spectrum for PD4 showed peaks at 1.47 ppm and 2.31-2.03 ppm which confirm the presence of 3-dimethylamino-1-propylamine, 1,3-propanediamine and potassium tetrachloroplatinate in the conjugate. The spectrum for PD5 displayed peaks at 0.99 ppm, 1.59 ppm and 2.50-2.40 ppm which indicate presence of 3-diethylaminopropylamine. Signals at 1.59 ppm, 2.50-2.40 ppm, 2.76 ppm and 4.54 ppm confirm the incorporation of 3-[4-ferrocenylketobutamido]propylamine onto the conjugate. Spectrum of PD6 showed peaks at 0.98-0.96 ppm, 1.57 ppm and 2.49-2.38 ppm which indicate the presence of 3-diethylaminopropylamine. Signals at 1.57 ppm, 2.49-2.38 ppm, 2.74 ppm and 4.51 ppm indicate the incorporation of the drugs; 3-[4-

ferrocenylketobutamido]propylamine and potassium tetrachloroplatinate. The spectrum for PD7 displayed signals at 1.18 ppm, 1.77 ppm and 2.98-2.51 ppm which indicate the presence of 3-diethylaminopropylamine. On the other hand, signals at 1.77 ppm, 2.44-2.39 ppm, 2.98-2.51 ppm and 4.54 ppm indicated presence of 3-[4-ferrocenylketobutamido]propylamine and cyclohexane-1,2-diamine dichloroplatinum(II).

4.4 SEM analysis

The polyamidoamine drug carriers and conjugates were further analysed by scanning electron microscopy to study surface morphology. Figure 4.7 and 4.8 displays micrographs of polyamidoamine drug carriers formed from selected amines, done at an accelerating voltage of 15 kV and viewed at various magnifications.

The images for carriers PC1, PC2, PC3, PC4, PC5 and PC7 (fig 4.7 and fig 4.8) showed smooth surface morphology and folded morphology which can be attributed to the successful polyaddition of the amines to MBA (Aderibigbe et al., 2015). Carrier PC9 showed a combination of both smooth and cracked surface topology. SEM image for PC6, PC8 and PC10 displayed spherical and smooth surfaces of the carrier indicating successful reaction of MBA and the amines to form the polymer. The SEM images cement the suggestion from FTIR results that the polyamidoamine carriers were successfully formed from the reaction of MBA and the selected amines.

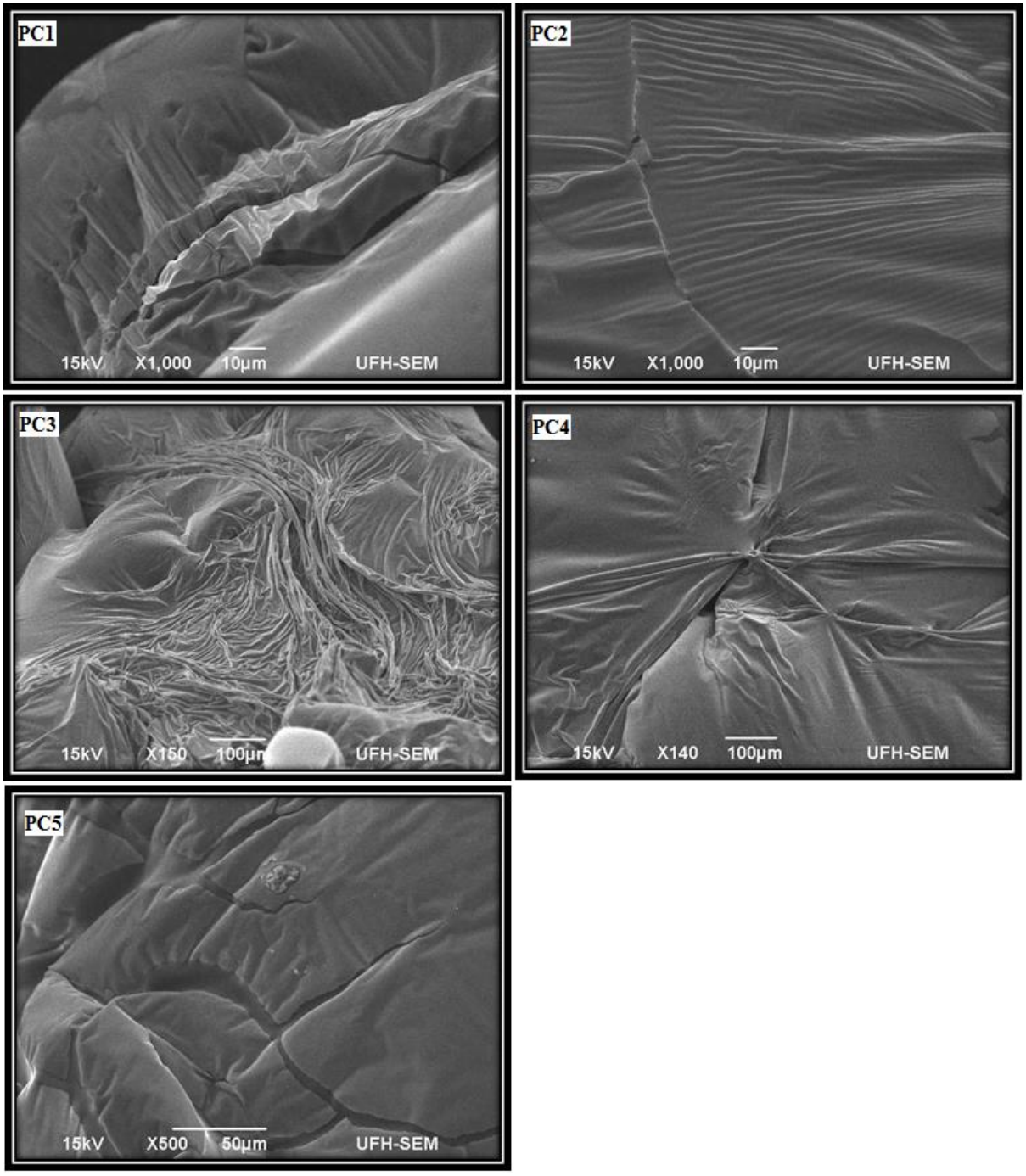

Figure 4.7: SEM images of polyamidoamine drug carriers PC1-5

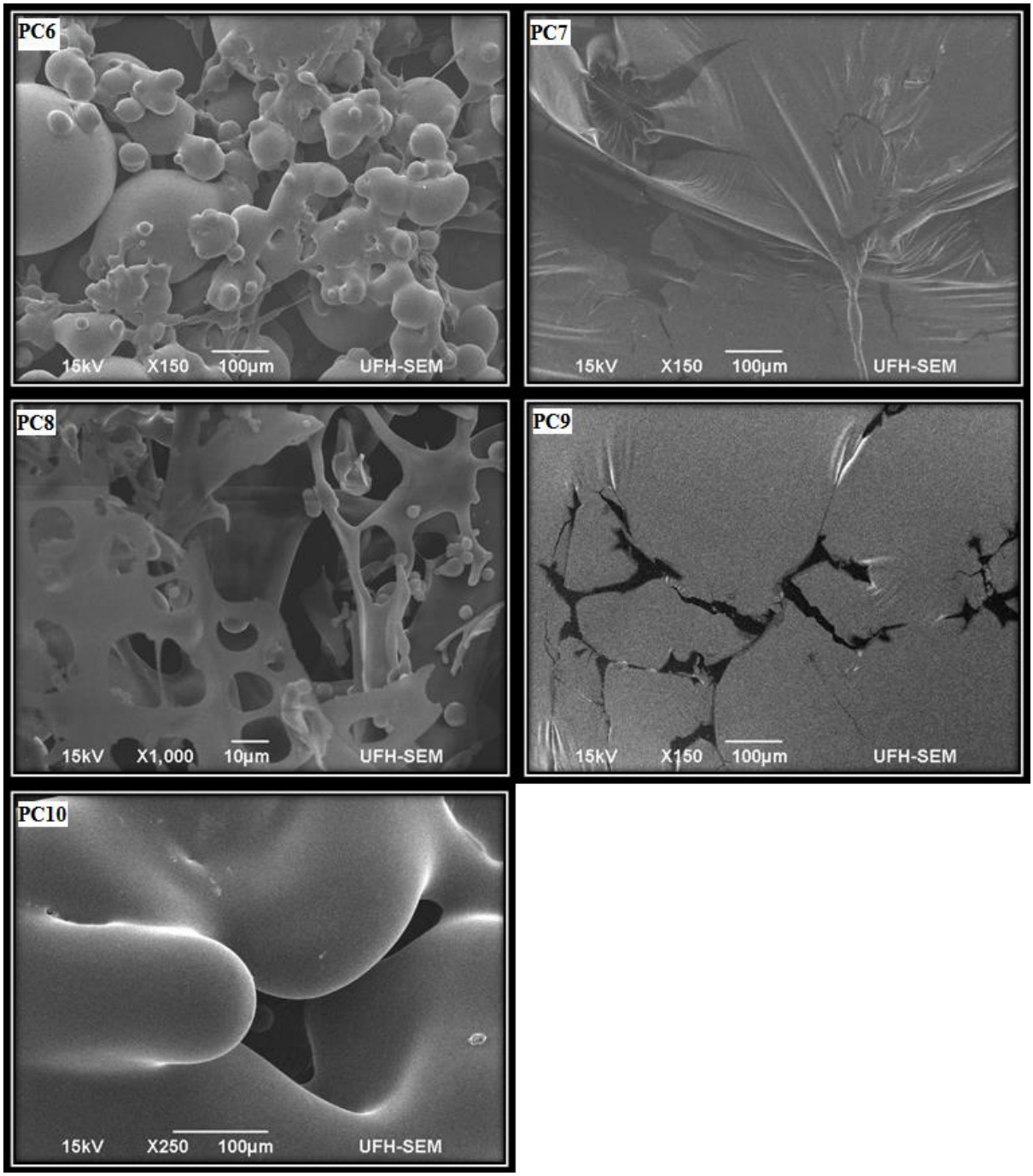

Figure 4.8: SEM images of polyamidoamine drug carriers PC6-10

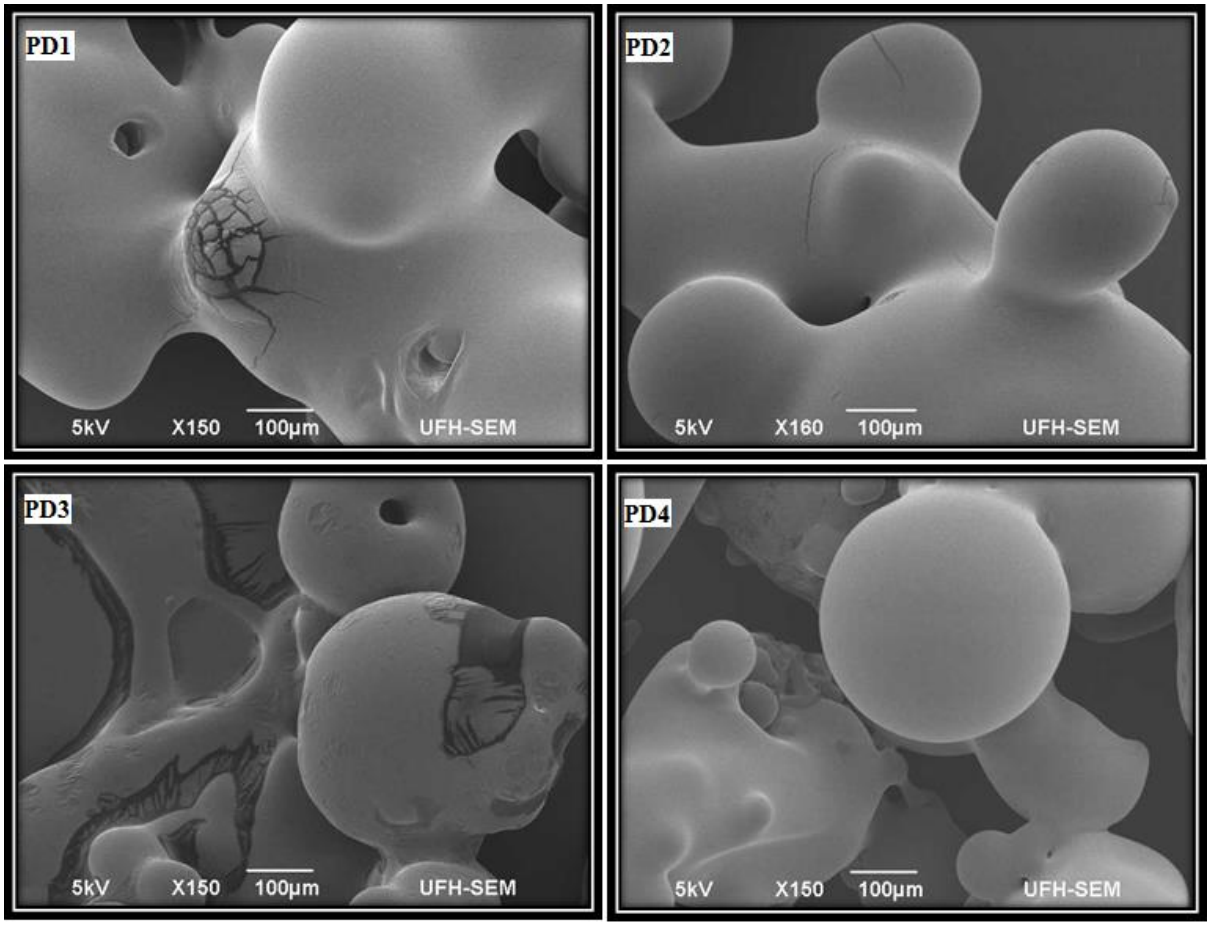

Figure 4.9: SEM images of polyamidoamine drug conjugates PD1-4

The surface morphology of the drug conjugates PD1, PD2, PD3 and PD4 (fig 4.9) did not differ much from each other. They all showed smooth surfaces with swollen spherical topologies which can be attributed to the successful polyaddition of amines to the methylenebisacrylamide (Aderibigbe et al., 2015). PD1 and PD3 displayed some sections of rough surface topologies.

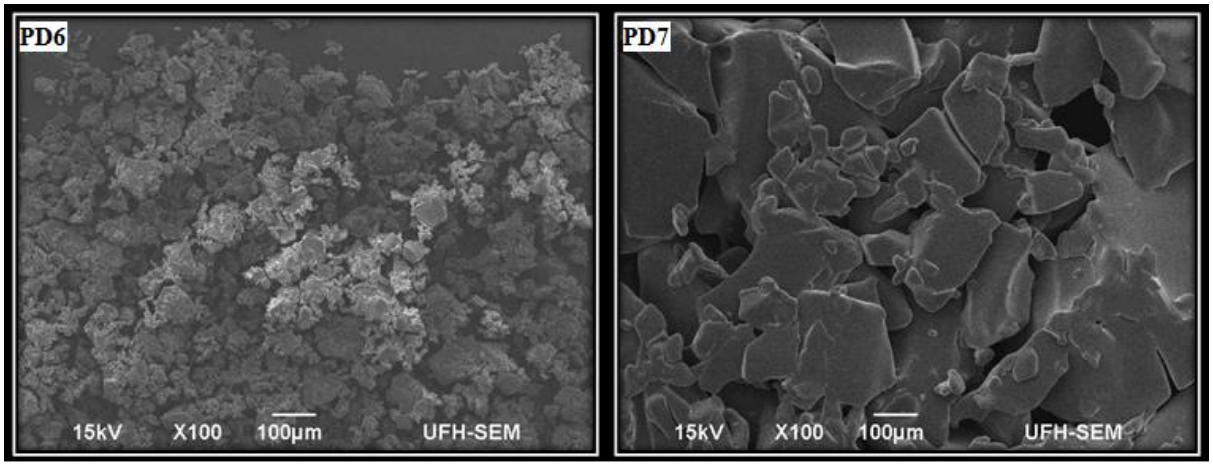

Figure 4.10: SEM images of polyamidoamine drug conjugates PD6-7

SEM image for conjugate PD6 displayed flacks with rough edges morphology. Smooth surfaced blocks topology was observed for SEM image of conjugate PD7.

4.5 EDX analysis

The elemental composition of polyamidoamine drug conjugates was obtained using energy dispersive x-ray analysis. EDX analysis data indicated that platinum and ferrocene based drugs were successfully incorporated to the polyamidoamine carriers as shown on table 4.3 below. The platinum content of the conjugates ranged from 1.59% in PD2 to 16.40% in PD6 while iron composition varied between 0.22% and 0.38%. Carbon composition ranged from 47.43% in PD7 to 25.52% in PD4. Nitrogen content was lowest at 3.15% in PD1 and highest at 18.70% for PD4. Oxygen composition varied from 13.32% to 39.0%. Chlorine content in the polyamidoamine drug conjugates ranged from 16.06% in PD6 to 23.38% in PD3.

	C %	N %	O %	Cl %	Pt %	Fe %
PD1	43.1	3.15	39.0	-	14.74	-
PD2	29.16	18.35	23.68	27.22	1.59	-
PD3	30.89	14.74	17.92	23.38	13.07	-
PD4	25.52	18.70	21.42	20.84	13.52	-
PD6	36.27	17.73	13.32	16.06	16.40	0.22
PD7	47.43	17.78	14.03	17.77	2.60	0.38

Table 4.3: Weight percent composition of drug conjugates from EDX data

4.6 TEM analysis

The polyamidoamine drug conjugates were also analysed by transmission electron microscopy to study the morphology. Figure 4.11 below displays micrographs of polyamidoamine drug conjugates. The sizes of particles can be estimated using the scale bar on the bottom left hand side of the images.

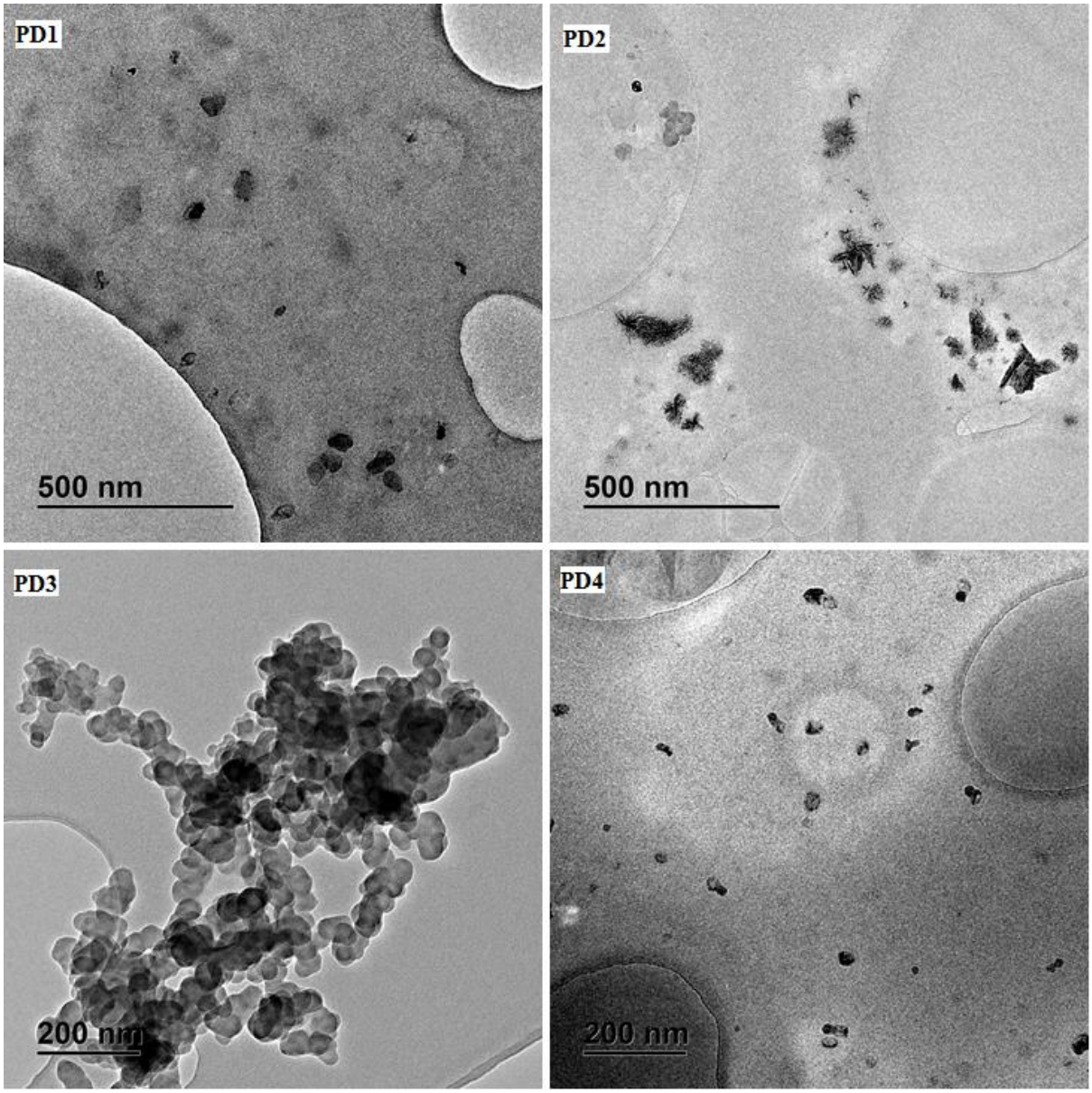

Figure 4.11: TEM images of polyamidoamine drug conjugates PD1-4

TEM analysis was performed on selected conjugates PD1, PD2, PD3 and PD4 as shown on fig 4.11. The TEM micrographs displayed smooth spherical topologies which also correlate to spherically shaped morphology observed for surface morphology studies (SEM) of the conjugates. The sizes of the particles were obtained in the nanometre range. The size of the particles making up the conjugates observed by transmission electron microscopy studies were in line with results obtained in particle size analysis discussed in the section below.

4.7 Particle size analysis

Compound	Average Particle Size (nm)	PDI (±SD)	Average Particle charge (±SD)
PC10	376.4 ± 92.70	0.390 ± 0.057	18.1 ± 6.35
PD3	258.3 ± 46.52	0.645 ± 0.158	30.2 ± 2.15
PD5	280.3 ± 25.48	0.533 ± 0.057	33.3 ± 4.54
PD6	247.1 ± 36.21	0.439 ± 0.125	29.0 ± 5.16

Table 4.4: Average particle size, polydispersity index (PDI) and surface charge of selected polymer drug conjugates and carrier

The polyamidoamine drug conjugate PD6 gave the smallest mean particle size (247.1 nm), followed by PD3 conjugate (258.3 nm), PD5 conjugate (280.3 nm) and PC10 carrier (376.4 nm). The carrier has the highest particle size compared to drug conjugates. The size of the particles making up the conjugates obtained from particle size analysis are comparable to the particle sizes observed by transmission electron microscopy studies. The polydispersity index (PDI) was highest in the conjugate PD3 and the least value was obtained for carrier PC10 at 0.390. The values for PDI are less than 1 indicating narrow molecular weight distribution which favours biomedical application of the polymers. Average particle charges ranged from 18.1 in carrier PC10 to 33.3 for conjugate PD5.

4.8 Drug release studies

Figure 4.12 shows the drug release profiles for conjugates PD3, PD5 and PD6 performed at pH 1.2 and 7.4 at a temperature of 37°C. All graphs showed a general trend of a sharp increase in the concentration of drug released that became steady after about 1500 minutes of the drug release experiments. Ferruti and co-workers reported similar drug release profiles of some of the PAA-platinates at pH 5.5 and 7.4 (Ferruti et al., 1999).

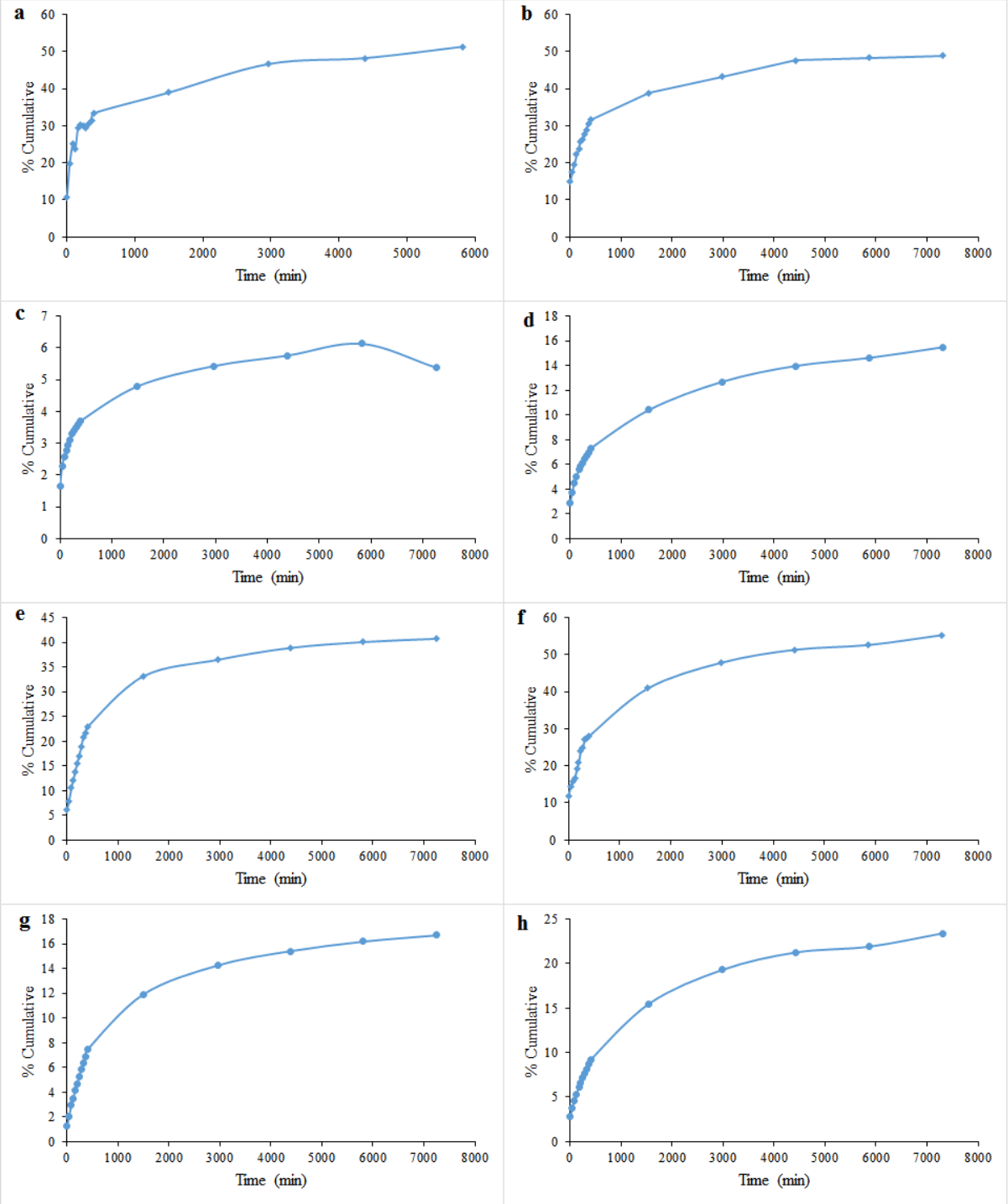

Figure 4.12: Percentage cumulative drug release profiles for (a) platinum drug release from PD3 at pH 1.2 (b) platinum drug release from PD3 at pH 7.4 (c) ferrocene drug release from PD5 at pH 1.2 (d) ferrocene drug release from PD5 at pH 7.4 (e) platinum drug release from PD6 at pH 1.2 (f) platinum drug release from PD6 at pH 7.4 (g) ferrocene drug release from PD6 at pH 1.2 (h) ferrocene drug release from PD6 at pH 7.4

Platinum drug release from conjugate PD3 at pH 1.2 was 51.4% after 5815 minutes. For the first 400 minutes, platinum drug release from conjugate PD3 was not linear but increased with time from 1495 minutes to 5815 minutes. On the other hand, platinum drug release for PD3 at pH 7.4 was faster in the first 400 minutes when 31.6% was released in the same period. 48.9% of drug was released in PD3 by 7300 minutes. The least amount of drug released from the conjugates was experienced in PD5 at pH 1.2 (fig 4.12c) where only 6% of the incorporated ferrocene drug was released in 5815 minutes of the experiment. 15.5% of drug was released in conjugate PD5 at pH 7.4 in the 7300 minutes carried out in the experiment. For conjugate PD6 at pH 1.2, 16.7% of the ferrocene drug was released in 7255 minutes. 40.7% of the platinum drug was released from PD6 at pH 1.2 in 7255 minutes. The percentage of ferrocene drug released was 23.4% for PD6 at pH 7.4 in 7300 minutes while 55.3% of platinum drug was released from conjugate PD6 at pH 7.4 in 7300 minutes of the experiment.

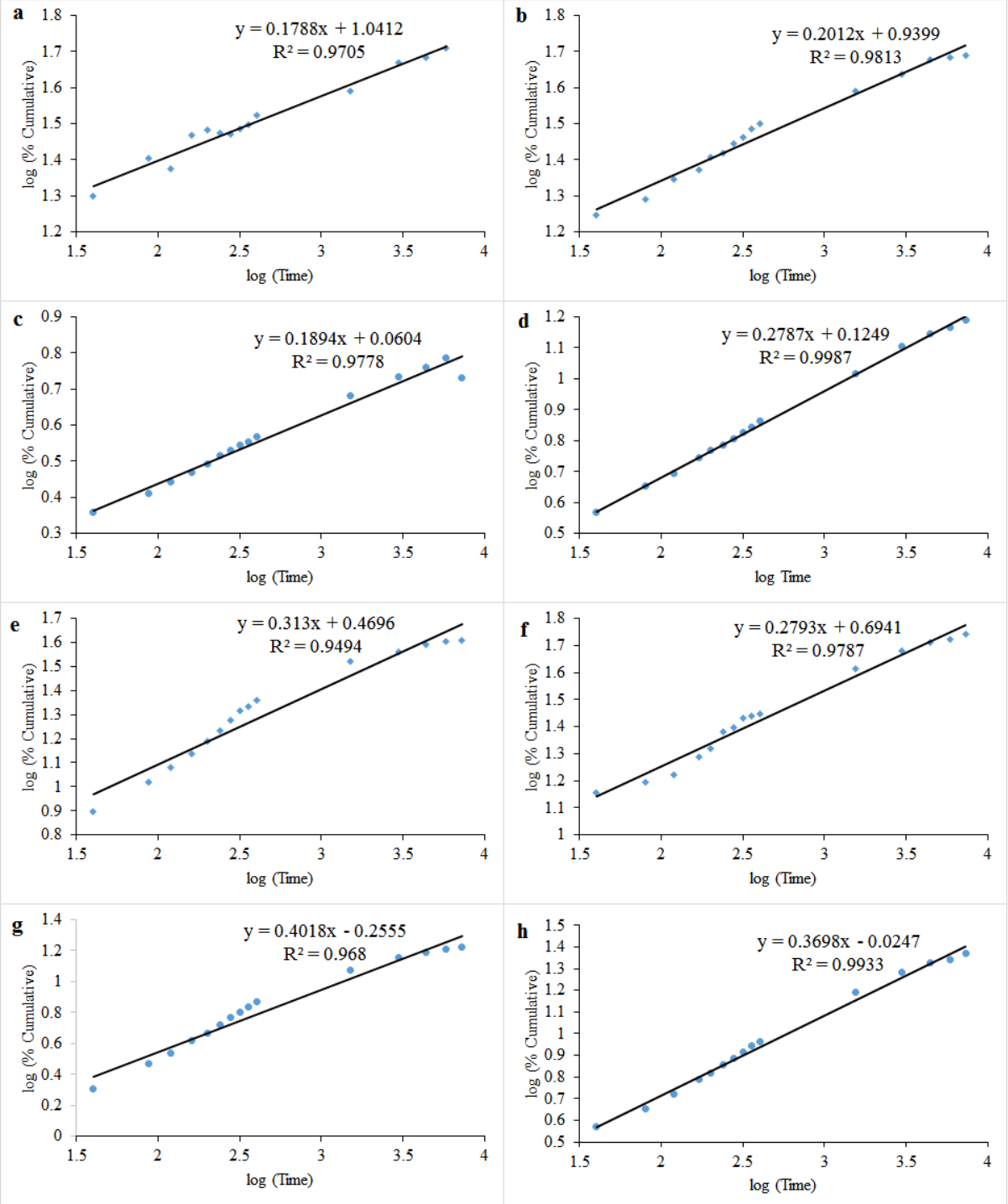

Figure 4.13: Korsmeyer-Peppas graphs for (a) platinum drug release from PD3 at pH 1.2 (b) platinum drug release from PD3 at pH 7.4 (c) ferrocene drug release from PD5 at pH 1.2 (d) ferrocene drug release from PD5 at pH 7.4 (e) platinum drug release from PD6 at pH 1.2 (f) platinum drug release from PD6 at pH 7.4 (g) ferrocene drug release from PD6 at pH 1.2 (h) ferrocene drug release from PD6 at pH 7.4

The mechanism of drug release of the polyamidoamine drug conjugates performed at a temperature of 37°C and at pH 1.2 and 7.4 was evaluated using Peppas equations 1 and 2 (Ritger & Peppas, 1987).

$$\frac{M_t}{M_T} = Kt^n \quad (1)$$

$$log\frac{M_t}{M_T} = n\log t + \log K \quad (2)$$

where M_t stands for the amount of drug released at time t, M_T is the total amount of polyamidoamine drug conjugate used, K is the kinetic constant and n is the diffusion or release exponent. Graphs of log (% Cumulative) against log (Time) of the experimental data were drawn and used to estimate diffusion exponent (n value).

		Korsmeyer-Peppas parameters	
Polymer drug conjugate	**pH**	**R^2**	**n**
PD3	1.2	0.9705	0.1788
	7.4	0.9813	0.2012
PD6	1.2	0.9494	0.313
	7.4	0.9787	0.2793

Table 4.5: Drug release studies for platinum based drug in polyamidoamine drug conjugates PD3 and PD6

		Korsmeyer-Peppas parameters	
Polymer drug conjugate	**pH**	**R^2**	**n**
PD5	1.2	0.9778	0.1894
	7.4	0.9987	0.2787
PD6	1.2	0.968	0.4018
	7.4	0.9933	0.3698

Table 4.6: Drug release studies for Fc-PDA in polyamidoamine drug conjugates PD5 and PD6 at pH 1.2 and 7.4

According to the conditions of Peppas equation, $n < 0.5$ indicates quasi-Fickian diffusion, $n = 0.5$ corresponds to Fickian diffusion, $0.5 < n < 1$ indicates anomalous or non-Fickian diffusion, $n = 1$ indicates case II (relaxation) transport while $n > 1$ corresponds to super case II transport (Costa & Lobo, 2001). The diffusion or release exponent (n values) for the drug release of the polyamidoamine conjugates at pH 1.2 and 7.4 was below 0.5 which indicate a quasi-Fickian diffusion mechanism.

4.9 Cytotoxicity activity evaluation

Samples of free drugs (K_2PtCl_4, Fc-PDA and DACH $PtCl_2$), conjugates PD1-4,6,7 and carrier PC10 were tested for cytotoxicity against human breast cancer cell lines (MCF-7 and MDA-MB-231) and normal cell lines (EA.hy926) as shown in table 7 below. Activities for the compounds are expressed as IC_{50}, the concentration of compound required for 50% inhibition in vitro.

Compound	IC_{50} ± SEM (µM)		
	MCF-7	**MDA-MB-231**	**EA.hy926**
PD1	10.68 ± 1.123	12.19 ± 1.10	88.04 ± 1.097
PD2	8.106 ± 1.224	9.353 ± 1.096	76.6 ± 1.096
PD3	8.613 ± 1.179	11.48 ± 1.168	> 100
PD4	12.45 ± 1.194	13.79 ± 1.175	> 100
PD6	> 100	> 100	> 100
PD7	1.455 ± 1.260	1.468 ± 1.209	> 100
PC10	73.01 ± 1.42	67.94 ± 1.154	> 100
K_2PtCl_4	> 100	> 100	> 100
Fc-PDA	> 100	> 100	> 100
DACH $PtCl_2$	2.49 ± 1.15	> 100	15.68 ± 1.13
Cisplatin	4.962 ± 1.267	4.124 ± 1.211	> 100

Table 4.7: Table showing results for in vitro analysis

The free drugs (K_2PtCl_4, Fc-PDA and DACH $PtCl_2$) exhibited weak cytotoxicity against all cell lines when compared to free drug cisplatin except for DACH $PtCl_2$ which showed good toxicity activity of 2.49 µM against MCF-7. The lack of cytotoxicity for Fc-PDA can be attributed to the presence of the ketone functional group next to the ferrocene ring since 4-ferrocenylbutanoic acid which lack the ketone functional group has been reported to exhibit high electrochemical reduction potential (Neuse, 2001). All samples showed weak activity against normal cell lines (EA.hy926) indicating selectivity towards cancer cell lines used in this study. The carrier PC10 was not conjugated to any drug and it showed negligible cytotoxicity activity against all cell lines screened as expected. Previous studies have also

shown that polyamidoamines generally exhibit low toxicity against various cell lines (Richardson et al., 1999; Ranucci et al., 1991). From the data obtained, polyamidoamine drug conjugate PD7 produced the highest toxic activity against both cancer cell lines (MCF-7 and MDA-MB-231) with IC_{50} values <1.5 µM whereas PD6 showed the least activity of all conjugates evaluated. In general, the conjugates (PD1-4,6,7) showed more activity against MCF-7 cell line than the other cell lines tested.

CHAPTER 5

Conclusion and Recommendations

5.1 Conclusion

Analogues of platinum and ferrocene, polyamidoamine carriers and conjugates were successfully prepared and characterized by various techniques such as FTIR, ^{1}H NMR, TEM, SEM and EDX. The polyamidoamine drug conjugates were formed from platinum and ferrocene based drugs by linking with amines. The conjugates particle size was obtained in the nanometre range as indicated by results from particle size analysis and transmission electron microscopy (TEM). The degree of conjugation of the drug onto the polymer varied from each conjugate.

Drug release from the conjugates occurred faster in the initial stages but become fairly constant after about 24 hour of the drug release experiments at both pH 1.2 and 7.4 at a temperature of 37°C. The highest percentage drug release was obtained for potassium tetrachloroplatinate drug release from conjugates PD3 and PD6. In PD3, 51.3% drug was released after 5815 minutes at pH 1.2 and 48.9% drug was released after 7300 minutes at pH 7.4 while in PD6, 40.7% drug was released after 7255 minutes at pH 1.2 and 55.3% drug was released after 7300 minutes at a pH of 7.4. Drug release from all polyamidoamine drug conjugates tested followed quasi-Fickian diffusion mechanism according to Korsmeyer-Peppas models for drug release.

The parent compounds bound to a polyamidoamine carrier showed more cytotoxicity compared to the free drug hence polymer conjugation has proved to be useful in enhancement of anticancer properties of unconjugated drug molecules. The combination of two drugs Fc-PDA and DACH $PtCl_2$ in polyamidoamine drug conjugate PD7 enhanced the cytotoxicity of

drugs as observed by the good results of <1.5 µM which is significantly more pronounced than the singly conjugated polyamidoamine drug conjugates. However, the observations were not the same in the case of conjugate PD6 which is composed of Fc-PDA and K_2PtCl_4 drugs.

5.2 Recommendations

Objectives of the research project were achieved but improvements of the yield of carriers and conjugates is necessary. Although established procedures were followed, conditions should be improved to elevate the yield of product obtained from the synthetic reactions. Different linkers other than 1,3-propanediamine, 3-dimethylamino-1-propylamine, dopamine and 3-diethylaminopropylamine which were used in this study need to be assessed to find out if they have an impact on effectiveness of the polyamidoamine conjugates. In vivo studies should be carried out for the cytotoxic conjugates to explore the potential of the polyamidoamine conjugates in living organisms. Evaluation of drug release at pH 5.8 which represent the pH of the biological environment of tumour tissue is also necessary.

REFERENCES

Aderibigbe, B.A., Sadiku, E.R., Sinha Ray, S., Mbianda, X.Y., Fotsing, M.C., Agwuncha, S.C. & Owonubi, S.J. **2015**. Synthesis and characterization of polyamidoamine conjugates of neridronic acid. *Polymer Bulletin*, 72(3): 417–439.

Alberts, D.S. & Noel, J.K. **1995**. Cisplatin-associated neurotoxicity: can it be prevented? *Anti-Cancer drugs*, 6: 369–383.

Alexis, F., Pridgen, E., Molnar, L.K. & Farokhzad, O.C. **2008**. Factors affecting the clearance and biodistribution of polymeric nanoparticles. In *Molecular Pharmaceutics*. 5(4): 505–515.

Allen, T.M. & Cullis, P.R. **2004**. Drug Delivery Systems: Entering the Mainstream. *Science*, 303(5665): 1818–1822.

Altered-states.net, **2015**. *Your body's pH levels*, http://altered-states.net/barry/update178/ [Accessed on 2 April 2015].

Bae, Y.H. & Kim, S.W. **1993**. Bae, Y.H. and Kim, S.W., 1993. Hydrogel delivery systems based on polymer blends, block co-polymers or interpenetrating networks. *Advanced Drug Delivery Reviews*, 11(1): 109–135.

Banerjee, S.S., Aher, N., Patil, R. & Khandare, J., **2012**. Poly(ethylene glycol)-prodrug conjugates: concept, design, and applications. *Journal of drug delivery*, 2012.

Bangham, A. D., & Horne, R.W. **1964**. Negative staining of phospholipids and their structural modification by surface active agents as observed in the electron microscope. *J. Mol. Biol.* 8(5): 660–668

Boulikas, T., Pantos, A., Bellis, E. & Christofis, P. **2007**. Designing platinum compounds in cancer: structures and mechanisms. *Cancer Therapy Vol Cancer Therapy*, 5(5): 537–583.

Boulikas, T. & Vougiouka, M. **2003**. Cisplatin and platinum drugs at the molecular level. (Review). *Oncology reports*, 10(6): 1663–1682.

Brunton, L.L., Chabner, B.A. and Knollmann, B.C., **2011**. Goodman & Gilman's The Pharmacological Basis of Therapeutics. 12th ed.

Bullinger, H.J. ed., **2009**. Technology guide: Principles-applications-trends. Springer Science & Business Media

Cavalli, R., Bisazza, A., Sessa, R., Primo, L., Fenili, F., Manfredi, A., Ranucci, E. & Ferruti, P. **2010**. Amphoteric agmatine containing polyamidoamines as carriers for plasmid dna in vitro and in vivo delivery. *Biomacromolecules*, 11(10): 2667–2674.

Chadha, R., Kapoor, V., Thakur, D., Kaur, R., Arora, P. & Jain, D. **2008**. Drug carrier systems for anticancer agents: A review. *J. Sci. Ind. Res.*, 67(3): 185–197.

Costa, P. & Lobo, J.M.S. **2001**. Modeling and comparison of dissolution profiles. *European journal of pharmaceutical sciences*, 13(2): 123-133.

Danusso, F. & Ferruti, P. **1970**. Synthesis of tertiary amine polymers. *Polymer*, 11(2): 88–113.

Desoize, B. & Madoulet, C. **2002**. Particular aspects of platinum compounds used at present in cancer treatment. *Critical Reviews in Oncology/Hematology*, 42(3): 317–325.

Duncan, R. **2006**. Polymer conjugates as anticancer nanomedicines. *Nature reviews. Cancer*, 6(9): 688–701.

Duncan, R. **2011**. Polymer therapeutics as nanomedicines: New perspectives. *Current Opinion in Biotechnology*, 22(4): 492–501.

Duncan, R. **2003**. The dawning era of polymer therapeutics. *Nature reviews. Drug discovery*, 2(5): 347–60.

Duncan, R., Cable, H.C., Lloyd, J.B., Rejmanová, P. & Kopeček, J. **1982**. Degradation of side-chains of N-(2-hydroxypropyl)methacrylamide copolymers by lysosomal thiol-proteinases. *Bioscience Reports*, 2(12): 1041–1046.

Duncan, R. & Kopeček, J. **1984**. Soluble synthetic polymers as potential drug carriers. *Polymers in Medicine*. 51–101.

Duncan R., Rejmanova P., Kopecek J. and Lloyd J.B. **1981**. Pinocytic uptake and intracellular degradation of N-(2-hydroxypropyl) methacrylamide copolymers. A potential drug delivery system. *Biochimica et Biophysica Acta (BBA)-General Subjects*, 678(1): 143–150

Duncan, R. & Vicent, M.J. **2010**. Do HPMA copolymer conjugates have a future as clinically useful nanomedicines? A critical overview of current status and future opportunities. *Advanced Drug Delivery Reviews*, 62(2): 272–282.

Emilitri, E., Ranucci, E. & Ferruti, P. **2005**. New poly(amidoamine)s containing disulfide linkages in their main chain. *Journal of Polymer Science, Part A: Polymer Chemistry*, 43(7): 1404–1416.

Farokhzad, O.C. & Langer, R. **2006**. Nanomedicine: Developing smarter therapeutic and diagnostic modalities. *Advanced Drug Delivery Reviews*, 58(14): 1456–1459.

Farrell, N. **2005**. Platinum anticancer drugs: From laboratory to clinic. *Medicinal Inorganic Chemistry*. 62–79.

Ferruti P. **1996** Ion-chelating polymers (Medical Applications). Polymeric Materials Encyclopedia 5: 3334-3359

Ferruti P., Danusso F., Franchi G., Polentarutti N. & Garattini S., **1973**. Effects of a series of new synthetic high polymers on cancer metastases. *J. Med. Chem*, 16(5): 496–499

Ferruti, P., Marchisio, M.A. & Barbucci, R. **1985**. Synthesis, physico-chemical properties and biomedical applications of poly(amidoamine)s. *Polymer*. 1336–1348.

Ferruti, P., Marchisio, M.A. & Duncan, R. **2002**. Poly(amido-amine)s: Biomedical applications. *Macromolecular Rapid Communications*, 23(5–6): 332–355.

Ferruti, P., Ranucci, E., Bignotti, F., Sartore, L., Bianciardi, P. & Marchisio, M.A. **1995**. Degradation behaviour of ionic stepwise polyaddition polymers of medical interest. *Journal of biomaterials science. Polymer edition*, 6(9): 833–44.

Ferruti, P., Ranucci, E., Sartore, L., Bignotti, F., Marchisio, M.A., Bianciardi, P. & Veronese, F.M. **1994**. Recent results on functional polymers and macromonomers of interest as biomaterials or for biomaterial modification. *Biomaterials*, 15(15): 1235–1241.

Ferruti, P., Ranucci, E., Trotta, F., Gianasi, E., Evagorou, E.G., Wasil, M., Wilson, G. & Duncan, R., **1999**. Synthesis, characterisation and antitumour activity of platinum (II) complexes of novel functionalised poly(amidoamine)s. *Macromolecular Chemistry and Physics*, 200(7): 1644-1654.

Francesco, A.M. Di, Ruggiero, A. & Riccardi, R. **2002**. Cellular and molecular aspects of drugs of the future: oxaliplatin. *Cellular and molecular life sciences*, 59(11): 1914–1927.

Fricker, S.P. **2007**. Metal based drugs: from serendipity to design. *Dalton Transactions*, (43): 4903–4917.

Galanski M. & Keppler B.K. **2007**. Searching for the magic bullet: Anticancer platinum drugs which can be accumulated or activated in the tumour tissue. *Anti-cancer agents in medicinal chemistry* 7(1): 55–73.

Ganta, S., Devalapally, H., Shahiwala, A. & Amiji, M. **2008**. A review of stimuli-responsive nanocarriers for drug and gene delivery. *Journal of Controlled Release*, 126(3): 187–204.

Gore, M.E., Fryatt, I., Wiltshaw, E., Dawson, T., Robinson, B.A. & Calvert, A.H. **1989**. Cisplatin/carboplatin cross-resistance in ovarian cancer. *British journal of cancer*, 60(5): 767–769.

Goren, M.P., Wright, R.K. & Horowitz, M.E. **1986**. Cumulative renal tubular damage associated with cisplatin nephrotoxicity. *Cancer Chemotherapy and Pharmacology*, 18(1): 69–73.

Greco, F. & Vicent, M.J. **2009**. Combination therapy: Opportunities and challenges for polymer – drug conjugates as anticancer nanomedicines. *Advanced Drug Delivery Reviews*, 61(13): 1203–1213.

Greenwald, R.B., Choe, Y.H., McGuire, J. & Conover, C.D. **2003**. Effective drug delivery by PEGylated drug conjugates. *Advanced Drug Delivery Reviews*, 55(2): 217–250.

Gros, L., Ringsdorf, H. & Schupp, H. **1981**. Polymeric Antitumor Agents on a Molecular and on a Cellular Level? *Angewandte Chemie International Edition*, 20(4): 305–325.

Gunatillake, P.A., Adhikari, R. & Gadegaard, N. **2003**. Biodegradable synthetic polymers for tissue engineering. *European Cells and Materials*, 5(1): 1–16.

Haag, R. & Kratz, F. **2006**. Polymer therapeutics: Concepts and applications. *Angewandte Chemie - International Edition*, 45(8): 1198–1215.

Hill, I.R.C., Garnett, M.C., Bignotti, F. & Davis, S.S. **1999**. In vitro cytotoxicity of poly(amidoamine)s: Relevance to DNA delivery. *Biochimica et Biophysica Acta - General Subjects*, 1427(2): 161–174.

Hoare, T.R. & Kohane, D.S. **2008**. Hydrogels in drug delivery: Progress and challenges. *Polymer*, 49(8): 1993–2007.

Hoffman, A.S. **2012**. Hydrogels for biomedical applications. *Advanced Drug Delivery Reviews*, 64: 18–23.

Kaluderović, G.N. & Paschke, R. **2011**. Anticancer metallotherapeutics in preclinical development. *Current medicinal chemistry*, 18(31): 4738–4752.

Kang, X., Xiao, H.-H., Song, H.-Q., Jing, X.-B., Yan, L.-S. & Qi, R.-G. **2015**. Advances in drug delivery system for platinum agents based combination therapy. *Cancer biology & medicine*, 12(4): 362–74.

Kartalou, M. & Essigmann, J.M. **2001**. Mechanisms of resistance to cisplatin. *Mutation Research - Fundamental and Molecular Mechanisms of Mutagenesis*, 478(1): 23–43.

Kelland, L. **2007**. The resurgence of platinum-based cancer chemotherapy. *Nature reviews. Cancer*, 7(8): 573–584.

Kidani, Y., Inagaki, K., Iigo, M., Hoshi, A. & Kuretani, K. **1978**. Antitumor activity of 1,2-diaminocyclohexane--platinum complexes against sarcoma-180 ascites form. *Journal of Medicinal Chemistry*, 21(12): 1315–1318.

Knox, R.J., Friedlos, F., Lydall, D. a, Ii, T. & Roberts, J.J. **1986**. Mechanism of cytotoxicity of anticancer platinum drugs: evidence that cis-diamminedichloroplatinum (II) and cis-diammine-(1, 1-cyclobutanedicarboxylato) platinum (II) differ only in the kinetics of their interaction with DNA. *Cancer Research*, 46(4 Part 2): 1972–1979.

Kociba, R.J., Sleight, S.D. and Rosenberg, B., **1970**. Inhibition of Dunning ascitic leukemia and Walker 256 carcinosarcoma with cis-diamminedichloroplatinum (NSC-119875). *Cancer chemotherapy reports*, 54(5): 325

Kopeček, J. **1984**. Controlled biodegradability of polymers - a key to drug delivery systems. *Biomaterials*, 5(1): 19–25.

Kopeček, J. and Ulbrich, K., **1983**. Biodegradation of biomedical polymers. *Progress in polymer science* 9(1): 1-58.

Köpf-Maier, P., Köpf, H. & Neuse, E.W. **1984**. Ferricenium complexes: A new type of water-soluble antitumor agent. *Journal of Cancer Research and Clinical Oncology*, 108(3): 336–340.

Kwon, G.S. & Okano, T. **1996**. Polymeric micelles as new drug carriers. *Advanced Drug Delivery Reviews*, 21(2): 107–116.

Larson, N. & Ghandehari, H. **2012**. Polymeric conjugates for drug delivery. *Chemistry of Materials*, 24(5): 840–853.

Li, C. & Wallace, S. **2008**. Polymer-drug conjugates: Recent development in clinical oncology. *Advanced Drug Delivery Reviews*, 60(8): 886–898.

Li, C., Yu, D.F., Newman, R.A., Cabral, F., Stephens, L.C., Hunter, N., Milas, L. & Wallace, S. **1998**. Complete regression of well-established tumors using a novel water-soluble poly(L-glutamic acid) paclitaxel conjugate. *Cancer Research*, 58(11): 2404–2409.

Li, W., Zhan, P., De Clercq, E., Lou, H. & Liu, X., **2013**. Current drug research on PEGylation with small molecular agents. *Progress in Polymer Science*, 38(3): 421-444.

Liechty, W.B., Kryscio, D.R., Slaughter, B.V. & Peppas, N.A. **2010**. Polymers for Drug Delivery Systems. *Annual Review of Chemical and Biomolecular Engineering*, 1(1): 149–173.

Malam, Y., Loizidou, M. & Seifalian, A.M. **2009**. Liposomes and nanoparticles: nanosized vehicles for drug delivery in cancer. *Trends in Pharmacological Sciences*, 30(11): 592–599.

Malgesini, B., Verpilio, I., Duncan, R. & Ferruti, P. **2003**. Poly(amido-amine)s carrying primary amino groups as side substituents. *Macromolecular Bioscience*, 3(1): 59–66.

Martin R.B. **1999**. Platinum Complexes: Hydrolysis and Binding to N(7) and N(1) of purines. *Cisplatin: Chemistry and biochemistry of a leading anticancer drug*. 183–205

Matsumura, Y. & Maeda, H. **1986**. A new concept for macromolecular therapeutics in cancer chemotherapy: Mechanism of tumoritropic accumulation of proteins and the antitumor agent smancs. *Cancer Research*, 46(12 I): 6387–6392.

Mellman, I. **1996**. Endocytosis and molecular sorting. *Annual Review of Cell and Developmental Biology*, 12(1): 575–625.

Mesotheliomaweb.org, **2015**. *Categories of Chemotherapeutic Agents*, http://www.mesotheliomaweb.org/categories.htm [Accessed on 30 April 2015].

Miller, R.P., Tadagavadi, R.K., Ramesh, G. & Reeves, W.B. **2010**. Mechanisms of cisplatin nephrotoxicity. *Toxins*, 2(11): 2490–2518.

Mohammadifar, E., Kharat, A.N. & Adeli, M. **2015**. Polyamidoamine and polyglycerol; their linear, dendritic and linear–dendritic architectures as anticancer drug delivery systems. *J. Mater. Chem. B*, 3896(3): 3896–3921.

Mufula, A.I. & Neuse, E.W. **2011**. Macromolecular carriers for methotrexate and ferrocene in cancer chemotherapy. *Journal of Inorganic and Organometallic Polymers and Materials*, 21(3): 511–526.

Muggia, F.M., Bonetti, A., Hoeschele, J.D., Rozencweig, M. & Howell, S.B. **2015**. Platinum antitumor complexes: 50 Years since Barnett Rosenberg's discovery. *Journal of Clinical Oncology*, 33(35): 4219–4226.

Mukaya, H.E., Neuse, E.W., van Zyl, R.L. & Chen, C.T. **2015**. Synthesis and preliminary bio-evaluation of polyaspartamide Co-conjugates of p-amino-salicylic acid chelated platinum (II) and ferrocene complexes. *Journal of Inorganic and Organometallic Polymers and Materials*, 25(3): 367–375.

N'Da, D.D. & Neuse, E.W. **2006**. Polyamidoamines as drug carriers: synthesis of polymers featuring extrachain-type primary amino groups as drug-anchoring sites. *South African Journal of Chemistry*, 59(1): 65–70.

Neuse, E.W., **2001**. Polymeric organoiron compounds as prodrugs in cancer research. *In Macromolecular Symposia*, 172(1): 127-138. WILEY-VCH Verlag GmbH.

Nguyen, A., Vessières, A., Hillard, E.A., Top, S., Pigeon, P. & Jaouen, G. **2007**. Ferrocifens and Ferrocifenols as New Potential Weapons against Breast Cancer. *CHIMIA International Journal for Chemistry*, 61(11): 716–724.

Nobelprize.org **2001**, The Nobel Prize in Physiology or Medicine for 2001 – Press Release, *Nobel Media AB 2014.* http://www.nobelprize.org/nobel_prizes/medicine/laureates/2001/press.html [Accessed on 16 May 2017]

Ornelas, C. **2011**. Application of ferrocene and its derivatives in cancer research. *New Journal of Chemistry*, 35(10): 1973.

Paramjot, Khan, N.M., Kapahi, H., Kumar, S., Bhardwaj, T.R., Arora, S. & Mishra, N. **2015**. Role of polymer–drug conjugates in organ-specific delivery systems. *Journal of Drug Targeting*, 23(5): 387–416.

Parhi, P., Mohanty, C. & Sahoo, S.K. **2012**. Nanotechnology-based combinational drug delivery: an emerging approach for cancer therapy. *Drug discovery today*, 17(17-18): 1044-1052.

Park, J.W. **2002**. Liposome-based drug delivery in breast cancer treatment. *Breast cancer research : BCR*, 4(3): 95–99.

Pasetto, L.M., D'Andrea, M.R., Brandes, A.A., Rossi, E. & Monfardini, S. **2006**. The development of platinum compounds and their possible combination. *Critical Reviews in Oncology/Hematology*, 60(1): 59–75.

Persidis, A. **1999**. Cancer multidrug resistance. *Nature biotechnology*, 17: 94–95.

Pizarro, A.M., Habtemariam, A. & Sadler, P.J. **2010**. Activation mechanisms for organometallic anticancer complexes. *Topics in Organometallic Chemistry*, 32: 21–56.

Qiu, Y. & Park, K. **2001**. Environment-sensitive hydrogels for drug delivery. *Advanced Drug Delivery Reviews*, 53(3): 321-339.

Rabik, C.A. & Dolan, M.E. **2007**. Molecular mechanisms of resistance and toxicity associated with platinating agents. *Cancer Treatment Reviews*, 33(1): 9–23.

Ranson, M. & Thatcher, N. **1999**. Paclitaxel: a hope for advanced non-small cell lung cancer? *Expert opinion on investigational drugs*, 8(6): 837–848.

Ranucci, E., Spagnoli, G., Ferruti, P., Sgouras, D. & Duncan, R., **1991**. Poly (amidoamine)s with potential as drug carriers: degradation and cellular toxicity. *Journal of Biomaterials Science, Polymer Edition*, 2(4): 303-315.

Rapoport, N. **2007**. Physical stimuli-responsive polymeric micelles for anti-cancer drug delivery. *Progress in Polymer Science (Oxford)*, 32(8–9): 962–990.

Raymond, E., Faivre, S., Chaney, S., Woynarowski, J. & Cvitkovic, E. **2002**. Cellular and molecular pharmacology of oxaliplatin. *Molecular cancer therapeutics*, 1(3): 227–235.

Reedijk, J. **1996**. Improved understanding in platinium antitumour chemistry. *Chemical Communications*, (7): 801–806.

Reedijk, J. & Lohman, P.H. **1985**. Cisplatin: synthesis, antitumour activity and mechanism of action. *Pharmaceutisch weekblad. Scientific edition*, 7(5): 173–180.

Rejmanová, P., Kopeček, J., Duncan, R. & Lloyd, J.B. **1985**. Stability in rat plasma and serum of lysosomally degradable oligopeptide sequences in N-(2-hydroxypropyl) methacrylamide copolymers. *Biomaterials*, 6(1): 45–48.

Richardson, S., Ferruti, P. and Duncan, R., **1999**. Poly (amidoamine) s as potential endosomolytic polymers: evaluation in vitro and body distribution in normal and tumour-bearing animals. *Journal of drug targeting*, 6(6): 391-404.

Ringsdorf, H. **1975**. Structure and properties of pharmacologically active polymers. *Journal of Polymer Science: Polymer Symposia*, 51(1): 135–153.

Ritger, P.L. & Peppas, N.A., **1987**. A simple equation for description of solute release I. Fickian and non-Fickian release from non-swellable devices in the form of slabs, spheres, cylinders or discs. *Journal of controlled release*, 5(1): 23-36.

Rosenberg, B. & VanCamp, L. **1970**. The successful regression of large solid sarcoma 180 tumors by platinum compounds. *Cancer Research*, 30(6): 1799–1802.

Rosenberg, B., Vancamp, L. & Krigas, T. **1965**. Inhibition of cell division in Escherichia coli by electrolysis products from a platinum electrode. *Nature*, 205(4972): 698–699.

Rösler, A., Vandermeulen, G.W. & Klok, H.A. **2001**. Advanced drug delivery devices via self-assembly of amphiphilic block copolymers. *Advanced drug delivery reviews*, 53(1): 95–108.

Ruiz-Esparza, G.U., Wu, S., Segura-Ibarra, V., Cara, F.E., Evans, K.W., Milosevic, M., Ziemys, A., Kojic, M., Meric-Bernstam, F., Ferrari, M. & Blanco, E. **2014**. Polymer nanoparticles encased in a cyclodextrin complex shell for potential site- and sequence-specific drug release. *Advanced Functional Materials*, 24(30): 4753–4761.

Ryan J. Burri and Nancy Y. Lee. **2009**. Anticancer Therapy, Concurrent Chemotherapy and Radiotherapy for head and neck cancer

dos Santos Guimarães, I., Daltoé, R.D., Herlinger, A.L., Madeira, K.P., Ladislau, T., Valadão, I.C., Junior, P.C.M.L., Teixeira, S.F., Amorim, G.M., dos Santos, D.Z. and Demuth, K.R., **2013**. Conventional Cancer Treatment. *Cancer Treatment-Conventional and Innovative approaches*

dos Santos Giuberti, C., de Oliveira Reis, E.C., Ribeiro Rocha, T.G., Leite, E.A., Lacerda, R.G., Ramaldes, G.A. & de Oliveira, M.C. **2011**. Study of the pilot production process of long-circulating and pH-sensitive liposomes containing cisplatin. *Journal of liposome research*, 21(1): 60–9.

Satchi-Fainaro, R., Duncan, R. & Barnes, C.M. **2006**. Polymer therapeutics for cancer: Current status and future challenges. *Advances in Polymer Science*, 193(1): 1–65.

Schaefer, S.D., Post, J.D., Close, L.G. & Wright, C.G. **1985**. Ototoxicity of low- and moderate-dose cisplatin. *Cancer*, 56(8): 1934–1939.

Schwall, C.T. & Banerjee, I.A. **2009**. Micro- and nanoscale hydrogel systems for drug delivery and tissue engineering. *Materials*, 2(2): 577–612.

Shenoy, D.B. & Amiji, M.M. **2005**. Poly (ethylene oxide)-modified poly (ε-caprolactone) nanoparticles for targeted delivery of tamoxifen in breast cancer. *International Journal of Pharmaceutics*, 293(1): 261–270.

Shiah, J.G., Dvořák, M., Kopečková, P., Sun, Y., Peterson, C.M. & Kopeček, J. **2001**. Biodistribution and antitumour efficacy of long-circulating N-(2-hydroxypropyl)methacrylamide copolymer-doxorubicin conjugates in nude mice. *European Journal of Cancer*, 37(1): 131–139.

Siddik, Z.H. **2003**. Cisplatin: mode of cytotoxic action and molecular basis of resistance. *Oncogene*, 22(47): 7265–79.

Silva, G.A., Marques, A.P., Gomes, M.E., Coutinho, O.P., & Reis, R.L. **2004**. Cytotoxicity screening of biodegradable polymeric systems. In Biodegradable Systems in Tissue Engineering and Regenerative Medicine, Reis, R.L. & San Róman, J. (Eds.), Chapter 19. Boca Raton, FL: CRC Press

Singh, A., Talekar, M., Tran, T.H., Samanta, A., Sundaram, R. and Amiji, M., **2014**. Combinatorial approach in the design of multifunctional polymeric nano-delivery systems for cancer therapy. *Journal of Materials Chemistry B*, 2(46): 8069-8084

van Staveren, D.R. & Metzler-Nolte, N. **2004**. Bioorganometallic chemistry of ferrocene. *Chemical reviews*, 104(12): 5931–5985.

Stewart, D.J. **2007**. Mechanisms of resistance to cisplatin and carboplatin. *Critical Reviews in Oncology/Hematology*, 63(1): 12–31.

Sugahara, S.I., Kajiki, M., Kuriyama, H. & Kobayashi, T.R. **2007**. Complete regression of xenografted human carcinomas by a paclitaxel–carboxymethyl dextran conjugate (AZ10992). *Journal of controlled release*, 117(1): 40-50.

Suri, S.S., Fenniri, H. & Singh, B. **2007**. Nanotechnology-based drug delivery systems. *J Occup Med Toxicol.*, 2(1): 16.

Talarico, T., Phillips, D.R., Deacon, G.B., Rainone, S. & Webster, L.K. **1999**. Activity and DNA binding of new organoamidoplatinum (II) complexes. *Investigational New Drugs*, 17(1): 1–15.

Thakor, A.S. & Gambhir, S.S. **2013**. Nanooncology: The future of cancer diagnosis and therapy. *CA: A Cancer Journal for Clinicians*, 63(6): 395–418.

Tong, R. & Cheng, J., **2007**. Anticancer polymeric nanomedicines. *Journal of Macromolecular Science, Part C: Polymer Reviews*, 47(3): 345-381.

Twaites, B., de las Heras Alarcón, C. & Alexander, C. **2005**. Synthetic polymers as drugs and therapeutics. *Journal of Materials Chemistry*, 15(4): 441.

Uchegbu, I.F. & Schatzlein, A.G. **2006**. *Polymers in drug delivery*. CRC Press.

Urbán, P., Valle-Delgado, J.J., Mauro, N., Marques, J., Manfredi, A., Rottmann, M., Ranucci, E., Ferruti, P. & Fernàndez-Busquets, X. **2014**. Use of poly(amidoamine) drug conjugates for the delivery of antimalarials to Plasmodium. *Journal of Controlled Release*, 177(1): 84–95.

Van Zutphen, S. & Reedijk, J. **2005**. Targeting platinum anti-tumour drugs: Overview of strategies employed to reduce systemic toxicity. *Coordination Chemistry Reviews*, 249(24): 2845–2853.

Vasey, P.A., Kaye, S.B., Morrison, R., Twelves, C., Wilson, P., Duncan, R., Thomson, A.H., Murray, L.S., Hilditch, T.E., Murray, T., Burtles, S., Fraier, D. & Frigerio, E. **1999**. Phase I clinical and pharmacokinetic study of PK1 [N-(2-hydroxypropyl) methacrylamide copolymer doxorubicin]: first member of a new class of chemotherapeutic agents—drug-polymer conjugates. *Clinical Cancer Research*, 5(1): 83–94.

Vicent, M.J. & Duncan, R. **2006**. Polymer conjugates: Nanosized medicines for treating cancer. *Trends in Biotechnology*, 24(1): 39–47.

Vichai V & Kirtikara K. **2006**. Sulforhodamine B colorimetric assay for cytotoxicity screening. *Nature protocols*, 1(3):1112-1116.

Wang, A.Z., Langer, R. & Farokhzad, O.C. **2012**. Nanoparticle Delivery of Cancer Drugs. *Annual Review of Medicine*, 63(1): 185–198.

Wang, D. & Lippard, S.J. **2005**. Cellular processing of platinum anticancer drugs. *Nature Reviews Drug Delivery*, 4(4): 307–320.

Wang, X. & Guo, Z. **2013**. Targeting and delivery of platinum-based anticancer drugs. *Chemical Society Reviews*: 42(1): 202–224.

Wheate, N.J., Walker, S., Craig, G.E. & Oun, R., **2010**. The status of platinum anticancer drugs in the clinic and in clinical trials. *Dalton Transactions*, 39(35): 8113-8127.

Wilkinson, G., Rosenblum, M., Whiting, M.C. & Woodward, R.B. **1952**. The structure of iron bis-cyclopentadienyl. *Journal of the American Chemical Society*, 74(8): 2125–2126.

Win, K.Y. & Feng, S.S. **2006**. In vitro and in vivo studies on vitamin E TPGS-emulsified poly(D,L-lactic-co-glycolic acid) nanoparticles for paclitaxel formulation. *Biomaterials*, 27(10): 2285–2291.

Wong, E. & Giandomenico, C.M. **1999**. Current status of platinum-based antitumor drugs. *Chemical reviews*, 99: 2451–2466.

World Health Organisation **2017**, *Cancer*, Media Centre, http://www.who.int/mediacentre/factsheets/fs297/en/ [Accessed on 14 May 2017].

Wysokiński, R., Kuduk-Jaworska, J. & Michalska, D., **2006**. Electronic structure, Raman and infrared spectra, and vibrational assignment of carboplatin. Density functional theory studies. *Journal of Molecular Structure: THEOCHEM*, 758(2):169-179.

APPENDIX

Selected ^{1}H NMR spectra

Carrier 1 (PC1)

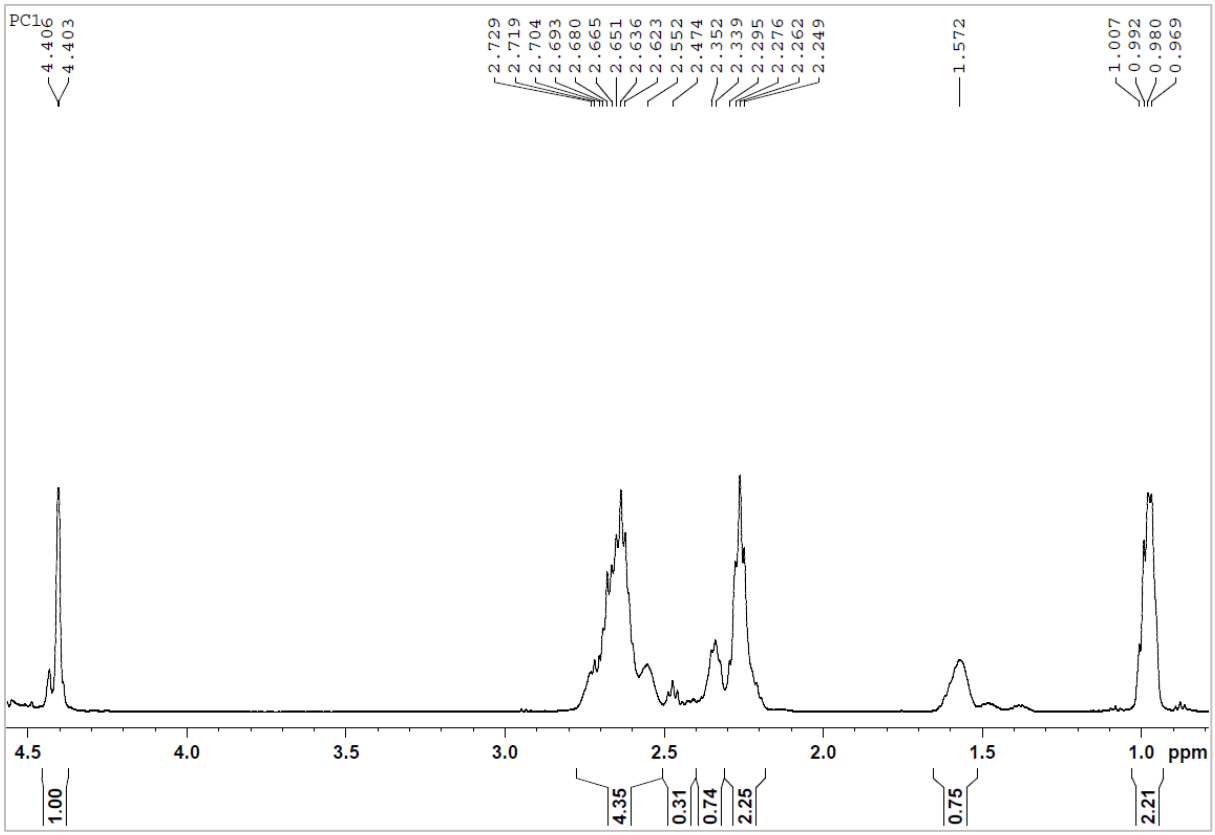

Carrier 2 (PC2)

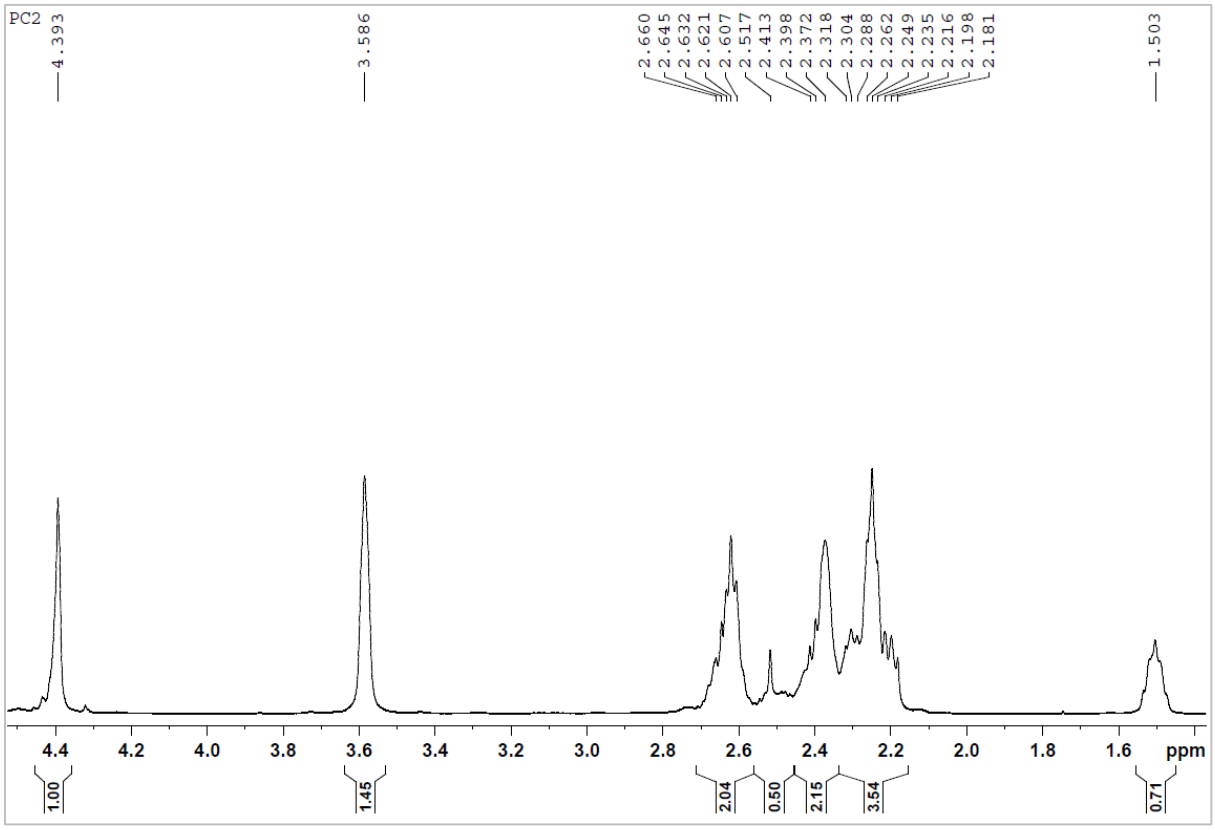

Carrier 3 (PC3)

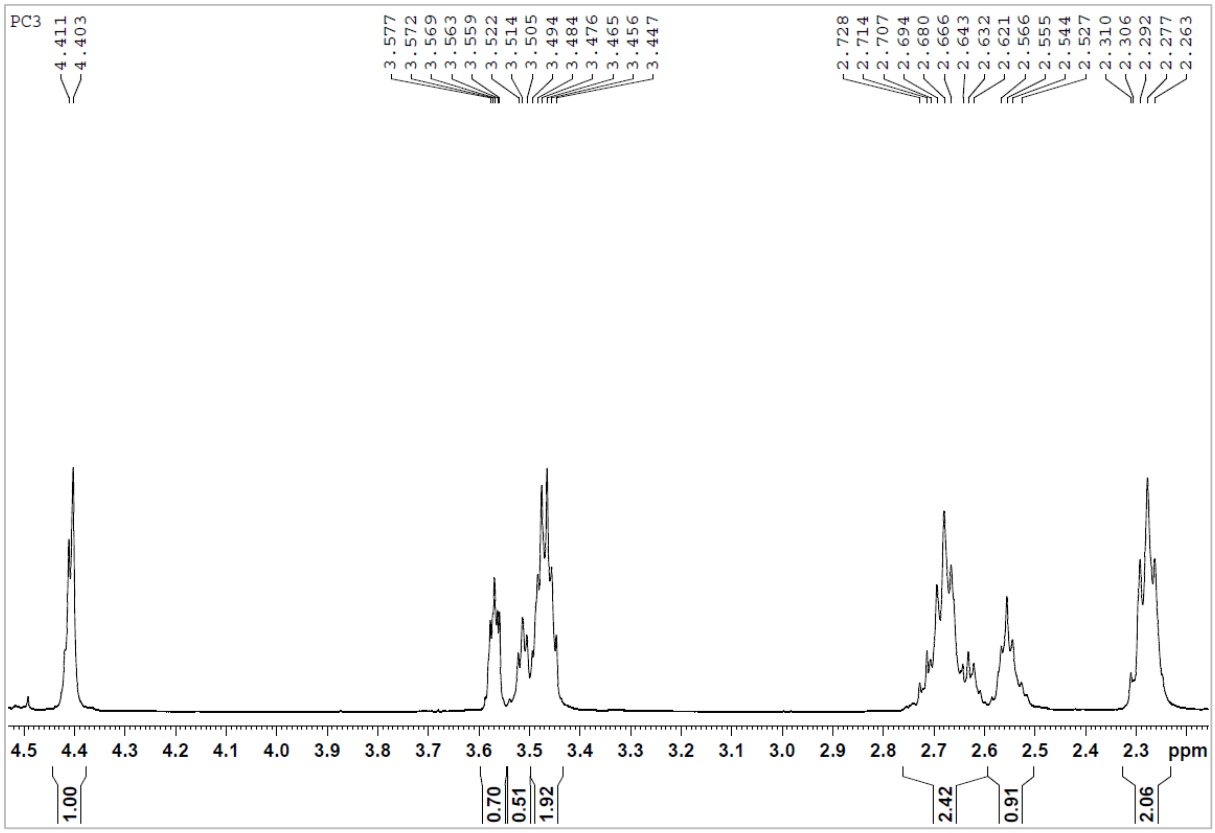

Carrier 4 (PC4)

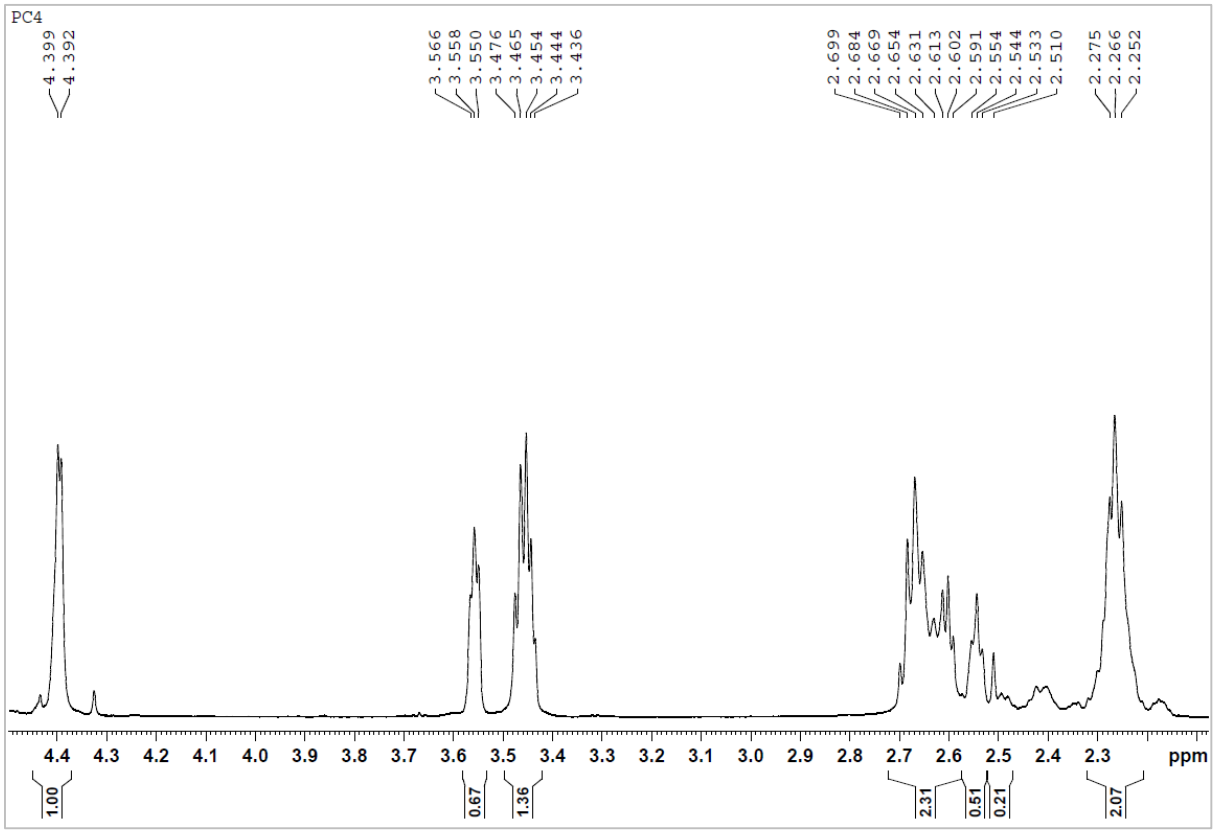

Carrier 7 (PC7)

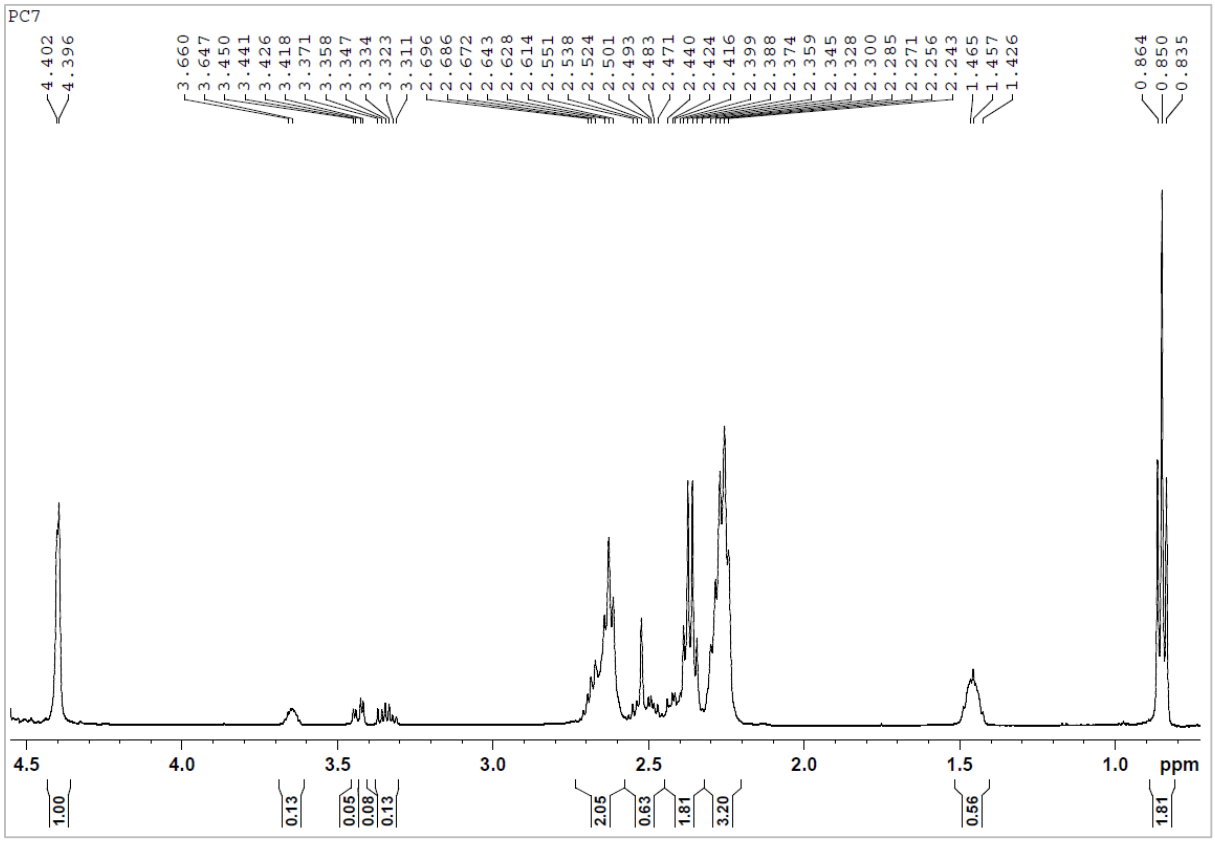

Carrier 9 (PC9)

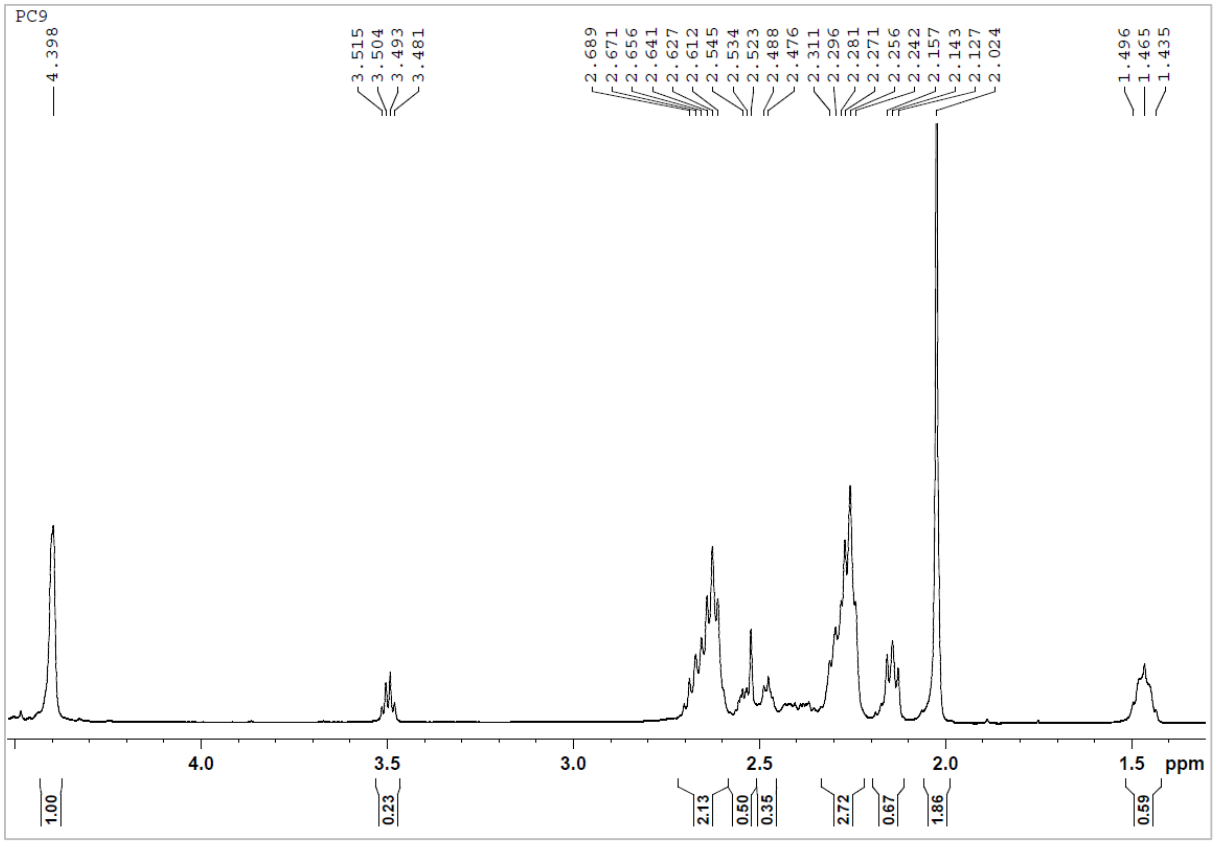

Conjugate 1 (PD1)

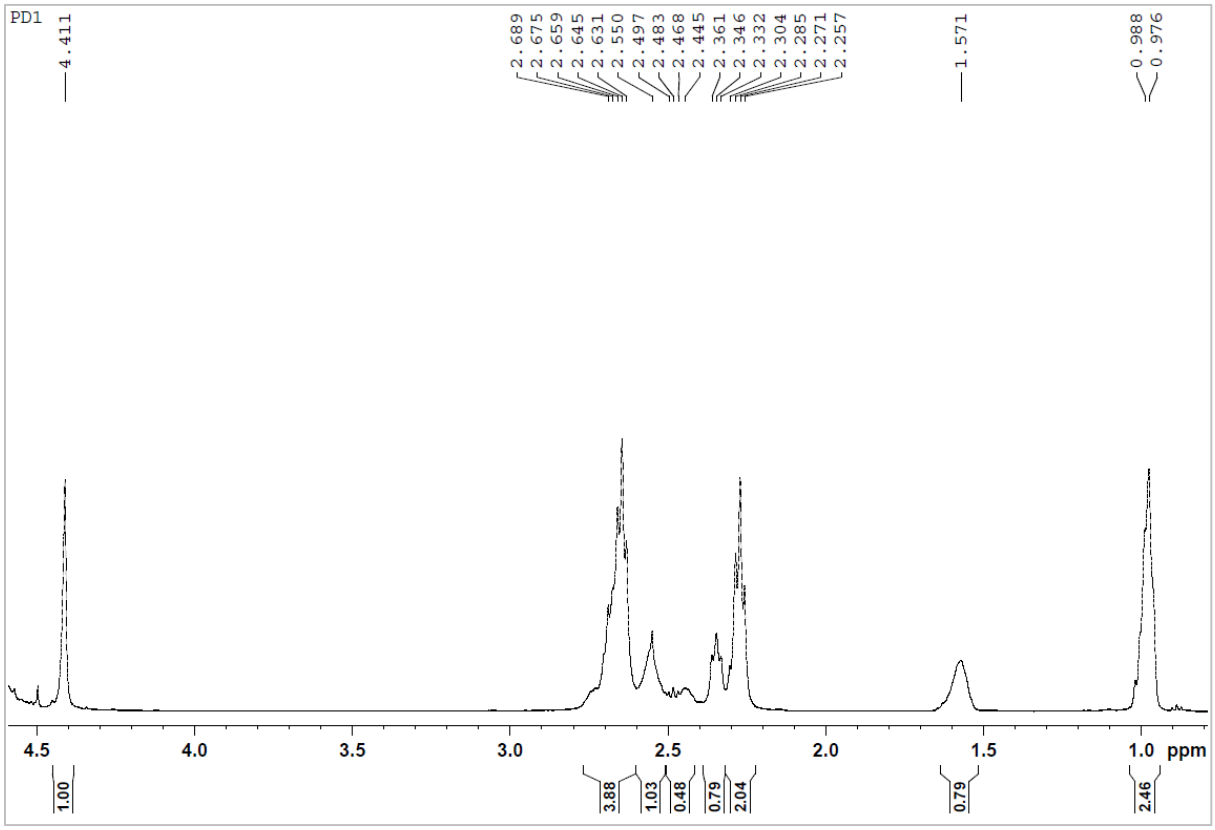

Conjugate 2 (PD2)

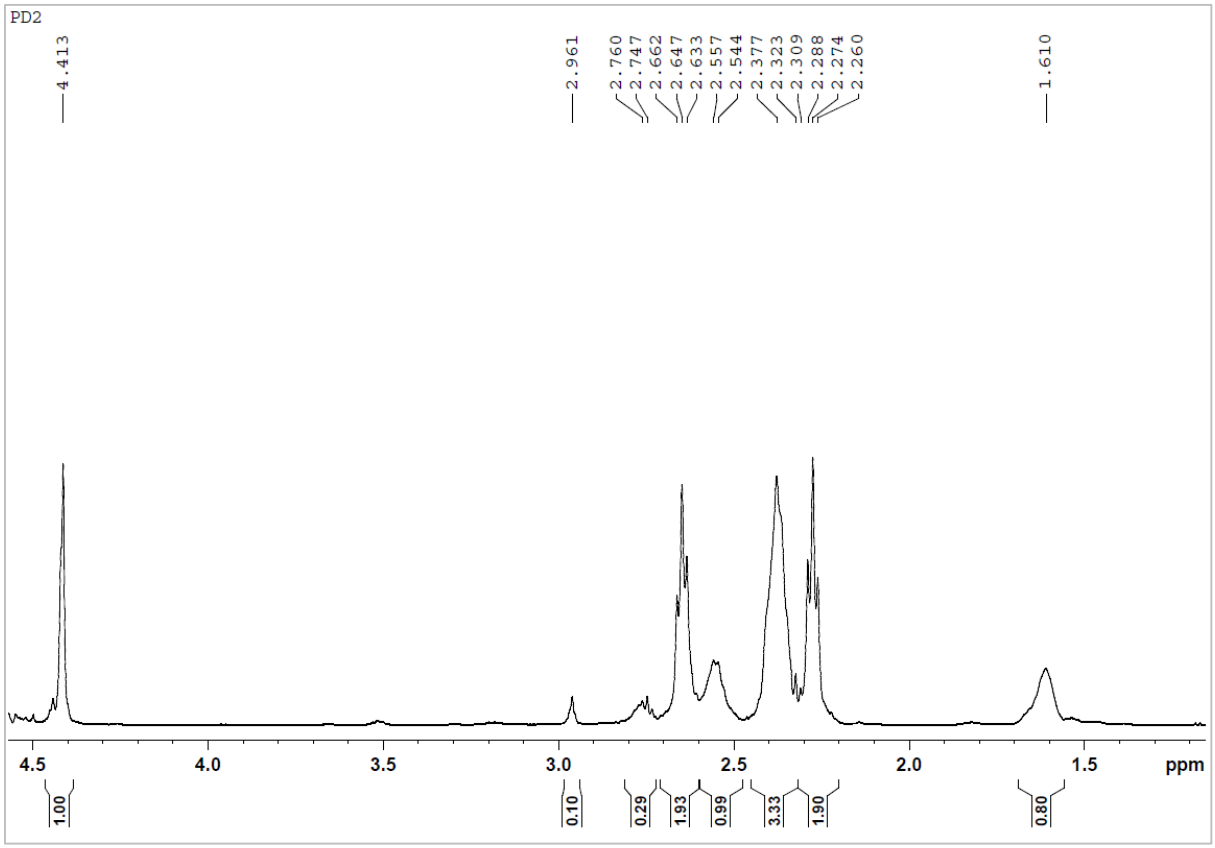

Conjugate 4 (PD4)

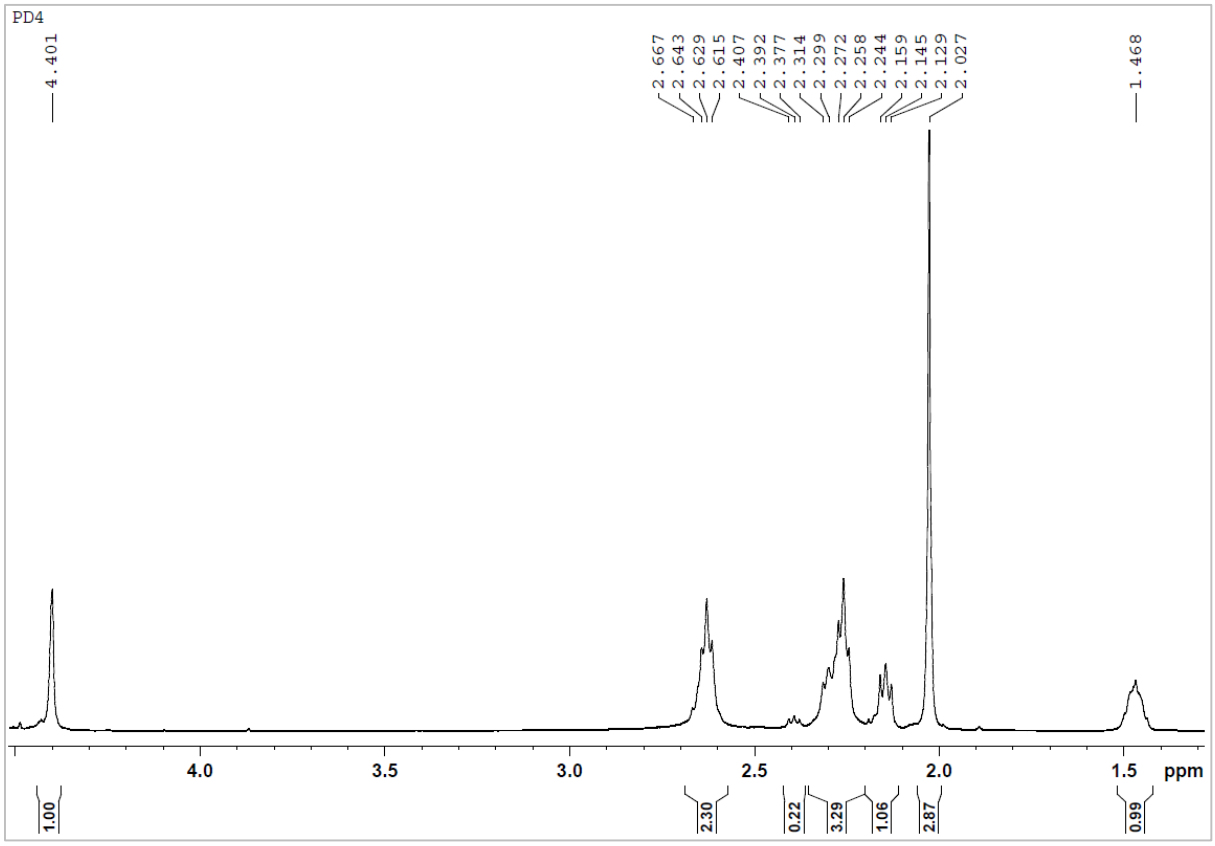

Conjugate 6 (PD6)

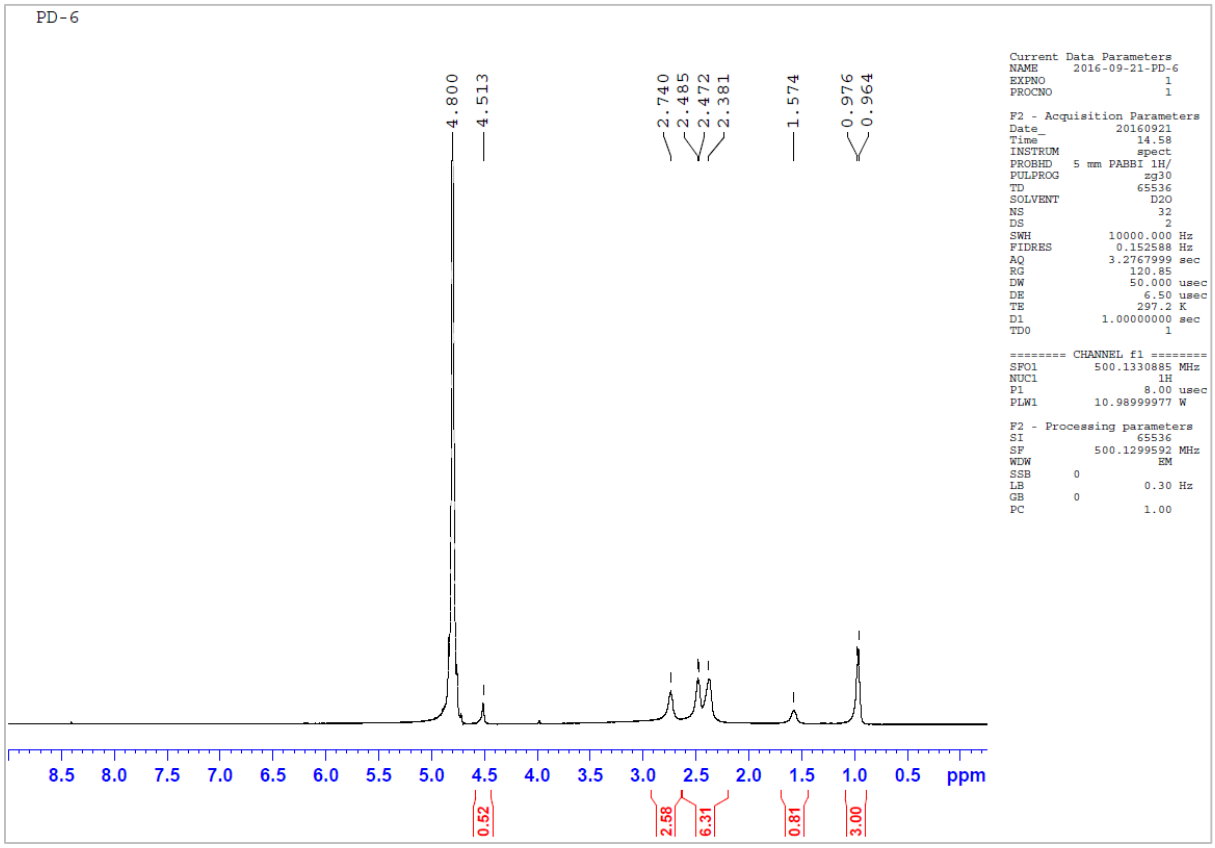

Selected EDX spectra

Conjugate 1 (PD1)

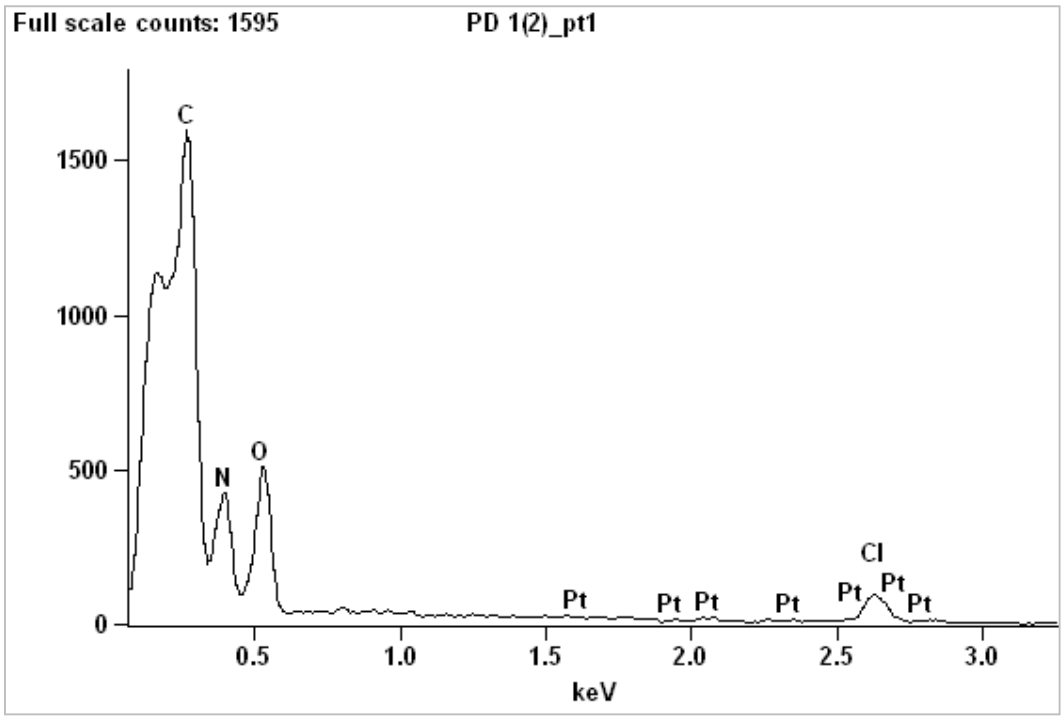

Conjugate 2 (PD2)

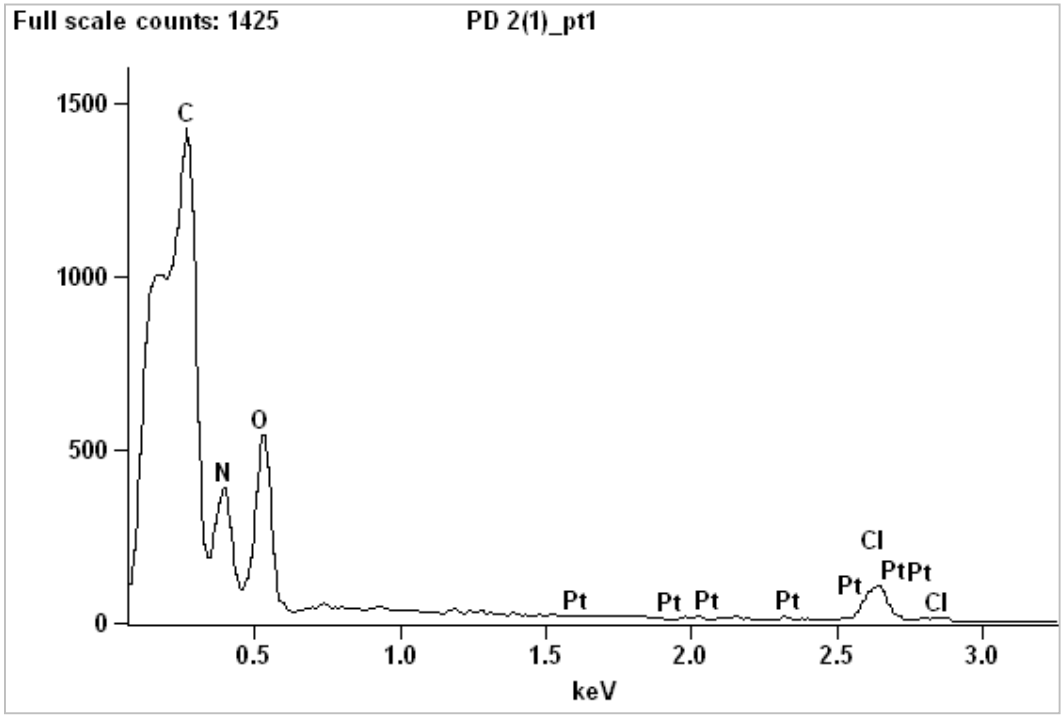

Conjugate 3 (PD3)

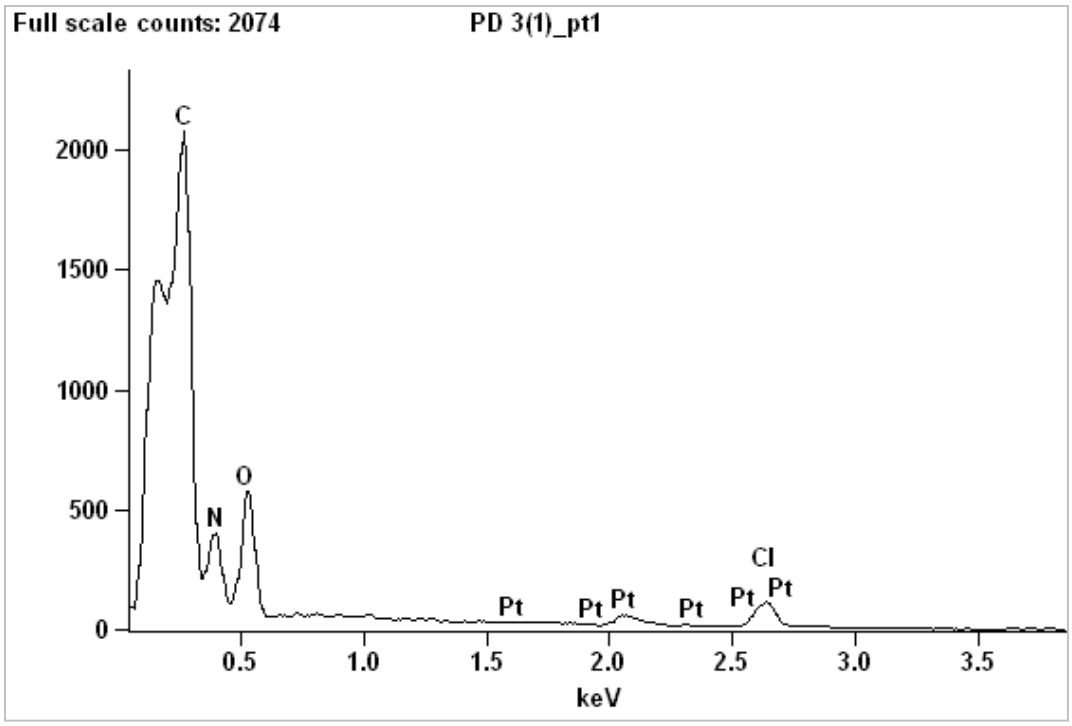

Conjugate 4 (PD4)

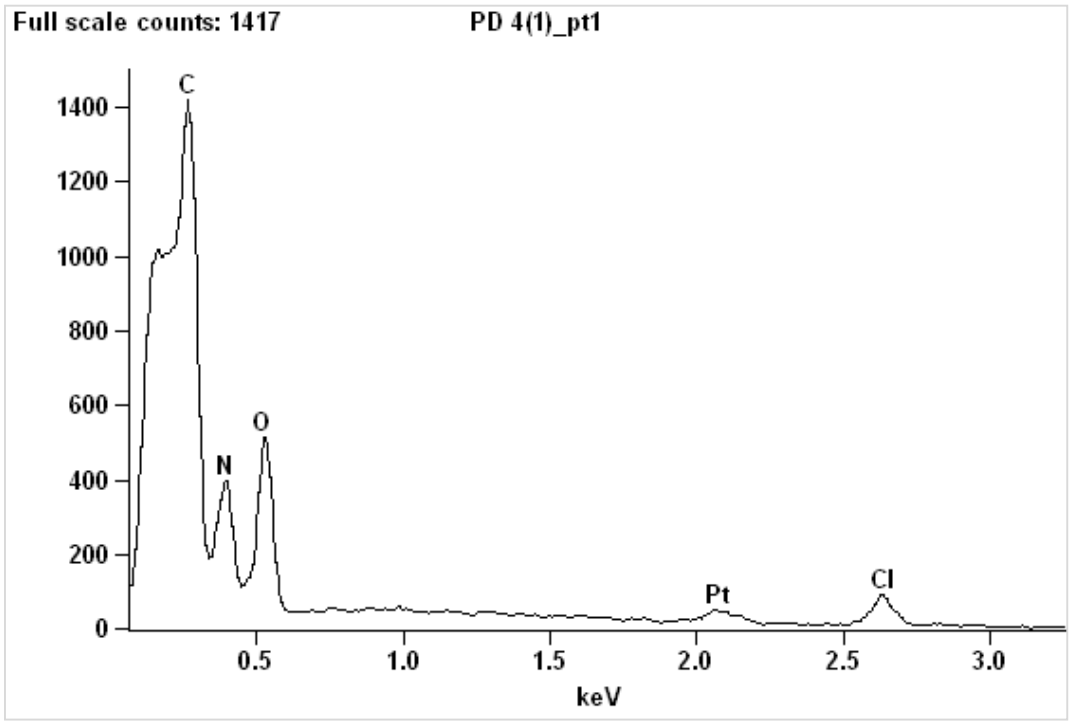

Conjugate 6 (PD6)

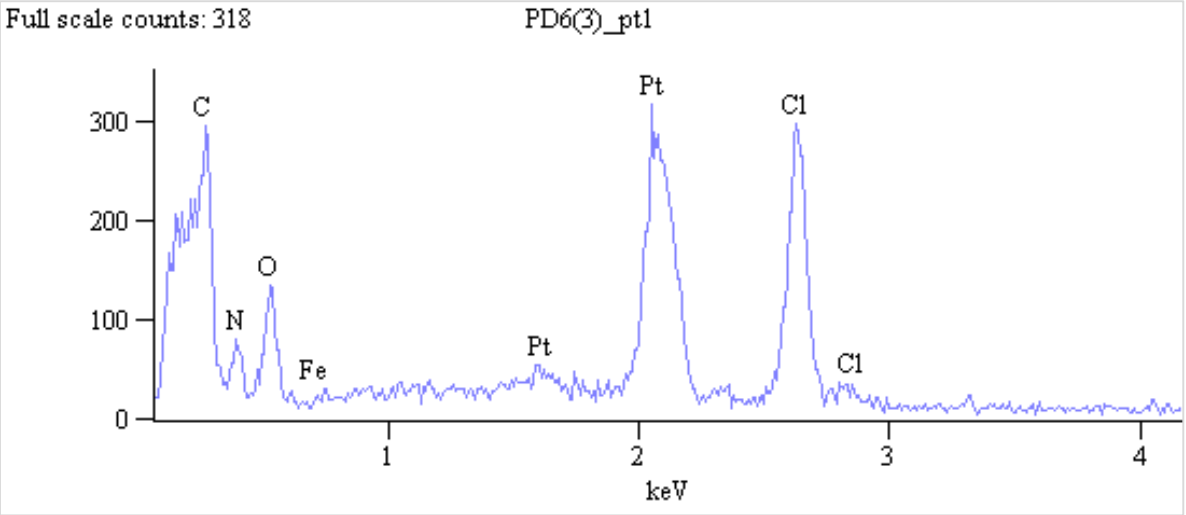

Conjugate 7 (PD7)